



<https://theses.gla.ac.uk/>

Theses Digitisation:

<https://www.gla.ac.uk/myglasgow/research/enlighten/theses/digitisation/>

This is a digitised version of the original print thesis.

Copyright and moral rights for this work are retained by the author

A copy can be downloaded for personal non-commercial research or study,
without prior permission or charge

This work cannot be reproduced or quoted extensively from without first
obtaining permission in writing from the author

The content must not be changed in any way or sold commercially in any
format or medium without the formal permission of the author

When referring to this work, full bibliographic details including the author,
title, awarding institution and date of the thesis must be given

Enlighten: Theses

<https://theses.gla.ac.uk/>
research-enlighten@glasgow.ac.uk

Depositional Environment, Geochemistry, and Diagenesis of
Paleocene and Early Eocene Carbonates of
Agdabia Trough, Libya

by

SHARIF S. AHMED

This thesis is submitted for the degree of Master of Science
(by Research) at the University of Glasgow, Department of
Geology and Applied Geology, February 1992

ProQuest Number: 11011465

All rights reserved

INFORMATION TO ALL USERS

The quality of this reproduction is dependent upon the quality of the copy submitted.

In the unlikely event that the author did not send a complete manuscript and there are missing pages, these will be noted. Also, if material had to be removed, a note will indicate the deletion.



ProQuest 11011465

Published by ProQuest LLC (2018). Copyright of the Dissertation is held by the Author.

All rights reserved.

This work is protected against unauthorized copying under Title 17, United States Code
Microform Edition © ProQuest LLC.

ProQuest LLC.
789 East Eisenhower Parkway
P.O. Box 1346
Ann Arbor, MI 48106 – 1346

ACKNOWLEDGEMENTS

I wish to express my thanks to the management of the Arabian Gulf Oil Company, especially the Exploration Department for their financial support during the course of the study, and for the release of the data which was essential to carry out this research.

I am indebted to my supervisor, Dr. C. J. R. Braithwaite, for his encouragement, constant support, fruitful discussion and valuable advice. I would like to thank the staff in the Geology and Applied Geology department for their understanding. My thanks also go to my friends and colleagues in the department, especially Joe Crummy for his help in the fluid inclusions. I am also grateful to Mr R. Morrison, Mr P. Ainsworth for his help in the SEM and Mr D. Maclean for his artistic photography.

My thanks are extended to Dr. A. Fallick and Dr. A. Boyce from the Isotope Geology unit at the SURRC for their enormous help, encouragement and support.

Finally, thanks go to my parents for their constant support, and to my wife, my son Ahmed and my daughter Marwa, for their patience and understanding.

TABLE OF CONTENTS

	Page
List of Figures	III
List of Tables	V
List of Plates	VI
Abstract	VII
Chapter 1 Introduction and Geology of Libya	
1.1 Aim of the study	2
1.2 Study area	2
1.3 Previous work	5
1.4 Methods of study	6
1.5 Problems	7
1.6 Geological history of Libya	9
1.6.1 Stratigraphy	9
1.6.2 Structure	12
1.7 Regional geology of Northeast Libya	18
1.7.1 Stratigraphy	18
1.7.2 Structure	25
Chapter 2 Lithofacies and environment of deposition	
2.1 Methods and techniques	33
2.1.1 Microscopy	33
2.1.2 X-ray Diffraction	34
2.2 Lithofacies description	36
2.3 Depositional model	63
Chapter 3 Diagenesis	
3.1 Chalk Diagenesis	83
3.2 Other lithofacies	86
3.2.1 Cementation	86
3.2.2 Dissolution	88
3.2.3 Compaction	89
3.2.4 Mineralisation	91
3.2.5 Dolomitization	92

3.4 Cathodoluminescence	93
Chapter 4 Geochemistry	
4.1 Methods and technique	103
4.1.1 X-ray Fluorescence analysis	103
4.1.2 Stable isotope analysis	108
4.2 Results and discussion	110
4.2.1 Trace element	110
4.2.2 Stable isotope	121
Chapter 5 Dolomite	
5.1 Distribution and description	129
5.2 Geology of the area during Tertiary	132
5.3 Geochemistry	133
5.3.1 Fluid inclusion	133
5.4 Mechanism of dolomitization	136
Chapter 6 Porosity analysis	
6.1 Porosity determination.....	140
6.2 Results and discussion	141
Conclusion	148
Future work	153
References	155
Appendix A	171
Appendix B	172
Appendix C	174
Appendix D	175
Appendix E	179

List of Figures

Figure	Page
1.1 Map of NE Libya showing wells in the area, including those in this study	3
1.2 Stratigraphic and structural cross-sections showing differences in thickness of the studied time units in the examined wells	4
1.3 Major sedimentary basins and the tectonic framework of Libya .	10
1.4 Map showing the present day basins and highs in Libya	15
1.5 Isopach map of the total Paleozoic in Cyrenaica	20
1.6 Major tectonic elements in Cyrenaica	23
1.7 Stratigraphic succession in Jabal AL Akhdar	28
2.1 Stratigraphic section of the studied core samples, illustrating the distribution of the different lithofacies as identified from the study of the Paleocene and Early Eocene	64
2.2 Schematic diagram, showing the correlation of the different lithofacies in the area	66
2.3 Schematic model for the depositional environment	68
3.1 Summary of the observed diagenetic events	83
3.2 X-section illustrate the correlation of similar CL signature in the Early Eocene sediments	95
4.1 Showing the vertical distribution of major and trace element concentration of the lithoclast bearing mudstone lithofacies in well A1-41	112
4.2 Showing the vertical distribution of major and trace element concentration of the chalky mudstone lithofacies in well B2-41	113
4.3 Showing the vertical distribution of major and trace element concentration of the the large Nummulite packstone lithofacies in well D1-41	114
4.4 Showing the vertical distribution of major and trace element concentration of the fine crystalline lithofacies D1-41	115
4.5 Showing the vertical distribution of major and trace element concentration of the coarse crystalline lithofacies in well C1-41 .	116
4.6 X-ray diffraction pattern, showing the existence of quartz and koalinite in the lithoclast bearing mudstone lithofacies	120

4.7	Relationship between $\delta^{18}\text{O}$ and depth in the dolomite	122
4.8	Oxygen-carbon isotopic composition of dolomite	122
4.9	Equilibrium relationship between $\delta^{18}\text{O}$ of dolomite temperature, and the predicted $\delta^{18}\text{O}$ of water	124
4.10	Relationship between depth and Na content in D1-41	124
6.1	Calculated sonic porosity in a cored interval in the chalky mudstone lithofacies (well B2-41)	143
6.2	Calculated sonic porosity in a cored interval in the large nummulite lithofacies (well J1-41)	145

List of Tables

Table	Page
2.1 Summary of the characteristic innate to each lithofacies	37
4.1 Chemical analyses for major elements in well A1-41	104
4.2 Chemical analyses for trace elements in well A1-41	104
4.3 Chemical analyses for major elements in well B2-41	105
4.4 Chemical analyses for trace elements in well B2-41	105
4.5 Chemical analyses for major elements in well C1-41	106
4.6 Chemical analyses for trace elements in well C1-41	106
4.7 Chemical analyses for major elements in well D1-41	107
4.8 Chemical analyses for trace elements in well D1-41	107
4.9 Results of carbon and oxygen isotope analyses of dolomite	109
4.10 Results of sulphur isotope analyses of calcium sulphate	109

List of Plates

Plate	Page
2.1 Showing characteristic of Lithofacies F1	73
2.2 Showing features of lithofacies F1	74
2.3 Showing characteristic of lithofacies F2	75
2.4 Showing constituent of lithofacies F2	76
2.5 Showing features of lithofacies F3	77
2.6 Showing constituent of nummulitic lithofacies	78
2.7 Showing features of lithofacies F4 and F5	79
2.8 Showing features of dolomites	80
2.9 Showing replacement in dolomite	81
3.1 Compaction and cementation	97
3.2 Stylolites in chalk and dolomite	98
3.3 Showing presence of mineralisation, anhydrite, NaCl	99
4.4 Types of Porosity	100
4.5 Types of luminescence	101

ABSTRACT

The study of the Paleocene and Early Eocene rocks of the Agdabia Trough, on the eastern edge of the Sirte basin of Libya, was undertaken to assess the depositional environment, the geochemistry, the succeeding diagenetic processes, and the resultant porosity of the sequence, and to investigate the causes of low permeability.

The results indicate predominantly slope deposition. The investigated sequence has been divided into seven lithofacies. These start with lithoclast bearing mudstones which are interpreted as debris flow deposits, associated with hemipelagic muds deposited at the base of the slope. These are overlain locally by thin pelletal packstones which are followed by chalks. The sequence is capped by lithofacies with large nummulites and finally by lithofacies with small nummulites. In the northern part of the area dolomite dominates sometimes co-existing with diagenetic evaporites. The slope stretched more than 30Km from the Cyrenaica platform to the basin centre where relatively deep water sediments dominated. The early Eocene interval documents a dramatic change in deposition and transition to shallow water sediments, represented by nummulitic limestones. The sedimentary pattern in the Eocene was dominated by shallowing upward cycles in the nummulitic limestone. These are believed to be due to falls in sea level which caused progradation of shallow water nummulitic banks over deep water slope deposit.

Many diagenetic alterations have been revealed. Diagenetic events began with dissolution and compaction, locally succeeded in the northern area by dolomitization. A second stage of dissolution followed by anhydrite deposition post dated the dolomitization. Equant calcite is the dominant cement and it is present mainly filling intraskeletal chambers of foraminifera. Dolomite dominates the Paleocene section in the northern part of the area. The geological, petrographical and geochemical evidence implies that the dolomitization process was accomplished by penetration of highly saline fluids derived from the Cyrenaica platform and took place under more than 1Km of burial. Cathodoluminescence petrography reveals four types of correlatable luminescence within the studied wells.

VIII

These include bright matrix and cement, dull luminescence, non luminescence and finally dull matrix with two cement stages. The distribution of these types in the area implies that oxic water driven from the Cyrenaica platform which gradually changed to a more reduced state down slope. The lateral changes in the luminescence types are paralleled by similar changes up section which are interpreted as due to progressive subsidence or burial.

Geochemical studies show moderate strontium (Sr) values, in the limestones ranging between 322 to 1600ppm, while in the dolomite Sr is relatively low. Other trace elements, such as iron (Fe) and manganese (Mn) are generally low, while sodium values are quite high in the dolomite reaching 7000ppm. The isotope analyses carried out chiefly on the dolomites, show depletion in $\delta^{18}\text{O}$, with quite negative values ranging between -2.4 to -8.3‰ (PDB). The equilibrium relationship calculation between $\delta^{18}\text{O}$ of the dolomite, the $\delta^{18}\text{O}$ of the precipitating water and the temperature reveals that the temperature of the precipitating water lay between 50-80°C and that the water was enriched by +5‰ in $\delta^{18}\text{O}$ with respect to the sea water. This implies that the water which was responsible for dolomitization was an evaporated sea water. The $\delta^{13}\text{C}$ values of the dolomites range between 0.6 to 2.5‰ (PDB), reflecting formation in water in equilibrium with marine sediments. The Sulphur isotope ($\delta^{34}\text{S}$) results from the anhydrite average 21.37‰ (CDT). This figure is consistent with the range of $\delta^{34}\text{S}$ isotopic values known for marine evaporites of Tertiary age. Fluid inclusions in the dolomites reveal an average recorded temperature of 105°C and salinity ranges between 162-210ppt NaCl equivalent.

Inspection of porosity in thin-sections and sonic logs suggests that the large nummulite lithofacies which apparently has good porosity might serve as a good reservoir rock, but more detailed study is required. Porosity and permeability are enormously influenced by calcium sulphate precipitation which occluded some porespace and narrowed porethroats, resulting in a reduction of the permeability in the area.

CHAPTER ONE

INTRODUCTION AND GEOLOGY

OF LIBYA

The area investigated is in northern Libya and lies on the western edge of the Agdabia trough, a small graben forming part of the Sirte basin and flanking the Cyrenaica Platform. The Paleocene and Early Eocene rocks present in the Agdabia trough form characteristic units, the Najah Formation, the Apollonia Formation and the Darnah Formation. These names were introduced by AGOCO exploration staff for subsurface sequences but the Apollonia and Darnah Formations have since been shown to have analogous sequences outcropping in the Jabal Al Akhdar area in northeast Libya. The thickness of the Paleocene and Eocene differs from place to place reflecting the almost continuous tectonic activity in the Sirte basin which began in the Upper Cretaceous. Hydrocarbon exploration activity in the region started in the early 1960'S and since then more than 27 wells have been drilled in the Agdabia trough. However, none have produced economic amounts of hydrocarbons. As a consequence of this failure geological studies have been intensified and it is thought that the cause of this apparent lack of hydrocarbons lies in a generally low permeability, but also in a poor understanding of either facies distribution or the depositional environments which facies represent.

1.1 Aims of the study

The central aim of recent investigations has been to better understand the geology of the Agdabia trough in order to determine the most prospective facies for hydrocarbon potential. The present research is part of this plan. The scope of this research is to reach an adequate depositional model for the Paleocene and Early Eocene rocks by examining their sedimentology, petrography and geochemistry. The study has examined lithofacies distribution and interpreted the environments of deposition. It has further considered the geochemistry and the diagenetic processes which have influenced the petrophysics of these facies. Core samples have been collected from five different wells scattered in the Agdabia trough at depths ranging between 5000ft. and approximately 13000ft. below sea level. These wells, A1, B2, C1, D1, and J1 are all located in concession 41 (now known as 129).

1.2 Study Area

The area investigated (Fig. 1.1) is located on the eastern edge of the Sirte basin between latitudes $30^{\circ} 40'$ and $31^{\circ} 45'$ and between longitude $20^{\circ} 00'$ and $20^{\circ} 50'$. The Agdabia trough forms part of the Sirte basin, and there are two hypotheses for the earlier history of this basin. The first

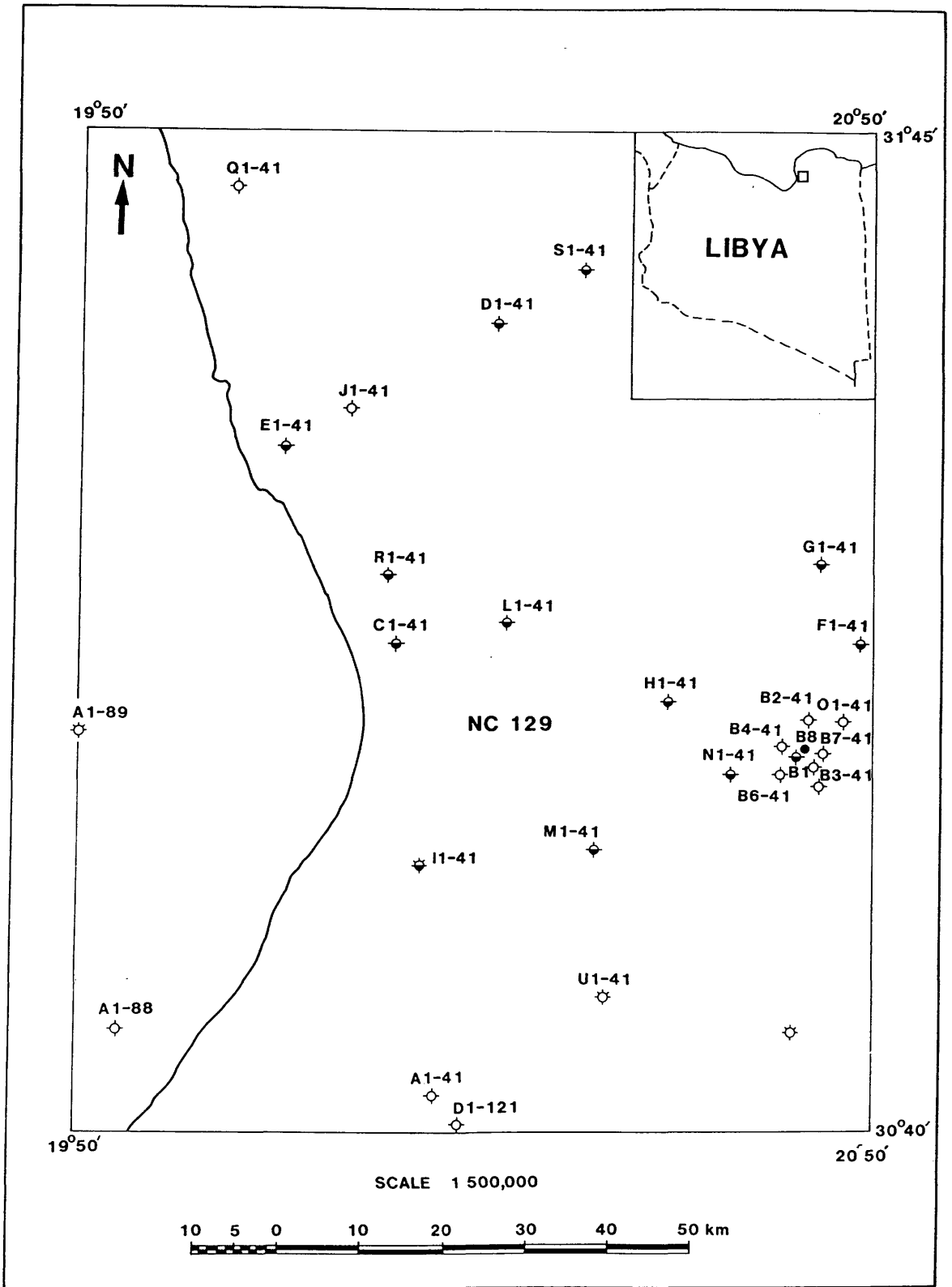


Fig. 1.1, Map of NE Libya showing wells in the area, including those in this study

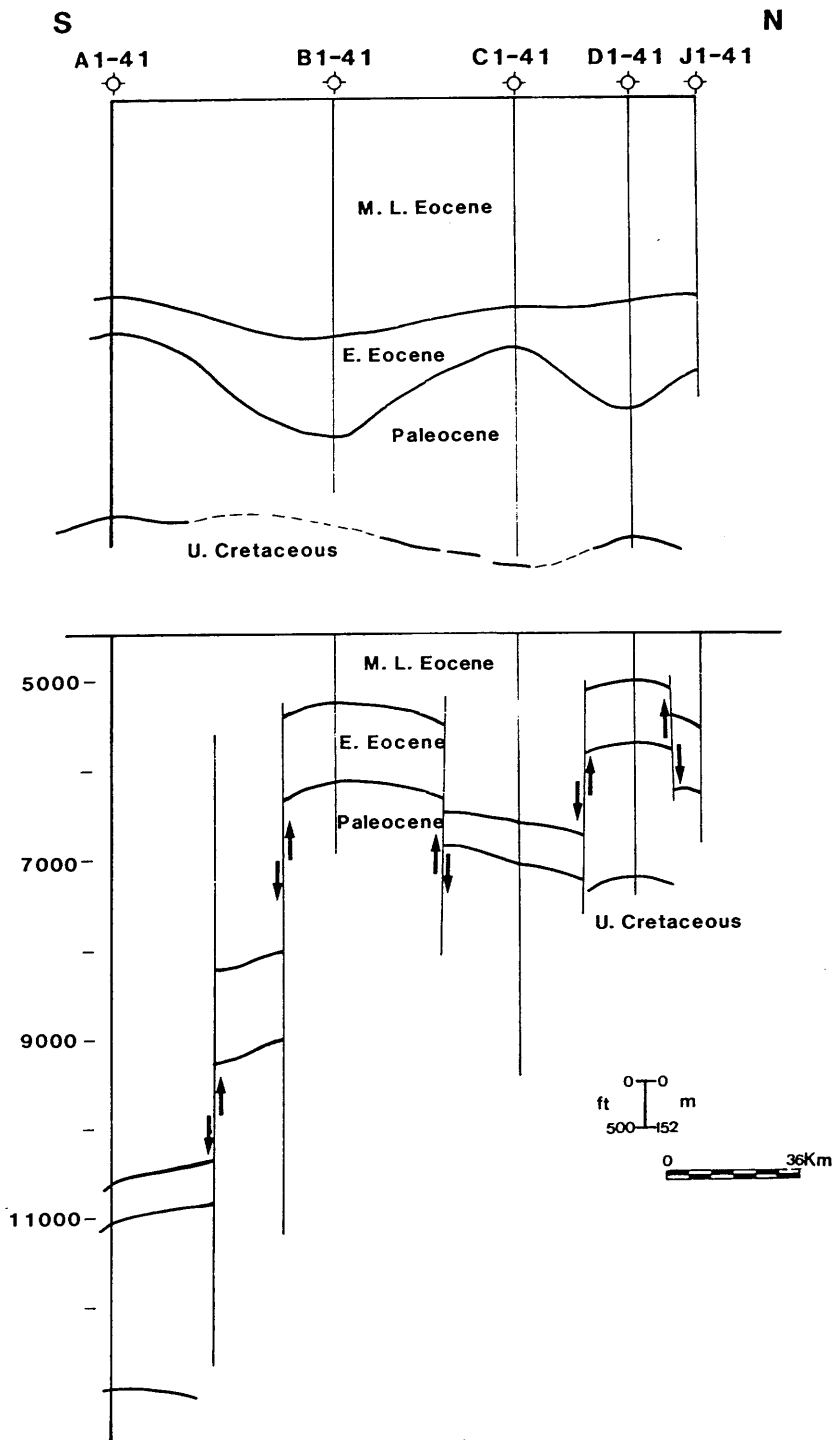


Fig. 1.2, Stratigraphic (top) and structural (bottom) cross-sections showing differences in thickness of the studied time units in the examined wells.

suggests that the area was a Paleozoic high and was essentially a non depositional area until Cenomanian time. The second that Upper Paleozoic and even Lower Mesozoic rocks were formerly present, and that they have been removed by uplift and erosion prior to deposition of the Late Jurassic or Early Cretaceous. There is as yet no firm evidence to support either of these views.

The largest influence on the sedimentation pattern in the trough was provided by the Cyrenaica platform. Sediments thicken from the platform margin towards the trough centre and are dominated by carbonates. The variation in thickness of the Paleocene and early Eocene sequence suggests local differences in subsidence and/or sedimentation rates (Fig. 1.2). The present day structural configuration of northeast Libya is dominated by the Cyrenaica Platform to the east and by Jabal Al Aḵhdar to the north. (see section 1.7)

1.3 Previous work

The geology of Libya has been the subject of numerous investigations. These were initially mostly on outcrops, but after oil was discovered in the early 1960'S most work has been concentrated in the subsurface, and most carried-out by oil companies. The Sirte basin is the most important basin in Libya in the production of hydrocarbons. Studies

have largely concentrated on the central and western parts of the basin, and relatively little attention has been given to eastern areas.

The subsurface Paleocene of the Sirte basin has been described by Conley (1971) who concluded that the sedimentary sequence in the subsurface was equivalent to that in outcrops. Berggren (1969, 1974) studied the distribution of Tertiary foraminifera in the Sirte basin and divided the sequence into a series of stratigraphic zones. In northeastern Libya most studies of the Eocene have been carried-out on the surface since most of the Tertiary succession is exposed in Jabal Al Akhdar. Rohlich (1974) discussed the tectonic development of Jabal Al Akhdar, and outlined the principal structural features of the area discussed in section 1.7.2. Recently El Hawat and others (1985; 1986) have examined Eocene and Miocene sedimentation and have identified a number of sedimentary cycles.

1.4 Methods of study

A number of investigative methods have been used in the course of this study. These will be listed here and details provided in the pertinent chapters.

The study started by collecting available core samples and describing them. Representative horizons were chosen for thin-section study. More than 160 thin-sections were prepared and were studied petrographically by conventional microscopy and by cathodoluminescence (CL). The scanning electron microscope (SEM) has been used for the investigation of the components and porespace of the fine grained sediments.

The geochemical investigation, comprises the determination of the calcite-dolomite ratio by X- ray diffraction (XRD), and the quantitative analysis of trace elements and major oxides by X-ray fluorescence spectrometry (XRFS). Isotope analyses, including carbon, oxygen and sulphur analyses were carried out mostly on dolomite. Porosity wirelines logs have been used to investigate the petrophysics of the sequence.

1.5 Problems

Little information on the subsurface geology of northeast Libya and in particular the Agdabia trough has been published. Most work in the area has been under the auspices of petroleum companies seeking time - stratigraphic control in their search for petroleum reserves. As a consequence it has sometimes been impossible to do more than speculate

about certain problems.

In addition, the extensive work carried out on core samples since they were drilled in the early sixties, has meant that a considerable part of the cores has been used. Poor storage facilities in the past have also had an effect on core sample quality. Data from other wells in the area was used to supplement that from the study wells to overcome these problems, but no extensive study was made of these wells.

1.6 Geological history of Libya

1.6.1 *Stratigraphy*

Libya is located on the Mediterranean coast of North Africa, and has an area of about 1,600,000 square kilometres. Geologically Libya is situated on the northern part of the African shield and over a long period has been the site for the accumulation of continental and marine sediments, expressed in a wide assortment of sedimentary rocks. Libya consist of four major sedimentary basins, Hammada basin and Murzuq basin are in the west and Serti basin in the middle while the southwest corner occupied by Kufra basin as shown in Fig. 1.3.

The southern part of Libya consists of basement exposures which include a wide variety of metamorphic and predominantly granitic igneous rocks. These outcrop north of the crest of the Gargaf arch, (shown in Fig. 1.3) but have been recognized subsurface in wells in many different parts of the country. Most of the exposed basement rocks are Precambrian in age but recent K-Ar dating of some of the granites beneath the Sirte basin suggests that these are early Paleozoic.

In eastern areas most of the Paleozoic rocks are non marine, although there were Silurian, Devonian and Carboniferous incursions of

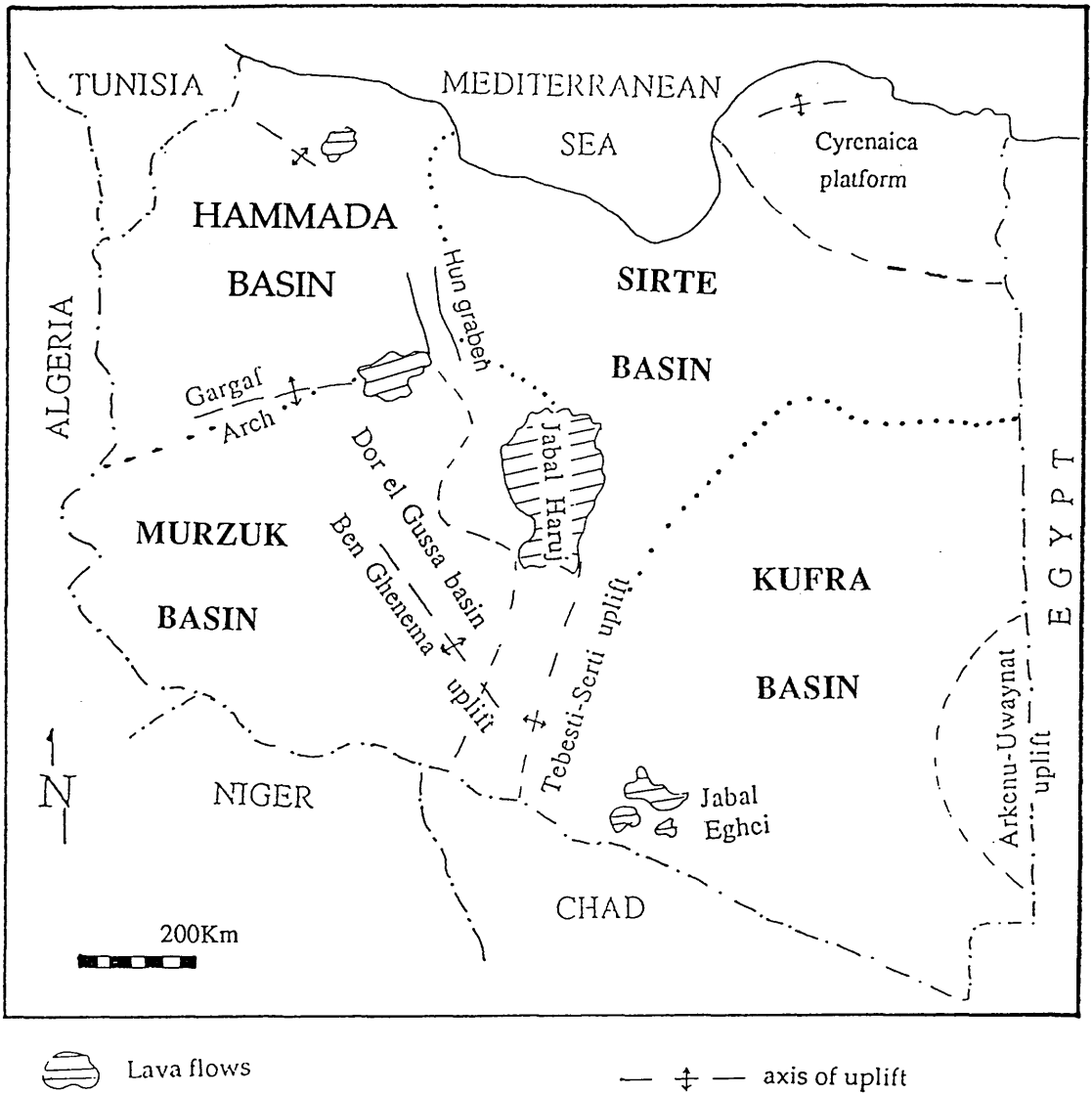


Fig. 1.3, Major sedimentary basins and the tectonic framework of Libya (after Conant and Goudarzi, 1967).

the sea, apparently of short duration. Further west in Algeria the Paleozoic section is dominantly marine.

The uplifted flanks of the Murzuq and Kufra basins (see Fig. 1.3) are covered by continental sandstones of Cambrian and Ordovician age which reach a thickness of about 900m. Although continental conditions prevailed over most of Libya during the Cambrian and Ordovician, they were interrupted in western Libya by a marine incursion which deposited fine grained clastic sediments which contain Middle Ordovician fossils (Conant and Goudarzi, 1967). The presence of an angular unconformity in some places indicates that beds below are Cambrian in age.

The first large scale marine transgression in western Libya commenced in the Silurian and lasted through much of this period. In the Murzuq basin the Silurian incursion deposited graptolitic shale which is overlain by thick regressive sandstones. The Devonian rocks in southern Libya are predominantly continental sandstones and reach a thickness of about 300m. Some marine units are present on the eastern and western flanks of the Murzuq basin. In the southern part of the Hamada basin a sequence of Devonian fine grained clastic rocks contains a marine fauna, while in the northern part of the basin an interbedded marine and non marine sequence has been penetrated by drilling.

The Carboniferous section is represented in western Libya by a thick sequence of shallow water marine and non marine fine grained clastic rocks which on the surface reach a thickness of 900m (Conant and Goudazi, 1967). Subsurface drilling documents much thicker sequences, although marine incursions have only been mentioned in western Libya

The Carboniferous rocks are overlain by a thick sequence of clastic sediments known as the Nubian sandstone. This is also present in much of northeastern Africa and in the Arabian peninsula. Most workers have interpreted the sequence as of continental origin, but recent studies have identified a marine incursion within the sequence and have suggested an Early Cretaceous. The source of these terrigenous clastics is still a matter of controversy, and their depositional environment and age remain in doubt.

Other Mesozoic rocks in Libya are predominantly of marine origin. They occur especially in the northwestern part of the country, but locally they grade laterally into near shore or continental facies. In the western part of Libya the Triassic and Jurassic rocks exposed consist mainly of gypsum co-existing with anhydrite (Gualtieri, 1962) but some Lower Cretaceous sequences are represented by continental sediments

In most of northern Libya Late Cretaceous deposits both in outcrop and subsurface are chiefly marine carbonate. Block faulting in the

Sirte basin, which coincided with sedimentation, developed different types of lithology. The grabens, representing the deepest parts of the basin, were filled by dark shales, while the shallower horsts part are represented by limestones and dolomites.

During the Tertiary northern Libya received widespread carbonate sediments. In the subsurface to the south, especially in the Sirte basin, sediments are much more varied. Fine grained clastic rocks of Oligocene and Miocene age are confined to deep troughs, and thin laterally over marginal highs where carbonates and evaporites were deposited. To the South the thick clastic sequence grades laterally into shallow marine and continental facies.

The Quaternary sediments of northern Libya are basically continental. Only one marine incursion has been reported and this commenced during the last European interglacial stage. Quaternary deposits are widespread and cover some of the bed-rocks. Sand is the predominant lithology, but alluvial gravel plains are also common.

1.6.2 *Structure*

Libya has been subject from time to time to tilting, warping into arches or basins, faulting, or covering by lava, (see Fig. 1.3). Two sets of faults have been defined in the literature, the first dated as near the end of Silurian which coincide with the Caledonian Orogeny and resulted in

several northwest-southeast trending structural elements of uplifts and troughs, later in the late Paleozoic the Hercynian Orogeny developed the second trend northeast-southwest (Fig. 1.4) and the intersection of these two trends has been the focus for most extensive volcanic activity in the country. Volcanics are aligned in a NW-SE trend, and are present in the north west near Tripoli and in the centre of Libya in Jabal Haruj. The fault trends are approximately parallel to the rift system of the Red Sea and East African rift system. The volcanic activity probably started in Oligocene time, and was contemporaneous with movements along deep-seated fractures perhaps related to the Alpine Orogeny.

Epeirogenic down warping, tilting and block faulting, have differentially depressed the Libyan part of the African foreland, allowing repeated transgressions of the Tethyan Sea upon it's border. As a consequence of these events sedimentary basins have been formed at different times, (see Fig. 1.3).

The Sirte Basin is one of the best known. It is an intracratonic basin on the northern margin of the African continent. The area is thought to have been a broad arch or domal structure during the late Hercynian but was subsequently eroded. Recent studies have reached the conclusion that the formation of the Sirte basin is perhaps the best documented evidence of extensive tensional fracturing of the African plate in Cretaceous time (Brown *et al.*, 1985; Almond, 1986).

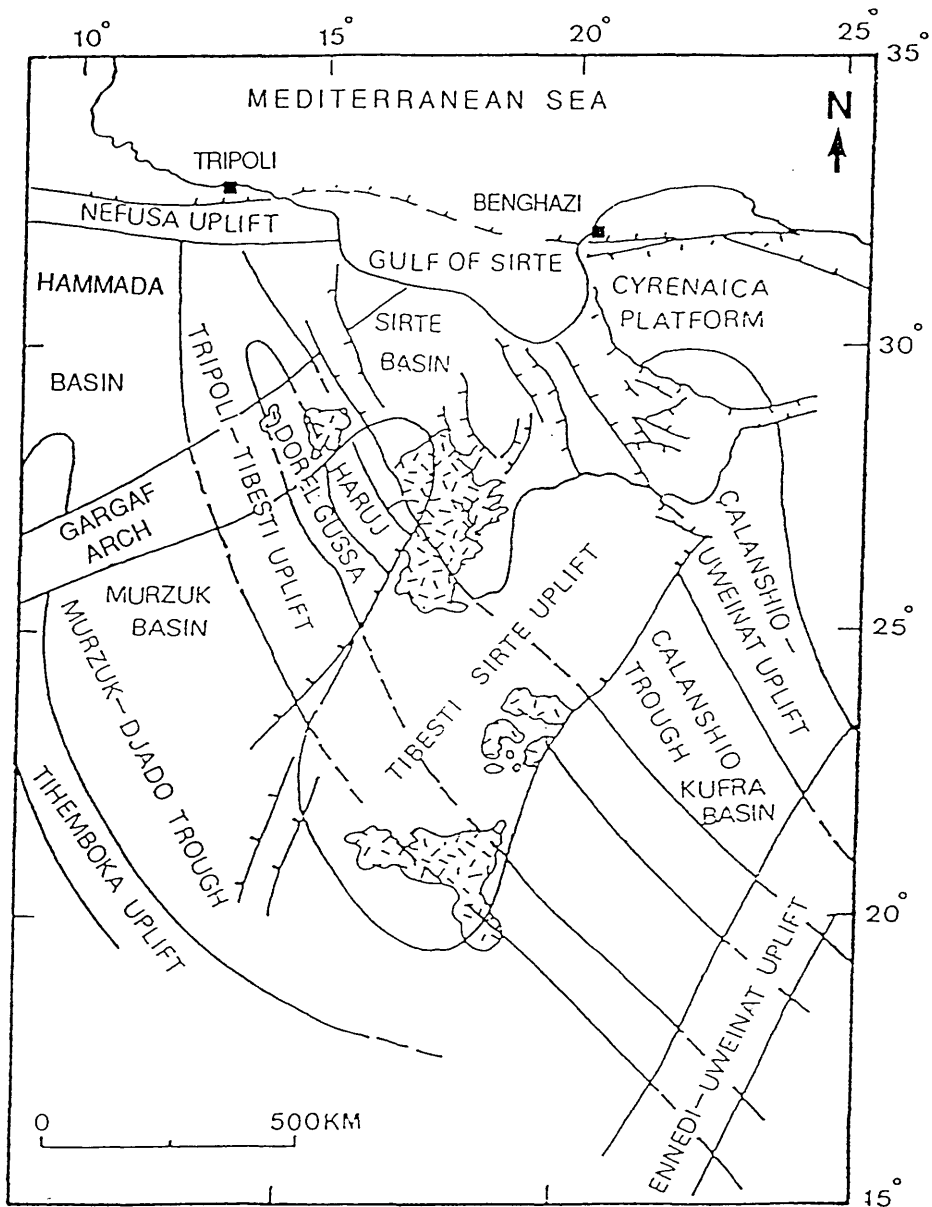


Fig. 1.4, Map showing the present day basins and highs in Libya resulting from the combined effects of two structural regimes (after Klitzch, 1971).

The formation of Serti basin started with large scale of subsidence and block faulting commenced in late Cretaceous and continued, at least intermittently, to the Miocene, perhaps even to the present day. The maximum subsidence have occurred during late and middle Eocene (Gumati, 1984). Drilling activity in order to find oil has provided an appreciable amount of information about the basement which chiefly consists of igneous and metamorphic rocks, but locally includes sedimentary rocks of probable Cambrian and Ordovician age.

At the beginning of late Cretaceous time, the grabens in the Sirte Basin received thick shale deposits while the horsts were covered with shallow water sediment or were out of water. During the Tertiary deep water carbonates were confined to the grabens that were still active, while reefs and shallow water deposits were present on the crests of the horsts. The carbonates grade into evaporites and terrigenous clastic rocks in the south as a result of shallowing of the sea.

The Hammada Basin, also known as the Ghadames Basin, is bounded to the South by the Gargaf Arch and to the east by the Hun Graben, but extends some distance to the West into Algeria. The geological succession in the Libyan part consists of rocks ranging from Cambrian to Paleocene. This sequence is interrupted by several unconformities, the most prominent being that following the Hercynian movement. The Hammada Basin is essentially a Paleozoic basin in which many thousands of meters of predominantly terrigenous clastic sediments were deposited

some of them are of marine origin.

The Murzuq Basin is located South of the Gargaf arch (Fig. 1.4) and is limited to the east by the Tibesti-Serti uplift and to the south by Precambrian rocks forming the Tibesti massif. The basin was influenced by a number of marine incursions but between these thick continental sediments were deposited. The Sea started to regress from the Murzuq basin in the early Carboniferous, by which time continental sediments were widespread. Rocks of all systems from Cambrian to lower Cretaceous are present around the periphery of the basin . The Dor el Gussa trough located in the northeastern part of the basin is separated by the concealed Ben Ghenema uplift (Fig. 1.4).

Low land to the East of the Murzuq basin, representing the southern extension of the Sirte basin, formed an arch trending more or less north-south known as the Tibesti-Serti uplift. This arch probably formed during the Carboniferous period (Klitzch, 1963), and by Tertiary time extensive erosion had exposed large areas of Precambrian rocks on both flanks of the Murzuq basin and on the southern margin of the Sirte basin.

The southeastern part of Libya is occupied by the Kufra basin. Rocks from Cambrian to Carboniferous age are present on the uplifted northern, western, and southern margins. Some marine sediments have been found on the eastern flank but the central part of the basin is filled by

Nubian sandstone underlying by the basement. In the eastern part of the basin, jabal Uwaynat and jabal Arkenu are high masses of Precambrian and late Paleozoic granitic rocks which rise abruptly hundreds of meters above the surrounding desert plain.

1.7 Regional geology of Northeast Libya

1.7.1 *Stratigraphy*

The Cyrenaica region occupies the northeastern part of Libya, and is bounded by longitudes 20° E and 25° E and latitudes from 29° N to 32° N. Cyrenaica is bordered to the north by the Mediterranean sea and extendeds to the east to the Egyptian border. It is bounded to the west by the Sirte basin and to the South by the Kufra basin (Fig. 1.3). It is considered to be part of the stable Saharan shield.

The most prominent surface geologic features in the region are the jabal Al Akhdar uplift (shown in Fig. 1.6) and the great sand sea. The Jabal Al Akhdar occupies the northern fringes of the Cyrenaica region and consists of sedimentary strata dipping steeply towards the north and cut by deep and wide wadis originating on the highs.

Several phases of epirogenic movement occurring in Cyrenaica since Precambrian time have produced troughs, horst blocks, or platforms, which have influenced the stratigraphical history of the area. In the southern and southeastern part of the area the basement is unconformably overlain by a partially marine Paleozoic sequence which is itself unconformably overlain by sediments of Jurassic or younger age.

In eastern and northeastern areas the basement is overlain by a wedge of marine Paleozoic rocks which thickens towards the east. The Paleozoic rocks reach a thickness of 3000m (shown in Fig. 1.5) and are unconformably overlain by marine of Late Cretaceous and Tertiary sediments. In parts of central Cyrenaica the Paleozoic rocks are absent and the non marine clastics of Late Jurassic to Early Cretaceous age rest directly on the basement.

Rocks of Cambro-Ordovician to Permian age are widespread in Cyrenaica and shows a variation of thickness attributed to post-Cambrian tectonic activity and to erosion which removed parts of the sequence. The dominant Cambrian lithologies are Quartz arenites interbedded with siltstones and shales. Occasional sandstones at the base of the sequence contain abundant feldspars and micas which suggest derivation from the granitic basement (Al-Arnauti and Shelmani, 1985).

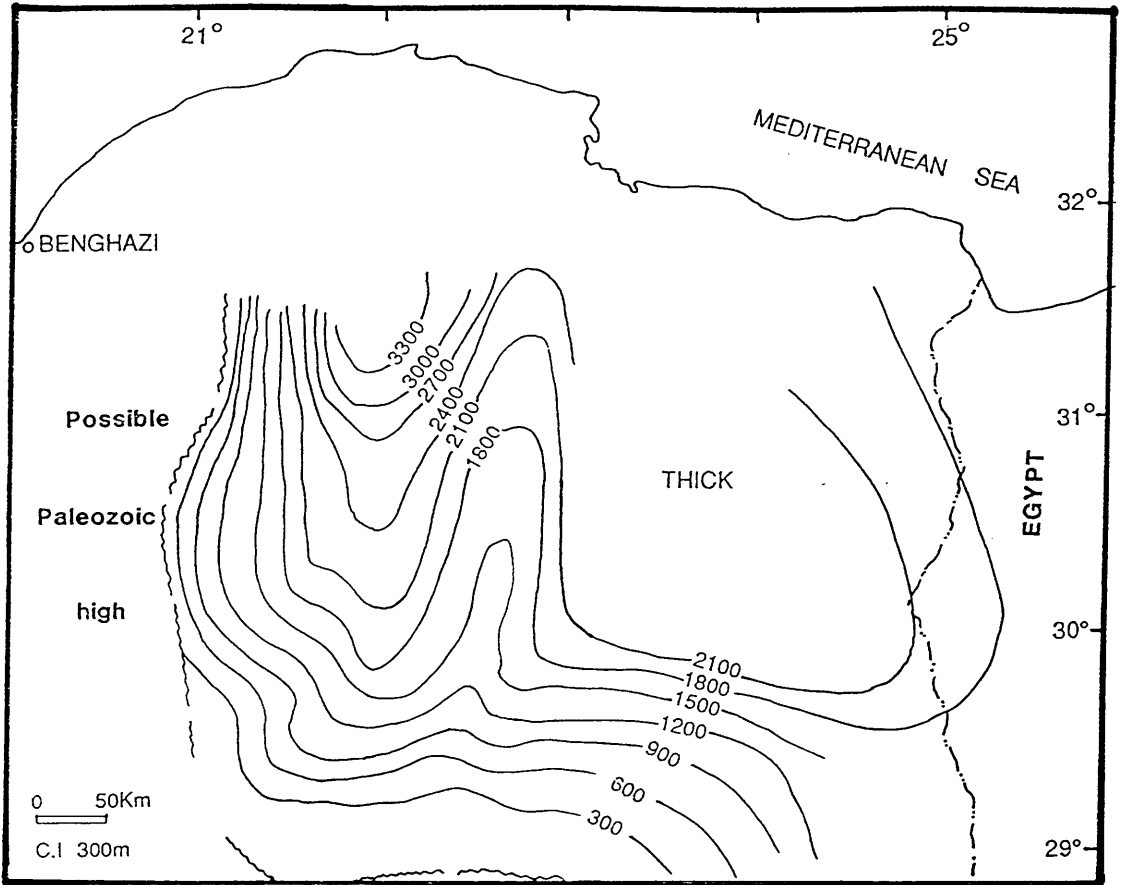


Fig. 1.5, Isopach map of the total Paleozoic in Cyrenaica (after Sola and Ozcicek, 1990).

Ordovician rocks vary from 150 to 600m thick and consist of subangular micaceous sandstones interbedded with dark grey shales and siltstones. They contain Acritarchs and chitinozoans which suggest a late Early Ordovician age and document the first marine transgression in the area.

The Silurian period is represented in Cyrenaica by two lithologies. Graptolitic shales have been dated paleontologically as Early Silurian and are overlain by sandstones and siltstones which are Late Silurian. The Silurian succession appears to have been deposited in a shallow marine environment but the transition from Lower Silurian graptolitic shale to Upper Silurian sandstone and siltstone suggest a possible regressive phase of sedimentation (El-Arnauti and Shelmani, 1985).

Early Devonian sediments are widespread in the area and reach a maximum thickness of 1000m. They consist of ferruginous sandstones and micaceous shales. The sedimentary facies, with the presence of acritarchs and miospores, suggest a near shore marine environment of deposition (EL-Arnauti and Shelmani,1985). Middle Devonian rocks have also been encountered in some wells. These consist of silty micaceous shales interbedded with calcilutite limestones which are considered to have been deposited in a shallow marine environment.

The thickest section of Carboniferous rocks reaches 1000m and consists of fine to coarse grained sandstones interbedded with red brown silty shales at the base and white chalky limestones at the top. The Carboniferous sediments show marked facies changes. In the South, they are represented by continental sediments, in the central area by mixed continental and marine facies, and in the North by shallow marine sediments. The complete lack of Carboniferous sediments in some areas is probably related to local erosion caused by the Hercynian Orogeny.

Permian sediments were not irregularly distributed over Cyrenaica. They consist of sandstones and shales with thin beds of lignite which suggest deposition in a continental environment. This is supported by the abundance of terrestrially derived miospores and palynodebris (El-Arnauti and Shelmani, 1985). Palynological studies also suggest that there is no evidence of Late Permian sediments in the region.

Recent studies by El Arnauti and Shelmani in 1985, have provided proof of the presence of Triassic sediments in northeast Libya. These are composed predominantly of sandstones and shales and are thought to have been deposited in a non-marine lagoonal environment. A slight marine incursion is indicated by the presence of glauconite in the sediments. There is no evidence for any early Triassic sediment being deposited, and only Middle and Late Triassic rocks have been identified in the area.

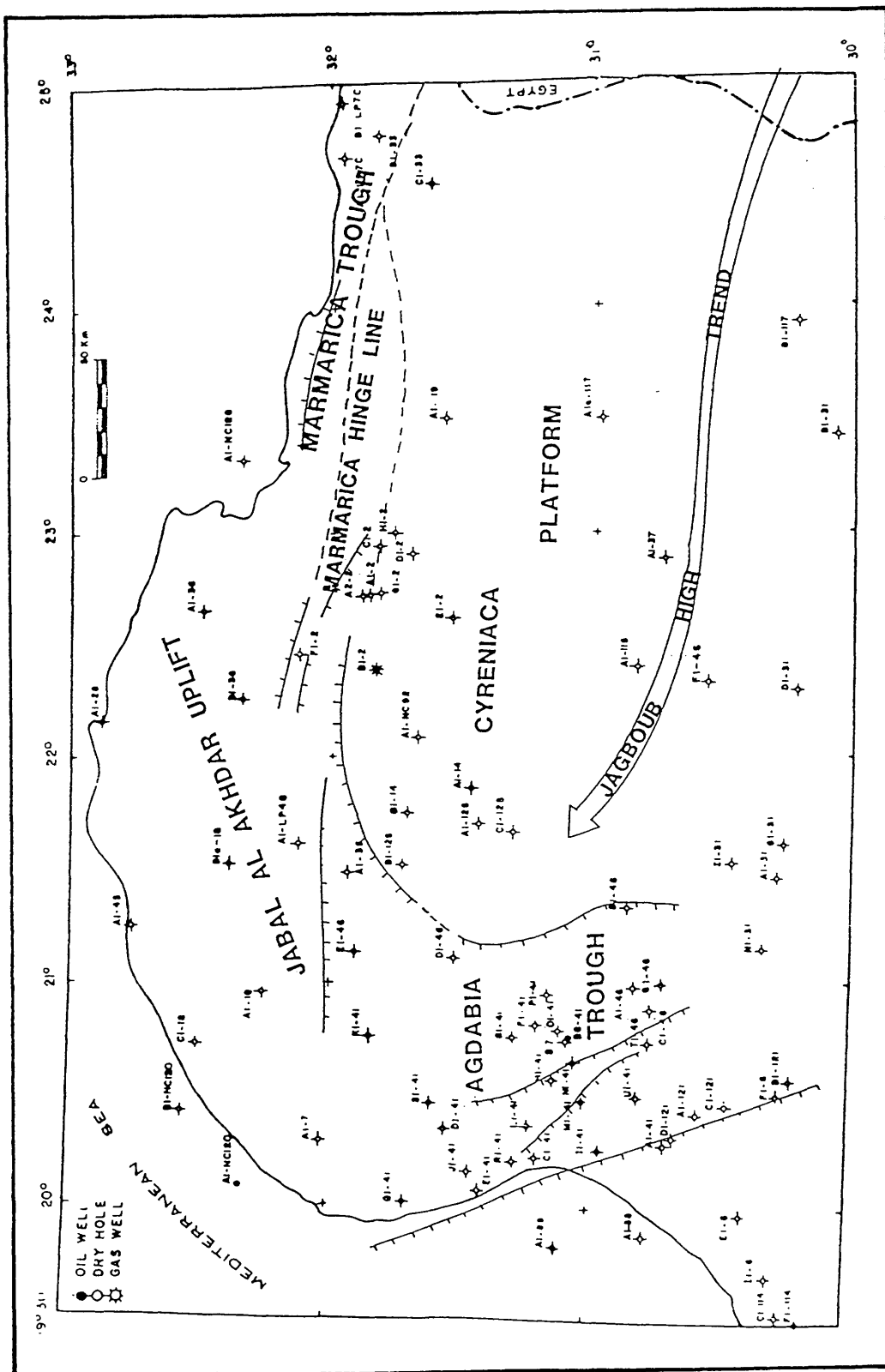


Fig. 1.6, Major tectonic elements in Cyrenaica (modified after AGOCO exploration staff, unpublished Report, 1989).

Jurassic sediments reach a thickness of 1000m in central Cyrenaica. Limestones dominate the succession, interbedded with sandstones in the upper part. This type of sedimentation changes towards the north to deeper marine facies represented by intercalations of shales and limestones. Palynological age dating confirms that these sediments are of Middle to Late Jurassic age.

Northern Cyrenaica is covered by Upper Cretaceous and Tertiary marine carbonate rocks and by recent sediments which include marine deposits. These formations have been subjects for many studies, Zert (1974), Klen (1974) and Rohlich (1974). The Early Cretaceous rocks consist of oolitic limestones with occasional chert beds, changing to dolomite at the base. Biostratigraphic investigation suggests a Neocomian to Albian in age.

North Africa witnessed a major transgression in the Late Cretaceous which advanced from the north to cover the entire region. This huge transgression deposited chalky limestones in a deep marine environment. These reached a thickness of 500m. In the central and coastal region of the Jabal Al Akhdar Late Cretaceous sediments are exposed. These range in age from Cenomanian to Maastrichtian and were deposited in a deep marine to neritic environment.

1.7.2 Structure

Tectonic activity in northern Cyrenaica ranges in age from the Caledonian to Middle Tertiary (Rohlich, 1980). The tectonic pulses which occurred during this period subjected the area to uplift, subsidence, faulting, tilting folding and erosion. The major structural element which appears in geological, geophysical and drilling data, is the stable platform which covers a great section of the area. This is bounded to the North by the Marmarica hinge line (Fig. 1.6) trending East- West and separating it from the relatively unstable *jabal Al- Akhdar* uplift.

The Cyrenaica platform is bounded in the east by the Marmarica-Tobruk trough, to the west by the Agdabia trough, and to the south by the Jagboub uplift. Goudarzi (1980) proposed a Tertiary fault line between the Cyrenaica platform and Sirte basin along its southwestern limits. The Cyrenaica platform consists of sediment believed to reach a maximum thickness of 4000m, (Fig. 1.5), and ranging in age from Cambro-Ordovician to late Carboniferous, these thin along the southern and southeastern limits of the platform. The Paleozoic strata were overlain by Mesozoic and Tertiary sediment.

Acute Mesozoic faults separate the Marmarica trough from the Cyrenaica platform in the eastern fringe (Fig. 1.6). The northern limit of Cyrenaica platform is defined by an Upper Cretaceous fault with an east-west trend. El-Arnauti Shelmani (1985) found thick marine sediments of

Jurassic age in the Marmarica trough. Along the southern limit of the Cyrenaica platform, drilling data suggest a basement high known as the Jaghboub uplift. This uplift is believed to have formed during the Caledonian orogeny and was possibly rejuvenated by Hercynian movement (Fig. 1.6).

In northeastern Cyrenaica the Paleozoic sequence has been tilted towards the north and northeast and there is an increase in marine influence within the Paleozoic sequence in the same direction. These two features assist in the development of a basinal structure called the Western desert basin. Early Mesozoic subsidence in this basin was appreciable and resulted in the deposition of thick sequences compared to those to the south, where subsidence was moderate or absent (Al-Arnauti and Shelmani, 1985). The Western desert basin (Fig. 1.6) is believed to be a Paleozoic-Mesozoic feature that became stable in the Jurassic and early Cretaceous.

To the north the Cyrenaica platform and the Marmarica trough terminate against the Jabal Al Akhdar uplift. This has a northeast-southwest trend. The abrupt thickening and the increasingly marine character of the associated sediments towards the north (especially those of early Cretaceous age) suggest that the Jabal Al Akhdar area was a fast sinking trough during the late Jurassic to early Cretaceous separated from the consolidated Western desert basin by a nearly East- West trending fault (Al-Arnauti and Shelmani, 1985).

In the late Cretaceous the basin inverted and subsidence reversed to uplift with the growth of a new fault system parallel or nearly parallel to the Jurassic-Early Cretaceous system. This idea is supported by two lines of evidence. First, the thickness of the lower Cretaceous is reduced and second the shallow marine conditions which prevailed in the central part of Jabal Al- Akhdar. Since the Cretaceous several tectonic movements have affected the area and left a series of unconformities.

Recently Rholich (1974, 1978, 1980) has studied the tectonic development of Jabal Al- Akhdar. The oldest outcropping formations Qaser Al Ahrar and Al Baniyah (Fig. 1.7) are U.Cretaceous and are exposed on the western margin of the uplift. They were deposited in a shallow neritic to bathyal environment and the sequences are composed mainly of carbonates and marls.

The first tectonic processes in Jabal Al-Akhdar occurred in the Santonian and produced a gentle anticlinorium which emerged as an elongated ridge trending ENE-WSW. This structure has three sets of high angle faults striking NE-SW, E-W, NW-SE. At the western limit of Jabal Al-Akhdar, variations in thickness of the Al Baniyah Formation (late Cenomanian- Coniacian) suggests intensive erosion of this ridge, while on the northern coastal margin sedimentation was uninterrupted and a bathyal facies sediments were deposited (Barr and Hammuda, 1971).

		JABAL AL AKHDAR	COASTAL REGION
MIOCENE	U		
	M	AR RAJMAH FM	
	L	AL FAIDIYAH FM	
OLIGOCENE	U	AL ABRAQ FM	
	L	AL BAYDA FM	
EOCENE	U	DARNAH FM	APOLLONIA FORMATION
	M		
	L		
PALEOCENE	U	AI UWALIH FORMATION	
	M		
	L		
UPPER CRETACEOUS	MASST.	WADI DUKHAN FM	AL ATHRUN FM
	CAMP.	AL MAJAHIR FM	
	SANT.		
	CONIAC.		AL HILAL FM
	TURON.	AL BANIYAH FM	
	CENOM.	OASER AL ABID FM	

Fig. 1.7, Stratigraphic succession in Jabal AL Akhdar (after Rohlich, 1978).

A transgression of shallow neritic seas which started in the Campanian covered the whole Cyrenaica region. A continuous succession was deposited up to and including the Paleocene. Another tectonic pulse is thought to have occurred in the early Eocene (Ypresian). This developed a mild folding in the axial part of the embryonic chain but produced another extensive flat topped anticlinal structure diagonal to the existing fold axis (Megerisi and Mamgain, 1980). This new axis trending WNW-ESE, overlaps with the main fold axis in the southern part of the area where upper Cretaceous chinks are overlain by the Oligocene Al-Abraq Formation. Rholich (1978) termed this elongated ridge the Mekhili uplift. The major part of it remained emergent until the late Oligocene. Barr (1978) recognized the same orogenic phase in the coastal region of Jabal Al Akhdar, beginning in the late Cretaceous and terminating in the early Eocene, which he termed the Cyrenaican orogeny.

The Paleocene has been documented in only two localities in the Jabal Al-Akhdar. The general absence of Paleocene rocks is thought to have been related to this "Cyrenaican orogeny" which is believed to have promoted suberial erosion after early Ypresian emergence. The Cyrenaican orogeny evidently began in the late Cretaceous and reached its maximum intensity in the early Tertiary, bringing the Paleocene to a close (Barr and Berggren, 1980).

The "Cyrenaican orogeny" was also responsible for the emergence of large areas in northeastern Libya and northwestern Egypt, up

nearly to latitude 28°. Islands and ridges developed, during the Cretaceous some of them remaining emergent until the late Oligocene and Miocene. The evidence for this found in Egypt, where lower Eocene rocks rest directly on the Senonian. The next tectonic phase in the jabal Al-Akhdar region was Late Ypresian-Middle Miocene and was marked by a mild warping producing fluctuations of sea level.

This sea level oscillation resulted in the deposition of five independent sedimentary cycles of which the last two were the most extensive. These sedimentary cycles, were in order of Formation (Fig. 1.7), the Apollonia and Darnah Formation, the Al Bayda Formation, the Al braq Formation, the Al Faidiyah Formation and the Ar Rajmah Formation (Rohlich, 1974). Thus, the upper Cretaceous seas which had covered the whole of the northern part of Libya were terminated by the end of the middle Miocene by the discontinuous pulsing of mildly transgressive and regressive phases.

During the slowing of the orogenic movements which affect Cyrenaica during the Tertiary, an early Eocene transgression started which covered the entire Cyrenaica region and continued to advance southward. By the Lutetian the present coastal area was covered by an outer neritic sea depositing on open sea facies the Apollonia Formation, while the shallower water of the Darnah formation was being deposited further south.

Further diastrophic movement defined in the relation between the Eocene and the overlying Tertiary deposits. The earliest of these coincided roughly with the Eocene/Oligocene boundary. At the beginning of this stage the sea probably withdrew from the whole Jabal Al Akhdar area for a short time. The new inundation came from the north during the Early Oligocene and covered an area different from that of the preceding cycle (Rholich, 1978). It was responsible for the deposition of the Al-Bayda formation

After the Early Oligocene Cycle of sedimentation some changes in the depositional area occurred. The next cycle is represented by the Al-Abraq Formation (Middle to Upper Oligocene), the distribution of this unit in the Jabal Al Akhdar emerged a new palaeotopographic features.

A further regression of the sea from Jabal Al Akhdar occurred in the Late Oligocene and is documented by the disconformable contact between the Al-Abraq and Al-Faidiyah Formations. The emergence which produced the sediment for the Al-Faidiyah Formation lasted from the late Oligocene to the early Miocene and covered most of the Jabal Al Akhdar region.

During the Middle Miocene the Jabal Al Akhdar witnessed the Last Tertiary transgression which deposited a shallow marine sediment known as the Ar-Rajmah Formation. At this time shallow marine

sediment covered the western and southern borders of Jabal Al Akhdar, while the central and eastern parts seems to have remained suberially exposed (Rholich, 1978).

The final uparching of Jabal Al Akhdar took place in the Middle Miocene and developed the present configuration, The Late Miocene was a period of emergence throughout the Mediterranean region (Barr and Walker, 1973), and no marine Pliocene deposits have been documented.

CHAPTER TWO
LITHOFACIES AND ENVIRONMENT
OF DEPOSITION

In order to assess a complete depositional model for the study area for the Najah, Apollonia and Darnah Formations. A detailed study has been made of more than 50 meters of cores from five wells considerable distances apart. More than 160 thin-sections have been described.

2.1 Methods and techniques

2.1.1 *Microscopy*

Samples were chosen for thin-section preparation from the detailed examination of the cores. Some rocks were impregnated with blue dyed epoxy before sectioning, a technique which facilitates the petrographic recognition of porosity, particularly microporosity, in thin-sections. All thin sections were partly stained with Alizarin Red-s following the method described by Friedman (1959) and Dickson (1966). This is a diagnostic stain which differentiates calcite from other minerals, especially dolomite. Conventional petrography and cathodoluminescence

(CL) were applied. The CL was generated using a Technosyn 8200 Mk II with autohold, typically run at 15 - 20kv and 200- 250 μ A. Subsequently fragments from some samples were coated using gold palladium and then examined in detail by means of the scanning electron microscope (SEM). This has proved valuable especially for the fine grained matrix and its components and microporosity. The SEM was a Cambridge Instruments S360 with integrated Link analytical system AN10,000 series. The energy dispersive X-rays (EDX) available on the SEM has been used to provide qualitative analysis.

2.1.2 X-Ray Diffraction

Samples were selected with special care to their position in the stratigraphic column. Particularly in places where there were close similarities in the lithology type or where there was obscurity in lithology identification. X-ray diffraction was used in order to differentiate between calcite and dolomite and also for semi-quantitative analysis in order to reveal the amount of calcite, dolomite, anhydrite and some other minor components in the chosen samples. (Appendix D).

The samples were prepared for the analysis by grinding small pieces from the whole rock for a few minutes. The powder (5-10 μ m) was then mixed with acetone to form a paste which was spread on one half of a petrographic glass slide. These slides were later analysed by a Phillips P W 1450/20 highly stabilized X-ray Diffractometer using Iron filtered cobalt K-alpha radiation. The generator setting was 20mA and 36kv and the

goniometer speed $2^\circ/\text{min}$. The intensities for the 3.03\AA calcite line, and the 2.88\AA dolomite line were measured at 34.31° and at 36.14° 2θ , respectively.

For semi-quantitative analysis, the samples were analysed by X-ray diffraction, again using $\text{Co K}\alpha$ radiation. A diffractogram was obtained for each sample over the range 4° - 50° 2θ . This gives a qualitative analysis for the minerals present above a threshold of 1-2%. A rough assessment of the concentration of each mineral present can be made by comparison of peak heights against peaks of pure mineral standards. It was subsequently decided to make new standards containing average concentrations of dolomite, calcite, quartz and anhydrite. Five standard mixtures plus pure calcite and dolomite were carefully weighed out and thoroughly mixed. Three separate samples were made from each standard mixture, and then all the standard samples were analysed on the diffractogram over the range 28° - 38° 2θ at 1° $2\theta/\text{min}$. using the same power setting. This range included the main peaks of the minerals under examination. Each main peak was measured in units of 2.5 millimetre and three samples of each standard were averaged to give one result

A calibration graph was drawn for each dolomite, calcite, quartz and anhydrite standard giving peak height in units against known concentration. The samples were analysed under the same conditions as the standards and the peaks obtained are measured against the standard calibration graphs. (Appendix D).

By using the above techniques the rocks of the study area have been classified into a number of distinctive lithofacies.

2.2 Lithofacies descriptions

The study of the cored intervals revealed seven separate lithofacies within the Najah, Apollonia and Darnah Formations, However, little is known about the detailed geometry of these facies and this would be very useful in more precise environmental interpretation. Lithofacies include (1) Lithoclast bearing mudstone, (2) Chalky mudstones, (3) Pelletal packstones, (4) Large Nummulites packstones, (5) small Nummulites wackestones, (6) Coarse crystalline dolomites and (7) Fine crystalline dolomites. The characteristics innate to each lithofacies are summarized in Table 2.1 and (Appendix E-1).

2.2.1 *Lithoclast bearing mudstone, F1*

The Paleocene sediments in the A1-41 and B2-41 boreholes are dominated by lithoclasts of millimetre size which are generally closely packed and surrounded by dark gray mud (Plate 2.1, A-C). The lithoclasts, which are predominantly grainstones and foram-bearing mudstones, contain both shallow and deep water fossils. These allochems are characterized by an abundance of planktonic forams such as *Globigerina* and the presence of calcareous algae, sponge spicules, rare agglutinated forams and abundant echinoderm fragments. Clay and silt size siliciclastic grains are common in the matrix, some K. feldspar also has been found.

LEGEND		LITHOFACIES																				
		F1			F2			F3			F4			F5			F6			F7		
		A	C	R	A	C	R	A	C	R	A	C	R	A	C	R	A	C	R	A	C	R
ALLOCHEMS	Lithoclasts	■	■	■																		
	Globigerinid	■	■	■																		
	Nummulites				■	■	■															
	Milioids				■	■	■															
	Fusulinids				■	■	■															
	Echinoid frag.		■	■																		
	Mollusca frag.		■	■																		
	Gastropoda		■	■																		
	Peloids				■	■	■															
	Algae				■	■	■															
	Coccolith				■	■	■															
	Micrite		■	■																		
	Sparite		■	■																		
	Arg. material		■	■																		
Quartz silt		■	■																			
Colour		light brown		pale cream		brown		gray		light gray		tan gray		dark gray								
Other features		laminated hemipelagic		laminated bioturbated				stylolitic compacted		stylolitic pyritic		stylolitic		brecciated								
TERRIG MAT.																						
ORTHO-CHEMS																						

Table 2.1, Summary of the characteristics innate to each lithofacies

Some of these bear authigenic overgrowths (Plate 2.2, C, D). Fractures are rare. Some contain partial fillings of calcite but remain open. Of more interest, however are a number filled by sediments (Plate 2.2, A, B). These may indicate synsedimentary fracturing and continuing lack of stability in the deposit. The lithoclasts which contain a shallow water fauna indicate a substantial distance of transport. These sediments are interpreted as debris flow deposits and it is proposed to discuss the general nature of such deposits before arguing the case for this area.

The name debris flows is commonly used to describe both a flow process and a deposit. Debris Flows are considered to be one of the major processes of transport of sediment of allochthonous origin. They are defined as a gravity transport mechanism entirely under subaqueous conditions and may be a significant agent of high density mass transport (Mountjoy *et al.* , 1972). The mechanism of support of granular solids in the flow is provided mainly by the strength of the debris. That means, that the matrix has strength and buoyancy to support grains and serves to lubricate grain irregularities.

Debris flows have the ability to move at speeds reaching several meters per second. In most cases the flow is laminar rather than turbulent but within-fluid mixing of large flows may be turbulent. The strength of debris flows depends upon the matrix property of cohesion and upon the granular friction caused by particle interlocking, in addition to the resistance to shear caused by the matrix "viscosity" (Johnson, 1970).

Deposition from debris flows occurs by "freezing", accompanied by partial preservation of the fluid phase as matrix mud. Hence, the presence of mud is a critical factor in documenting debris flows (Enos, 1977, p.140). The exact mechanism by which these sediments are transported is not clear. It has been suggested that debris flows depend on the critical thickness of the flow as well as slope angle, and that flows are capable of travel on slopes as low as 0.5° for distances of several hundred kilometres, either continuously or intermittently (Hampton, 1972).

Occasionally, where such resedimented deposits lack a muddy matrix, the transport mechanism is thought to have been a combination of debris flow and grain flow (Middleton & Hampton, 1973). However, grain flow is characterised by grain to grain collision and no friction reduction occurs in such flows. Hence, they occur only on steep slopes with angles that exceed 18° and so are probably a very localised process in deep sea environments.

The geometry of carbonate debris flow deposits typically corresponds to an extended lense like form rather than a channel, although these do occur. Channel filling may occur within the depositional area and may also represent a prephase of turbidite sedimentation, as more and more ambient fluid is mixed into the flowing slurry. Finally, debris flows may occupy channels cut by other processes but can not cut channels themselves (Leeder, 1982).

It has been shown experimentally (Hampton, 1972), that subaqueous debris flow fronts are unstable and may give rise to superimposed turbidity currents. Mixing at the front of the debris flow is suggested as being a major mechanism for generating turbidity currents in the ocean. This mechanism is favoured because it requires no special condition in order to operate, it is a natural consequence of debris moving through water.

Debris flows probably give rise to turbidity flows as more and more ambient fluid is mixed in with the flowing slurry. Normal turbidity flows originate from gravity driven dilute mixtures of granular solids and water and are widely considered to be an important transporting agent for oceanic sediment. Turbidites may be deposited in proximal as well as in distal positions, depending on the source area, which is generally a shallow shelf area or upper slope region.

Turbidity successions vary greatly in their textural features. Variation is controlled by the distance between the source of the material and the depositional area, by the paleoslope, by the amount and composition of the sediment available, the topography of the depositional area and by the density of the turbidity current (high density or low density suspension). The vertical sequence of turbidite facies is controlled by decreasing current intensity during the deposition of the turbidite sequence. The complete sequence described by Bouma can be observed in only a small percentage of all turbidites, and is generally less complete in

the down current direction (Hampton, 1972).

In the study area the sediments of the Agdabia trough and interpreted as debris flows were deposited during the Paleocene and represent the most interesting part of the slope succession and consequently the area. In well A1-41 the debris flow or flows are sandwiched by hemipelagic muds while in well B2-41 they are intercalated with chalk deposits. In J1-41 the whole Paleocene is represented by debris flow deposits, although the texture has been almost obliterated by dolomitization (Plate 2.1, D). The significance of this distribution will be discussed below.

The allochthonous origin of these deposits is indicated by their stratigraphic position within the basin environment, their texture and their wide variety of clast types containing intermixed, bank and basin microfossils surrounded by a lime mud matrix. Clasts have a wide variation in size and shape and show poor sorting. They can be divided into two types, according to their origin, those originating high up the slope in shallow water, and those from lower down the slope. The shallow water clasts generally are light coloured and are prominent against basin sediments. They are of a range of lithologies, sizes and shapes. Clasts thought to have originated on the slope are lime mudstones of slope facies, and these are generally of uniform size and shape.

The lithoclasts signify substantial disintegration of the platform margin and slope, leading to the nearly instantaneous erosion and deposition of thick accumulations of debris. The slope instability which led to the generation of such large mass movement may have resulted from sediment loading (Crevello & Schlager, 1980; Mullins et al. ,1984) and/or tectonic steepening and seismicity (Cook et al., 1972; Mutti et al. , 1984). The fact that these blocks have a different chemical signature (luminescence) from the matrix supports the view that there was erosion of a lithified mass rather than simply collapse of unconsolidated sediment.

Two sorts of fabric have been distinguished in the cores studied, clast supported and mud supported. While the latter is the most common, the matrix supported fabric with floating clasts occurs locally in the lower part of the succession and suggests proximal debris flow deposits (compare Mullins & Cook, 1986). The large size of lithoclasts in A1-41 suggests proximity to a steep slope. The polymict nature of the clasts reflects the complexity of the source area which might indicate either a diversity of lithified environments or sampling of a varied stratigraphy to some depth.

Lithoclasts which float in a muddy matrix represent an unsupported framework. Such a framework develops when debris flows with high density, high viscosity and strength, freeze in place. An unsupported framework rules out any suspension settling of particles. Lithoclast sizes ranges from the finest particles to several millimetres.

Clasts show differing degrees of rounding and have a random distribution, but are often densely packed and show very poor to poor sorting.

Even where sediments are matrix-supported, the interfragmental space is not an open framework filled with sparry calcite and/or light coloured mud, as is common in shoal water breccias and some reef margin facies. Rather, the interfragmental space is filled with dark lime mudrock with intermixed bank and basin microfossils and with mud to grain supported texture. The shallow water origin of fossils and rock clasts is easily inferred; the pervasive lime mud matrix probably represents loose sediment from the slope and basinal environments.

However, the input of displaced carbonate sediment to the basin should decrease with increasing distance from the source. The coarse textured allochthonous deposits in well A1-41 have a wide variety of light coloured lithoclasts which offer a striking contrast to the enclosing dark gray muds of the basin facies. Since the data available are entirely from the subsurface, it is impossible to determine whether flows were deposited in sheet like or channel form.

In the studied area there is thought to be a minor contribution to the sequence from turbidites, poorly sorted, thinly laminated beds representing the uppermost parts of Bouma sequences. These, however, seem to be volumetrically unimportant.

The debris flows show a diversity in grain size and in grain lithology. Some lithoclasts are foram grainstones (Plate, 2.1, C) and others pelletal mudstones. These grains have to be derived either from different places or from different parts of a stratigraphic sequence. In addition the grains had different diagenetic histories which means that they also had different burial histories (Plate 2.1, B). Some muddy lithoclasts might have been lithified on the sea floor and thus be both younger and more locally derived.

The hemipelagic sediments in well A1-41 are dark mudstones with a massive homogeneous appearance in core. They are occasionally laminated but show no evidence of current control during deposition or vertical sequences of facies. The hemipelagic sediments are characterized by their dark colour and abundance of terrigenous mud. They have a small variable amount of microfossil fragments, typically *Globigerina*, and a shallow water biota which was presumably incorporated during transport of the debris flows. The dark brown colour of the hemipelagic sediments suggests deposition in an enclosed or deep water environment with limited water circulation. There are no indications of bioturbation whatsoever and this suggests that the water was not well oxygenated enough for a fauna to flourish. In other words, the bottom conditions during the deposition of these sediments remained anoxic. The presence of scattered phosphate fragments reflects high fertility and oxygen poor bottom waters because phosphate genesis is favoured by such conditions. However, these are probably derived from an environment higher on the slope.

These allochthonous facies, have been recognized in wells A1-41 and B2-41, which are thus more proximal, and are absent in C1-41 and D1-41. They were deposited during the Paleocene and show a gradual upward decrease in the numbers of lithoclasts, indicating that the activity of the source was declining. They occur in the transitional area between the platform and the more distal parts of the basin, and are anomalous deposits enclosed in the usual mudrock of the basin facies. Although the phenomenon responsible for the transport and deposition of the debris flows was repeated during the Paleocene (especially in well A1-41), and the deposits represent a fair proportion of the succession the debris flow sediments form a quantitatively small proportion of the total time of the basinal filling. The relative contribution of shallow and deep water bioclasts reflects the distance from the platform and the intensity of the transport process.

The essentially heterogenous texture and fabric of the debris flow deposits implies a type of flow that involved extensive mixing of the source material during transport. The overall character of most clasts suggest that they formed by breaking-up of earlier deposits, partially or thoroughly lithified materials of the platform margin. The internal motion of the clasts in the debris flows during transport was probably not turbulent. This is suggested by the general absence of grading throughout nearly the whole thickness of the sequence. The unsorted matrix, unsupported framework and chaotically oriented clasts strongly support the interpretation that at any point along the debris flow sediment body, deposition took place essentially as a mixed mass rather than as a gradual

upward accumulation.

The triggering mechanism for transport and allochthonous deposition of these flows is thought to have been gravitational instability and/or seismic shocks caused by small movements along faults. The collapse of the Agdabia trough commenced in the Upper Cretaceous by means of step faulting. The effect of tectonism may have enhanced slope instability, first by the downbowing and oversteepening of the slope, and second by active faulting which may have developed fault scarps or created zones of weakness along which slope failures could occur.

The tectonic significance of these deposits is of special interest as they were apparently formed at a time when the basin was experiencing a high rate of tectonic subsidence. The interbedding of the debris flow deposits and hemipelagic deposits implies multiple episodes. As a speculation these episodic debris flows probably corresponded with tectonic pulses associated with basin subsidence.

The economic significance of debris flows is that they indicate proximity to the margin of an adjacent carbonate shelf. They may assist in determining the time of cementation and dolomitization, and may also help in correlation and better interpretation of the genesis of carbonate facies. Such poorly sorted deposits generally have low porosity but selective dissolution may generate valuable porosity capable of being

occupied by hydrocarbons. Unfortunately there is no evidence that such dissolution has occurred in the area examined.

2.2.2 Chalky mudstone, F2

The chalk in the studied area is typically a pure calcitic, fine grained, pelagic limestone that is weakly cemented. It is a *Globigerina* bearing nannofossil limestone with occasional larger allochems (Plate 2.3, A, B). The *Globigerina* sediment may have been deposited in a relatively deep water environment. In other areas chalk results almost entirely from a submarine "rain of faecal pellets" of plankton feeders because coccolith debris would never reach the sea floor by settlement alone (Bromley, 1979).

The SEM has been used to investigate the microfabric of chalks in the Paleocene and lower part of the early Eocene in the Agdabia trough. The matrix consists of coccolith remains (Plate 2.3, D), occurring either as whole coccospheres, which have a spherical calcareous exoskeleton with a diameter ranging between 12 to 30 μm , or as separated coccolith plates, each plate consisting of a tablet-shaped crystal of low Mg calcite ranging between 0.5 to 1 μm in diameter. A variable amount of relatively coarse carbonate debris such as echinoderm plates and a few other minor constituents is also present.

Partially disaggregated thoracosphaerids are common in the sequence, with large numbers of complete tests. Mapstone (1975) defined thoracosphaerids as unicellular calcareous marine nannoplankton algae. Their tests can be a single layered hollow ball, a flask or bell shaped structure. The test is perforated and in addition may also contain an aperture. Most of the thoracosphaerids (Plate 2.4, A, B) in the sequence are spherical and range from 18 to 22 μ m in diameter . The paleontological charts of Bramlette & Martini (1964), and Hay & Mohler (1967) show that thoracosphaerids were very abundant in Danian time.

Detailed petrographic study has suggested that two chalk facies are present, an argillaceous chalk and a non argillaceous chalk. The non argillaceous chalk is a white to pale cream, friable to moderately hard lime mudstone. It appears to be free from dispersed argillaceous materials. The argillaceous chalk consist of grayish, moderately consolidated, finely laminated lime mudstone. The recent work of Matter (1974), Schlanger & Douglas (1974), Hancock and Scholle (1975) and others has shown that all nannofossil deposits undergo progressive lithification as a function of depth of burial and other factors. Thus any distinction between soft, intermediate, and hard deposits is completely arbitrary and of no major significance (Scholle,1977).

Within this lithofacies dolomite is observed as widely scattered isolated rhombs floating in the chalk matrix without any preferred orientation. However, minor aggregates of more than one crystal are

sometimes present (Plate 2.4, C,D) and interlocking crystals are occasionally found in close association with stylolites. The diameter of individual crystals ranges from 25 to 40 μ m.

No visible intergranular porosity has been observed in the chalk sequence of the studied area under the petrographic microscope. Under the SEM, however, intergranular and Intragranular porosity are visible (Plate 3.4, A, B) although in some places not clear. In general, in most parts of the sequence the chalk facies has an excellent porosity, and this applies to the investigated core samples mostly as moldic porosity. Scholle(1977) explained the retention of porosity in some settings as governed by the scarcity of chemically unstable components such as aragonite or high magnesium calcite. Neugebauer (1974) suggested that, it is the magnesium content of the pore fluid of which inhibits dissolution but overpressuring may also be responsible. Adelseck *et al* (1973) showed that the pressure solution lithifies chalk at shallower depth when the magnesium content of the pore fluid is exhausted. The chalk lithofacies in the studied core samples are characterized by fair to excellent porosity which is thought to be due to the less pervasive cementation, and it's likely that this is due to the amount of magnesium in the pore fluid rather than overpressuring.

conditions of deposition : a-salinity : It has been well documented that most of the chalks in Europe were deposited in waters of normal marine salinity. This is shown by the widespread occurrence of fossils of groups such as echinoderms that cannot flourish in lower salinities. In contrast,

in the chalk of the central United States there is a curious absence of a variety of Porifera, Brachiopoda and echinoderms (Hattin & Cobban, 1965) which may indicate either marginally lower salinity or a periodic influx of fresh water. Chalks are present in a wide variety of environments largely because coccoliths as a group have a wide salinity tolerance (Bukry, 1974). The chalk present in the studied area is similar to the European chalks in its constituents and therefore the salinity parameters are also expected to have been similar.

b-depth of water: There is controversy between two extreme interpretations of the depth of water in which the European Chalk was deposited. The first is the assumption that the Chalk was deposited in water several thousand meters deep and hence is a deep sea ooze. As Reid (1973), Jenkyns & Hsu (1974) and Hakansson *et al.* (1974) have indicated, such interpretations have failed to distinguish between a pelagic organism and a deep sea sediment.

The second assumption is based on the superficial similarity between Chalk and aragonite muds which are deposited in shoals not more than 6-9 m deep in the Bahamas. This led to the idea that the Chalk was a very shallow precipitate. However this comparison was shown by Black (1953) to be untenable.

As indicated, the chalks of the Agdabia trough are rich in coccoliths. Coccoliths are pelagic organisms which have an extremely wide environmental and latitudinal distribution (McIntyre *et al.*, 1967). The minimum depth for coccoliths to be produced in abundance around the British isles today is 10-20m. In the tropics the maximum concentration is at about 50 m (Black, 1965). In the Indian Ocean, the maximum of pigmented coccolithophorids is found at 200 m (Provasoli, 1963). Moreover, for coccoliths and their laths to settle, the bottom must have been below normal wave base (Reid, 1973) which probably means deeper than 20 m (Sverdrup, Johnson & Fleming, 1942,529). This is not to say that bottom currents were negligible.

In Europe White Chalk facies grade off present land areas into probably deeper water chalks in fault bounded troughs in the central North sea (Hancock & Scholle, 1975), and in the open oceans, Cretaceous chalks has been found down to depths now of nearly 4000m in the Central Pacific (Schlanger & Douglas, 1974). The good preservation of the calcitic coccolith material (Hancock and Kennedy, 1967, Scholle, 1974) provides evidence of maximum depths because coccoliths composed of low Mg calcite, consider to be the stablest polymorph of CaCO_3 . Roth and Berger (1975) suggested etching is common below 1500m, while Honjo (1975) found etched coccoliths between 600-1000m in depth, but the majority were complete and intact (Hancock, 1975).

Many discussions about water depth of the Cretaceous chalk have ignored the evidence of facies above, below and alongside it. According to Walther's law of facies, the interpretation of the Chalk facies should be compatible with them . In the Paleocene and Early Eocene of the investigated area, deposition took place in a relatively deep water environment.

C-rate of deposition: Rate of deposition calculations depend on the length of time over which the measurement is made. That means that the longer the time of deposition the thicker the sequence which will have accumulated . In addition, sediments rich in chinks are typically present in areas that have low rates of clastic terrigenous input, that do not overwhelm the microfossil and nannofossil production. The accumulation rate of chinks is controlled by the production of the constituent organisms. Moreover, because of compaction after deposition, most figures are really thicknesses of compacted chalk that represent a stated time.

In the Agdabia trough during Paleocene time the total rate of deposition was apparently of 83 m/my. This number is tremendously high but in fact the thickness which has been calculated is not the real thickness. It consists of the real thickness plus debris flow sediments which contain resedimented materials from older rocks.

2.2.3 *Peloidal packstones, F3*

This facies is characterized by dark brown packstones, occasionally grainstones and is commonly slightly dolomitic. It is well defined only in well B2-41 in the Najah Formation (Paleocene) which formed before deposition of the debris flow lithofacies. The allochems consist predominantly of foraminifera and peloids (allochems composed of micrite with no genetic sense or size restriction) with abundant echinoderm fragments, rare bivalve and gastropod fragments and a mixture of lithoclasts with different sizes (Plate 2.5, A-D). These were transported from higher up the slope. The forams are dominated by fusulinids, miliolids and rare nummulites.

The peloids are uniform in size and are mostly ovoid in shape. The micrite which they consist of includes very fine grains with clear boundaries. The peloids show a remarkable loose packing and some seem to float in the matrix. The peloids might be micritized skeletal fragments, but are very uniform in shape and cryptocrystalline and their origin remains uncertain. The matrix is generally homogeneous with clotted groups of pellets which may represent burrow fills. It is commonly stylolitic and slightly dolomitized.

The abundance of foraminifera and echinoderms indicates generally open marine conditions. This lithofacies is very similar to the

standard microfacies 2 of Wilson (1975) which he referred to as a Microbioclastic calcisiltite. It contains a mixture of fine bioclasts and peloids in a very fine grainstone to packstone. It was regarded by Wilson (1975) as representing part of the lower slope characterized by water depths reaching few hundred meters, and by generally oxygenated water of normal marine salinity with good current circulation. Waters were deep enough to be below wave base but intermittent storms may have affected the bottom sediment.

2.2.4 Large *Nummulites* packstones, F4

This lithofacies is characterized by gray to dark gray packstones, occasionally grainstones in parts. The allochems are dominated by *Nummulites gizensis* (Forskal) which makes up the bulk of the fossils. Rare fusilinids, echinoderm fragments, rare bryzoa, and peloidal grains, are present (Plate 2.6, A). Replacement by silica chalcedony is also common (Plate 2.7, B). The facies is typically stylolitic and anhydritic (Plate 2.7, A, C). Most of the large Nummulite chambers filled by calcite cement (Plate 2.6, D). It forms the uppermost part of the marine Early Eocene which represents a separate cycle of sedimentation and shows a considerable distribution in the studied area.

In well D1-41 the sequence is interrupted by about 30 cm of sandstone which consists of quartz grains (Plate 3.3, A) ranging from subangular to angular with clear point contacts . There are no other sandstones in the sequence. The odd stratigraphic position of these sediments may be explained in terms of down slope movement of surface deposits, with the sediment contorting and the sand breaking up into isolated pockets. As the sand is not a characteristic facies of the supposed source area it was probably incorporated into the flow by erosion or by an associated failure of the slope sediment.

The accumulation of allochems is composed almost exclusively of *Nummulites gizensis*. These can form non reef buildups or banks (Aigner, 1982). Other benthonic organisms are restricted to burrowing echinoids, gastropod and bivalves, and are relatively sparse in the bank environment.

Nummulites, often associated with other larger Foraminifera, are common in neritic and shelf ramp facies in many parts of the Mediterranean Paleogene (Aigner, 1983). The nummulitic facies which is exposed in Libya and Egypt have been subject to a long debate concerning their environment of deposition and the physical factors responsible for the deposition of *Nummulites gizensis* .

Aigner and Futterer (1978) both found that nummulite bank facies exhibit abundant examples of high energy sedimentary structures, such as erosive pockets and pot holes which are mostly filled with nummulitic grainstones and suggested intense bottom scouring during high energy events like storms. Furthermore, Aigner (1982) found in some units that the *Nummulites gizensis* form imbricated sets oriented obliquely to the bedding planes. Futterer (1982) and Seilacher (1973) both observed that whenever nummulites start to form dense accumulations they develop "contact imbrication". This occurs preferentially towards the shallowing top of the nummulitic bank facies, Nummulites may also show edge-wise imbrication and chaotic stacking, and these might indicate wave influence.

Nummulites may have lived on relatively soft lime muds (Blondeau, 1972). Arni and Lantern (1972) studied the sediment texture and biofabric in nummulitic banks and both are agreed that the winnowing away of a considerable amount of mud and the concentration of the foraminiferal tests has been by physical processes. However, Aigner (1983) found a close correlation between the proportion of small and large nummulites in the reworked sediments and that assumed for the original population. He suggested that reworking must have occurred without large scale lateral transport by in situ winnowing.

According to Blondeau (1972), nummulite development is optimal in well-aerated warm and shallow waters, and such conditions are

likely to have dominated during the deposition of the nummulitic limestone in the studied area. Aigner (1983) added that the shallow waters would have been increasingly subject to hydrodynamic forces such as storms. These therefore seems to have been an interaction of productive development of the nummulitic community accompanied by winnowing, and it is to that the accumulation and growth of the nummulitic sediment body is attributed. Aigner (1983) speculates that the seagrasses (which are not preserved due to their low fossilisation potential) might have contributed to bank growth by trapping sediments.

analogy of Early Eocene sediments on the surface: The Early Eocene sequence outcrops in several areas, notably in the type section of jabal Al Akhdar. In the outcrops the Early Eocene sequence begins with chalk deposits full of coccoliths overlain by nummulitic limestones (packstones). The Apollonia Formation, which corresponds to the chalk, has been described in the literature as a light coloured massive fine grained chalk with chert nodules. Occasionally, the chalk becomes marly and there is a rhythmical alternation of limestones of varying grain size. Sometimes the sediments show graded bedding, probably caused by turbidity currents (Banerjee, 1980).

Gregory (1911) placed the "Apollonia limestone" in the Lower Eocene because of it's stratigraphic position below his Lutetian "Darnah limestone". Stefani (1923) supported this view on the evidence of the presence of *Nummulites globules* and of *Plecanium niloticum*, and placed

it in the Ypresian (Lower Eocene). Rholich (1974, pp.34-35) and Zert (1974, p.14) reported some planktonic deep sea forams from this formation. Macrofossils are few, bivalves being most common. The lithology and the faunal assemblage indicates a deeper marine environment, probably deep neritic to bathyal.

The lower boundary of the Apollonia Formation is exposed only in the marsa al Hilal area where the Formation rests unconformably on the Upper Cretaceous Althrun Formation. The upper boundary is conformable and gradational with the Darnah Formation which correspond to the nummulitic limestone lithofacies. On a regional scale there is interfingering between the upper part of Apollonia and the lower part of the Darnah Formation. This interfingering is explained by submarine transport of sorted organodetrital material to deeper parts of the basin (Banerjee, 1980).

The lower boundary of the Darnah Formation is taken at the first appearance of *Nummulites gizensis* (Forskal) in fine grained limestone. This is followed by a nummulitic limestone with occasional intercalations of dolomite . The lower part of the Darnah Formation consists of Lutetian *Nummulites*: *Nummulites gizensis lyelli* D'Archiac, and *N.cf.globulus* Leym. Hanzlikova (in Klen 1974, p.28) found an assemblage corresponding to the Priabonian base (*Nummulites* ex.gr. *gizensis* Forskal, etc.). Generally the nummulite assemblage indicates an Upper Lutetian to Priabonian age for the Darnah formation. These

sediments show a continual rhythmical shallowing and reflect a shallow neritic to littoral environment with normal marine salinity.

The upper part of the Darnah Formation is characterized by algal to coral limestones with whole nummulites alternating with nummulitic gray limestones. The Darnah Formation terminates the Eocene sedimentary cycle, and is unconformably and transgressively overlain by Oligocene or Miocene sediment elsewhere.

2.2.5 *Small Nummulites wackestone, F5*

This lithofacies is a continuation of the same depositional pattern as the large nummulites packstone. It is represented by light gray mudstones to wackestones. There are fewer large nummulites than in lithofacies F4 and the bulk of the facies is represented by muddy sediments with small *nummulites* (Plate 2.6, B, C) and a few mollusc shells. The sediments are occasionally laminated, and show patchy dolomitization. The chambers in the small *nummulites* are sometimes filled by calcite cement.

The presence of small *nummulites* indicates that this facies maintained approximately similar environmental conditions to those of

F4. Open marine conditions with normal marine salinities predominated. Compared to the lithologies discussed so far, this facies association represents a lower energy environment. Only the depth of the water had changed and this had a direct relationship to the hydraulic energy levels. In F5 the water became deeper and the energy level less than in F4. This might be related either to fluctuation in sea level or to tectonics or both.

Aigner (1983) found that in this facies there was less disturbance by physical processes than in the nummulitic bank. High energy episodes are indicated by packstone beds consisting mostly of fragmented bioclasts. Aigner (1983) also suggested that nummulitic banks which accumulated on topographic highs were frequently struck by storm events. Such events were less effective in these slightly deeper and protected "back bank" environments.

2.2.6 *Fine crystalline dolomite, F6*

Dolomite forms the predominant lithology in wells C1-41, D1-41 and J1-41 in the Paleocene and parts of the Early Eocene. It is generally replacive but is also present as a cement. The dolomite in the area has been divided according to grain size into two facies, fine and coarsely crystalline. Both are widespread and there is no areal or stratigraphic separation.

The fine crystalline dolomite is characterized by a unimodal, planar-e, dolomite (Sibley and Gregg, 1987) with partly mimetic replacement of allochems (Plate 2.9, A, C, D). Most of the dolomite crystals have a grain size less than 0.01mm. In most cases the original rock was a bioclast wackestone to mudstone, occasionally it was a homogeneous muddy sediment, now a fine grained dolomite with a cloudy appearance. Coarse rhombs lining pores are also common. Interlocking crystals are rare (Plate 2.8,D). Anhydrite is abundant at some levels and usually co-exists with the dolomite. It commonly postdated the dolomite and often acts as a cement filling pores, rarely as a replacement (Plate, 2.9, B). Dissolution seams are also common (Plate 3.2, C).

2.2.7 Coarse crystalline dolomite, F7

The coarse crystalline dolomite is unimodal, Planar-s, dolomite (Sibley and Gregg, 1987), Most coarse dolomite crystals are full of inclusions although crystals with cloudy centre and clear rims are present (Plate 2.8, A, B). Most of the crystals are more than 0.1mm in in diameter. Pyrite is present but is not common (Plate 2.8, C). The original lithology, before the dolomitization, seems to have been a bioclast packstone, or occasionally a grainstone. The allochems show non-mimetic replacement, that means that their form is preserved but not their structure. Dissolution seams are generally common and usually associated with fracturing. There is some

sort of brecciation in the Najah formation which is especially pronounced in well C1-41. Anhydrite is also present, most often as a cement but also as a replacement of dolomite. A few areas of dolomite crystals have a granulated appearance. Dispersed and irregular dolomite grains with sutured boundaries suggest collapse. Generally this type of brecciation might be due to a volume reduction which accompanied dolomitization or to dissolution during diagenesis of evaporites.

2.3 Depositional model

In the uppermost part of the Paleocene, a pattern of deeper water deposition commenced in the Agdabia trough. This continued throughout the Eocene and resulted in association of different lithofacies, the vertical sequence and the lateral distribution of these lithofacies is shown in fig. 2.1, 2.2, (Appendix E). Pelagic sedimentation dominated and is expressed in a variety of planktonic foraminifera, and other pelagic fauna, debris flows, and hemipelagic sediments (Fig. 2.3). These accumulated on a deep basinal floor which was perhaps hundreds of meters below effective wave base, but above the carbonate compensation depth (CCD).

Both slopes and basins are sites of extensive fine grained pelagic and hemipelagic sedimentation. The slope facies is transitional between the rapid and active calcium carbonate production of shallow water and the slow accumulation of fine grained pelagic sediments in the basin. The transition from platform to basin may in places be abrupt, in the form of a steep cliff, but more commonly is a gently inclined slope.

However, one of the most distinctive differences between basin and slope sediments reflects the instability of the slope and base of slope. The disruption and reorientation of the sediment into slides and chaotically deformed masses may be very common on slopes, but the frequency and scale of such features is usually dramatically reduced in

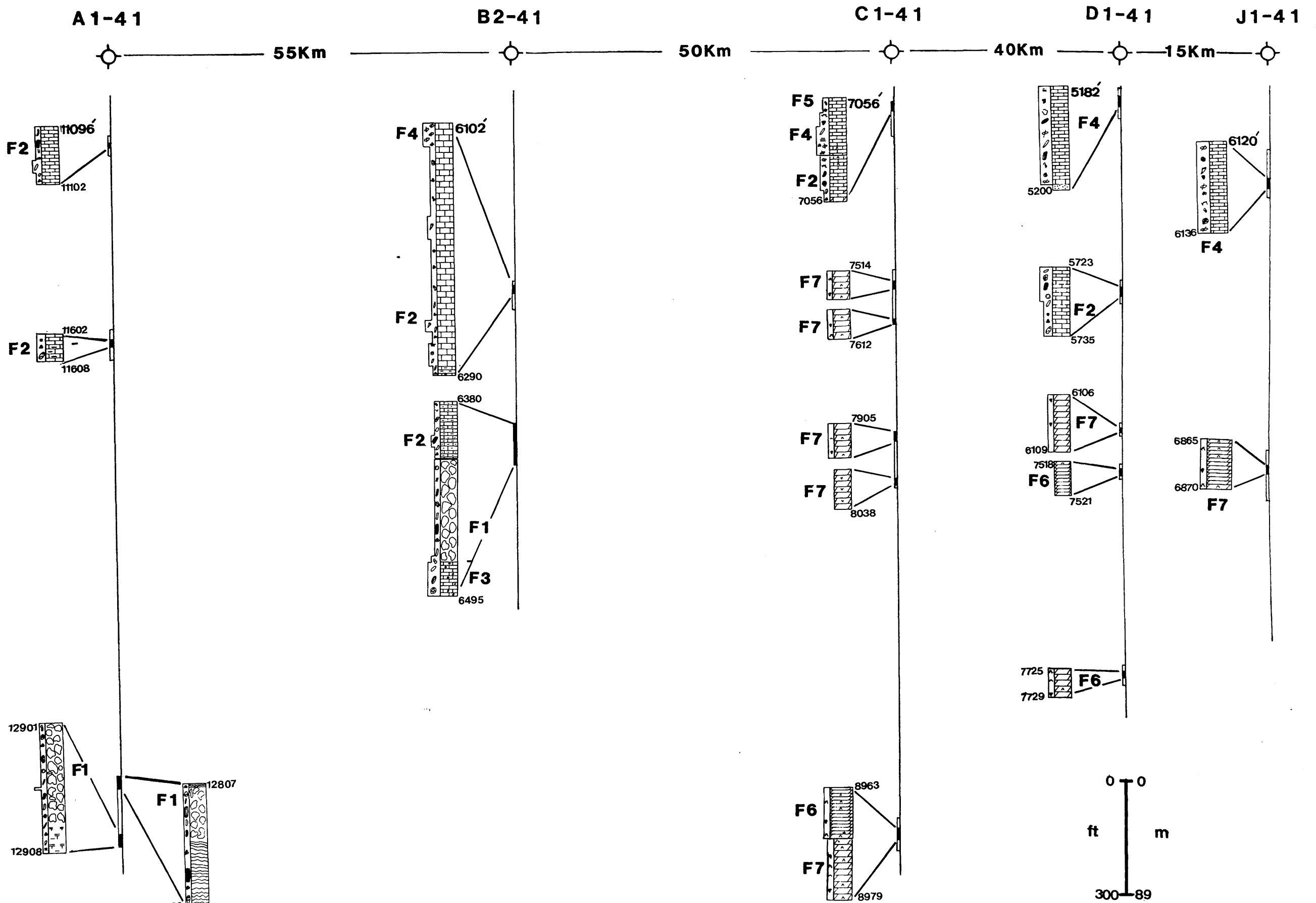
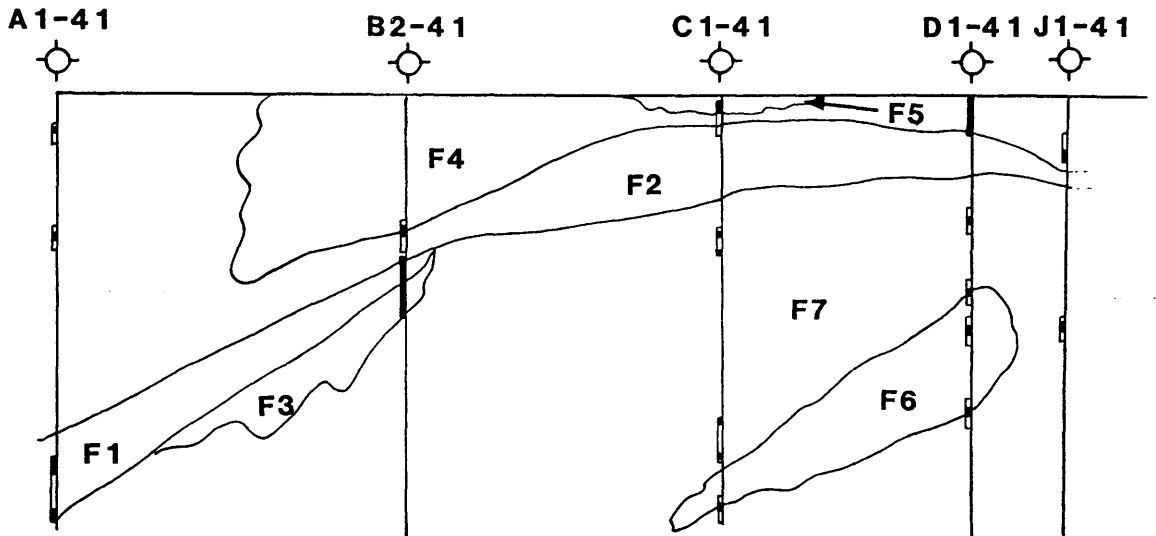


Fig. 2.1, Stratigraphic section of the studied core samples, illustrating the distribution of the different lithofacies as identified from the study of the Paleocene and Early Eocene. (Datum is the top of L. Eocene).

LEGEND

	Limestone
	Dolomite
	Argillaceous carbonate
	Lithoclast bearing mudstone
	Hemipelagic sediments
	Calcium sulphate
	Peloids
	Benthonic Foraminifera
	Fusulinid
	Globigerinid
	Gastropoda
	Nummulite
	Miliolid
	Bryozoa
	Echinoderm Frag.
	Brachipoda Frag.
	Mollusck Frag.
	Bioclasts
	Stylolites
	Lamination
	Collapse breccia



0 50Km

Horizontal Scale

Vertical Scale 1 : 300

LEGEND

- F1 = Lithoclast bearing mudstone
- F2 = Chalky mudstone
- F3 = Pelletal packstone
- F4 = L. Nummulites packstone
- F5 = S. Nummulites wackstone
- F6 = Fine crystalline dolomite
- F7 = Coarse crystalline dolomite


 Cored interval

Fig. 2.2, Schematic diagram, showing the correlation of the different lithofacies in the area. (Datum is the top of L. Eocene).

carbonate basins. Another important difference between slope and basin relates to the texture and geometry of their sediment gravity flow deposits. Slope and base of slope deposits commonly include massive large size lithoclasts, which are interpreted as having been transported by debris flows. Deposits are either sheet like fans or confined to relatively narrow erosional channels. In contrast sediment gravity flow deposits in basinal settings are usually fine textured and can even occur in well organized and fining upwards sequences (Cook & Egbert, 1981)

The slope is generally located above the lower limit of oxygenated water and stretches from above the wave base to below it. The Debris flow deposits which are recognized in wells A1-41 and B2-41 were deposited during the Paleocene. In A1-41 the debris flow deposits are intercalated with hemipelagic basin sediments while in B2-41 they overlie pelletal packstone lithofacies and are themselves overlain by chalk deposits.

Since the debris flows occurred during the Paleocene, and the Agdabia trough is believed to have subsided in the latest part of the Cretaceous. The Cyrenaica platform which lay to the east, adjacent to the Agdabia trough, had been a site of extensive sediment accumulation since the Paleozoic. Probably these massive deposits which have an apparent lack of sedimentary structures were the product of down slope mass movement of lithified carbonate sediments produced at a rapid rate near the platform margin, but it's more likely the source of these sediment from

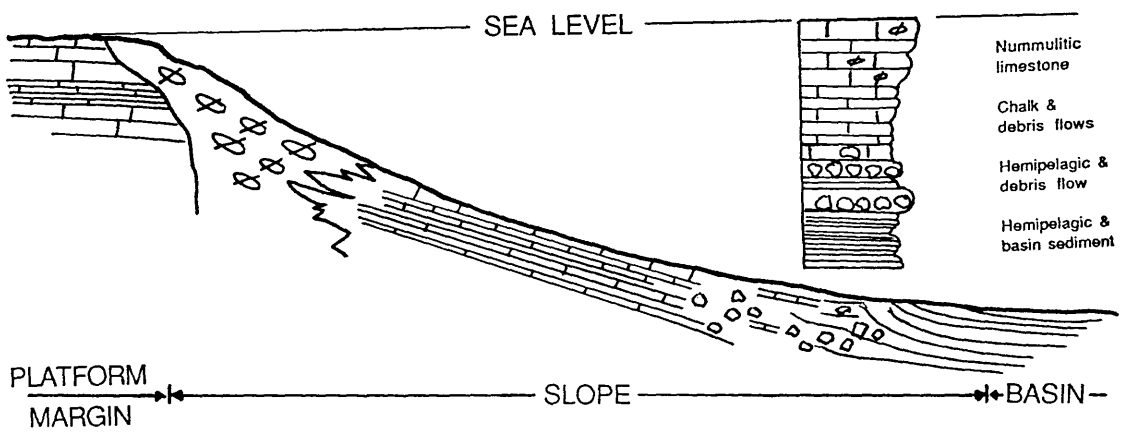


Fig. 2.3, Schematic model for the depositional environment in the studied area.

sampling of diverse lithologies to some depth.

The regional facies pattern of the Eocene sediments is consistent with an open shelf, with the shallow, wave agitated, facies of the near shore zone passing down slope without a marked break, into deeper water with low energy pelagic facies. The widespread distribution of pelagic cherts and occasional cherts in the early Eocene reflects a uniform gentle slope and this period was also characterized by world-wide high sea level (Haq *et al.* , 1987). Local and possibly regional gravitational instabilities provoked mass movement towards the basin. These movements were induced by basinward slopes, and as a result appreciable amounts of the Paleocene section especially in wells A1-41 and B2-41, are allochthonous with large amounts of interbedded "in situ" pelagic sediment (Fig. 2.1).

The appearance of argillaceous limestones at great depth (below 13000 ft = 3800m), accompanied by debris flows and chalk deposits suggests a deep marine environment in the lower part of the section, contrasting with the widespread increase in shallow water forams high up in the section, providing evidence for a gradual upwards shallowing, although these was occasionally interrupted by pelagic deposition at the platform edge in response to changes in sea level.

In the Middle East there were significant changes in the regional depositional environment in the latest early Eocene, with evidence of a

marked eustatic fall in sea level (Haq *et al.* , 1987). The same features have been found elsewhere in Libya (Barr & Berrgren, 1980), where shallow water nummulitic lithofacies were developed, and rapid buildup from deeper and quieter waters into shallower and more turbulent waters resulted eventually in capping by shoal deposits (Wilson, 1975). Generally the upper most part of the Paleocene and the whole of the Eocene represent a continuation of the same depositional style.

Sea level changes may be either local or world wide (eustatic) and affect the sedimentary facies in many different ways. Usually shallow marine sediments reflect transgressions and regressions some of which are the result of eustatic change. Eustatic sea level changes may give rise to major transgressions and regressions affecting the whole system, but are unlikely to produce frequent rapid sea level changes expressed for example as cyclothems. Whatever the causes, sea level changes occur on different time scales and may be global, regional or local. They need to be taken into consideration whenever facies models are constructed. The deposition of the upper slope facies represented by the nummulitic facies may coincide with a global lowering of sea level at the end of the Middle Eocene (EL-Hawat *et al.*, 1986)

Cyclic sedimentation can be explained by many factors whose relative importance varies between different environments. In the Darnah Formation several cycles have been documented in the literature. Tectonic and eustatic sea level changes appear to be the most effective

factors in the repetition of these cycles, and may have been working together or individually. In the investigated cores one complete cycle has been distinguished. The formation is generally rich in fossils and the most abundant are the nummulites.

The small sedimentary cycle in the nummulitic facies, which started at the contact with the underlying chalky mudstone facies, consists of a number of lithologies and is represented first by packstones to grainstones which contain considerable numbers of large nummulites. Often the nummulites form the dominant constituent of the rocks. These grade upwards to a mixture of small and large nummulites (Plate 2.6, D), and then the cycle is terminated by mudstones to wackestones with abundant of small nummulites and echinoderm fragments (Appendix E-2). Occasionally the facies is affected by diagenetic dolomite and anhydrite. Sometimes it is interrupted by small debris flows, represented by sandstone in the case of the well D1-41. El-Hawat *et al.* (1986) studied the exposed part of the Darnah Formation in detail and divided it into five depositional facies. These are: fore bank, bank, reef, shoal, and back bank facies. These are stacked in repeated coarsening upwards and progressively shallowing upwards cycles. He found that bank complexes exhibit large scale massive, trough, and draping structures which he attributed to bank reworking, and accretion, in response to sea level changes.

These cycles represent a progradation of shallow water nummulitic banks, over deep water slope deposits (Apollonia Fm.). The

coarsening upwards cyclicity of the nummulitic facies, suggests a progressive winnowing and removal of small nummulites and fine grained matrix (small nummulites lithofacies) as banks grow upwards close to the wave base (El-Hawat, 1985).

The upward coarsening which might be accompanied by a thickness increase in the shoal to slope transition is considered to reflect a steady fall in sea level, causing the platform to aggrade vertically as well as prograde into increasingly deeper water. Both processes would result in the expansion of the lateral and vertical extent of the shoal to slope transition.

Plate 2.1

A) Photomicrograph of different sizes of lithoclast and bioclast from lithoclast bearing mudstone with dissolution seam (arrow). Bar scale=0.5mm. Well A1-41, depth 12905ft.

B) Photomicrograph of lithoclasts in lithofacies F1 under cathodoluminescent light. The lithoclasts give different luminescence which implies different origins. Note some of the lithoclasts have more than one stage of cementation. Bar scale=0.3mm. Well A1-41, depth 12817ft.

C) General view to lithofacies F1, where the foram grainstone lithoclast (centre) represents one of the different shallow water lithologies which make up the debris flows. Bar scale=0.5mm. Well A1-41, depth 12814ft.

D) Photomicrograph of lithofacies F1 in well J1-41. Showing that most of the lithoclasts have been obliterated by dolomitization. Bar scale=0.5mm. Well B2-41, depth 6868ft.

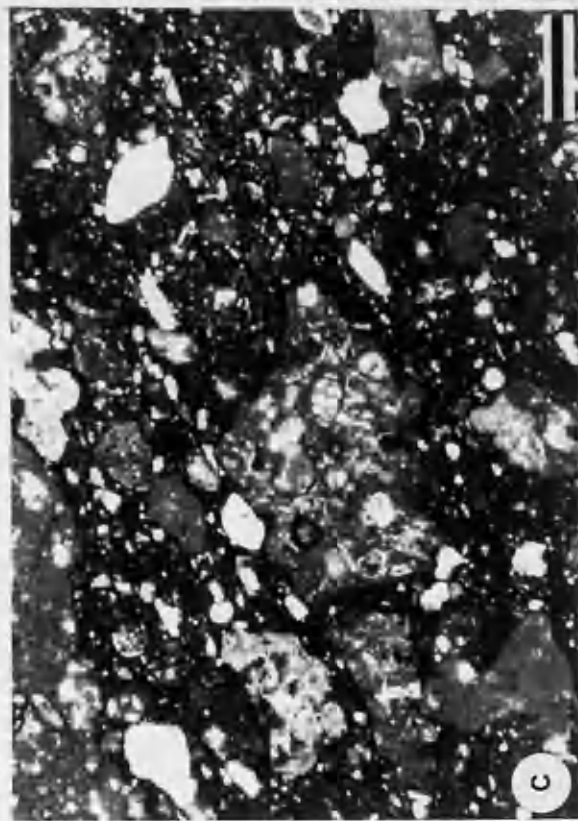
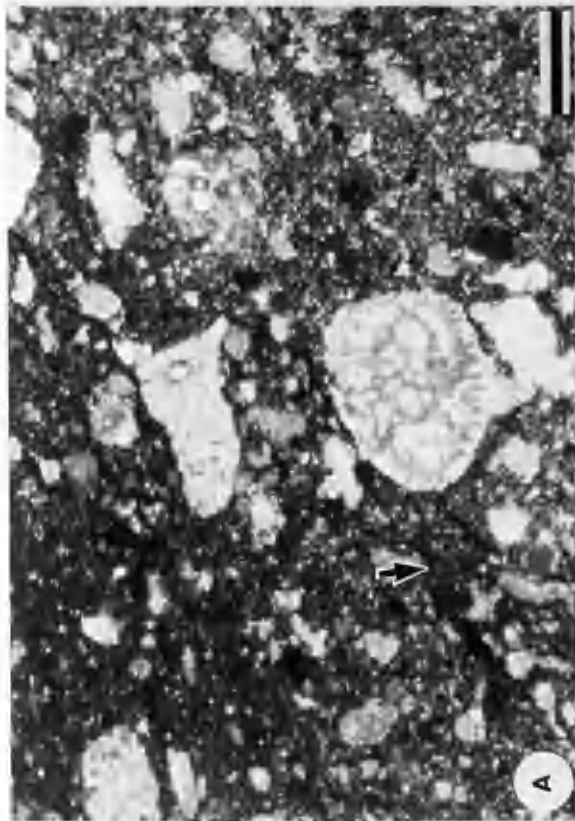
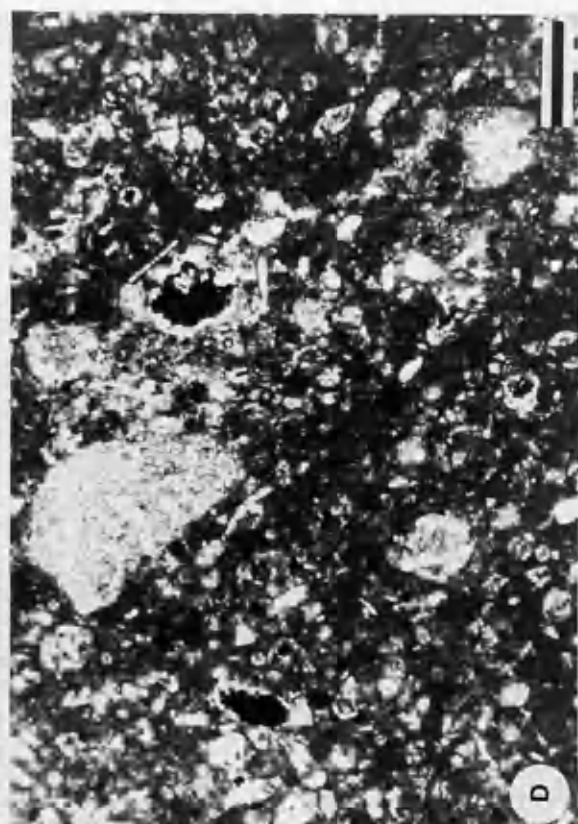
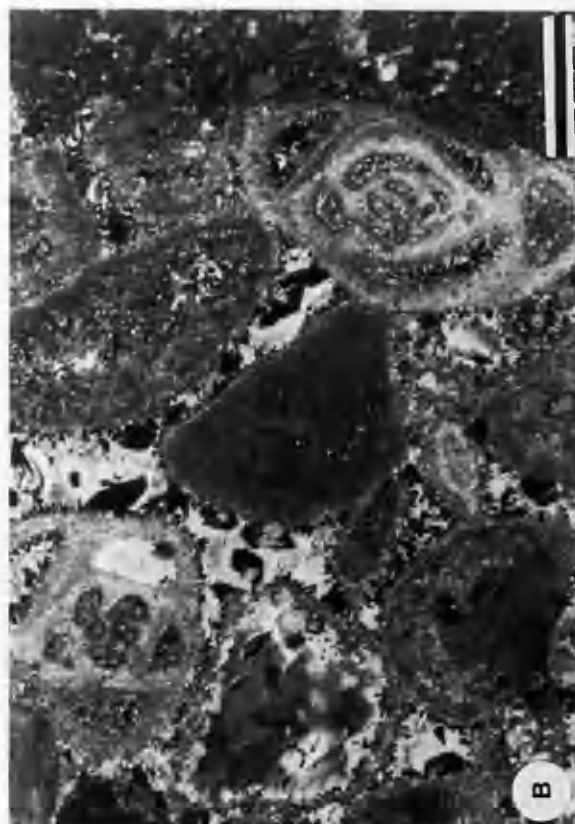


Plate 2.2

A) Photomicrograph of late fracture (arrow) in lithofacies F1, filled with calcite. Bar scale=0.5mm. Well A1-41, depth 12817ft.

B) Photomicrograph of internal sediment filling fracture (arrow) in lithofacies F1. Bar scale=0.5mm. Well A1-41, depth 12817ft.

C,D) SEM examination of K-feldspar in lithofacies F1. C) Authigenic K-feldspar crystal. D) EDX spectrum of the same crystal as (C) showing composition. Bar scale=10 μ m.

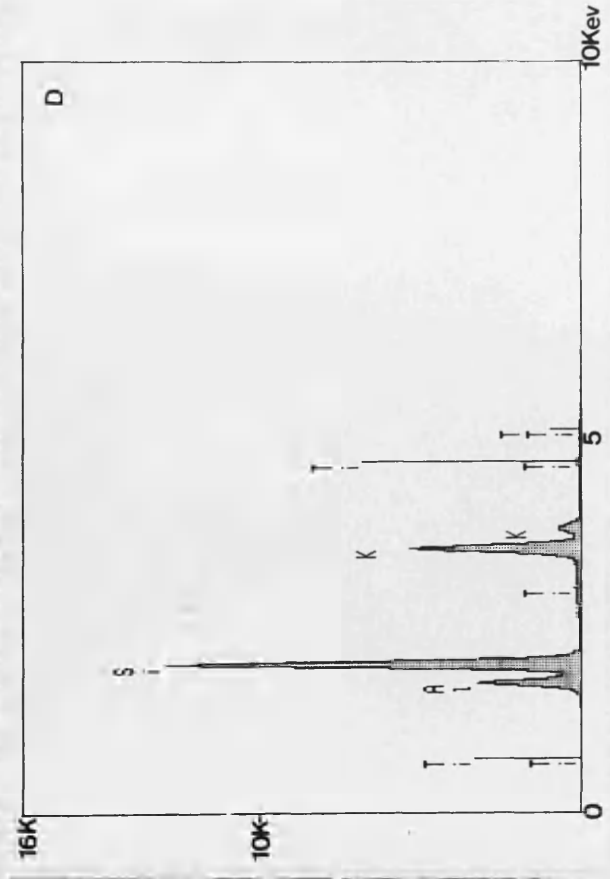
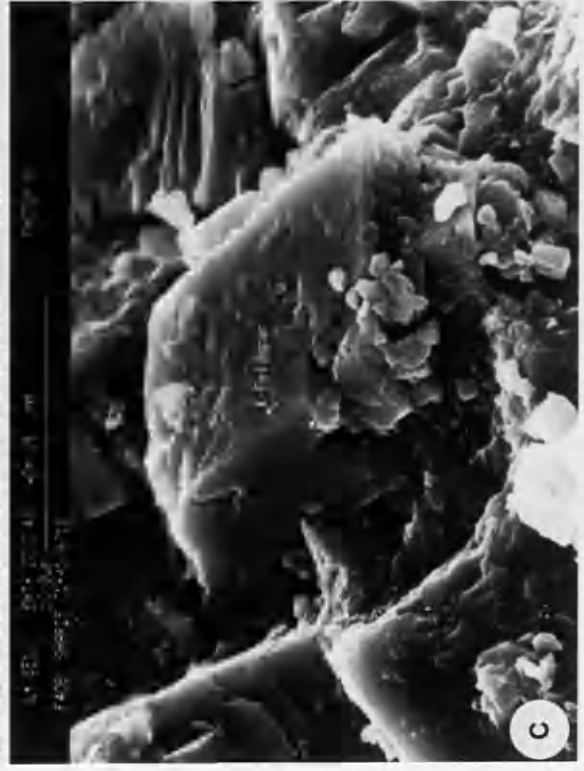
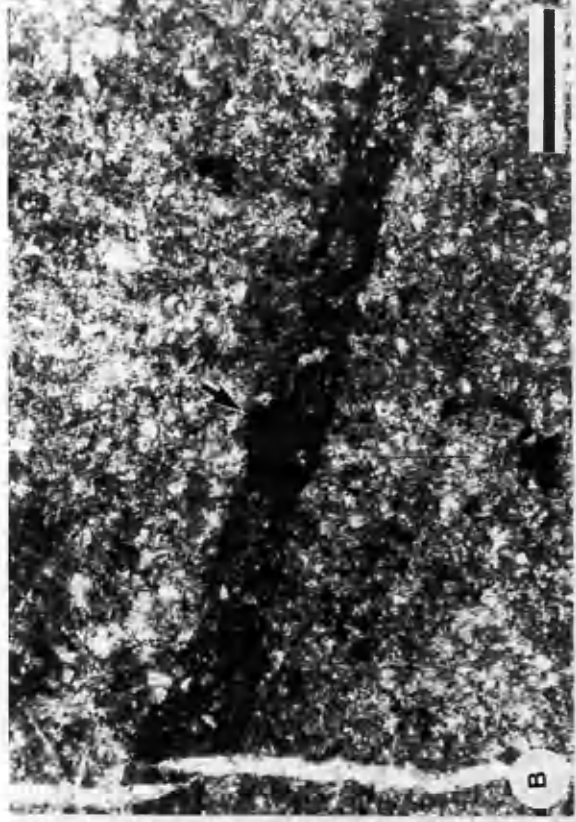
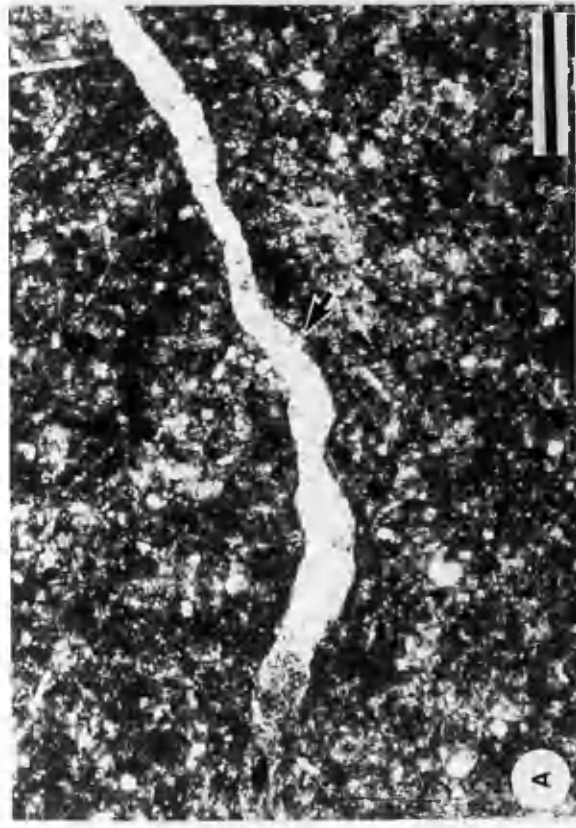


Plate 2.3

A) Photomicrograph of F2 showing globigerinids concentrated in laminae, dissolution seams (arrow) commonly present. Bar scale=0.5mm. Well B2-41, depth 6430ft.

B) Photomicrograph illustrate typical micrite with abundant of globigerinids (a), gastropoda (b). The bioclast mostly filled with sparry calcite and have undergone compaction. Bar scale=0.2mm. Well B2-41, depth 6415ft.

C) Photomicrograph by SEM of well developed crystals of calcite, usually found in foram chamber. Well C1-41, depth 5195ft.

D) Photomicrograph under SEM of the chalk component. Abundant of coccoliths in cluster. Also characterized by good porosity, and no clear cement is visible. Well C1-41, depth 6400ft.

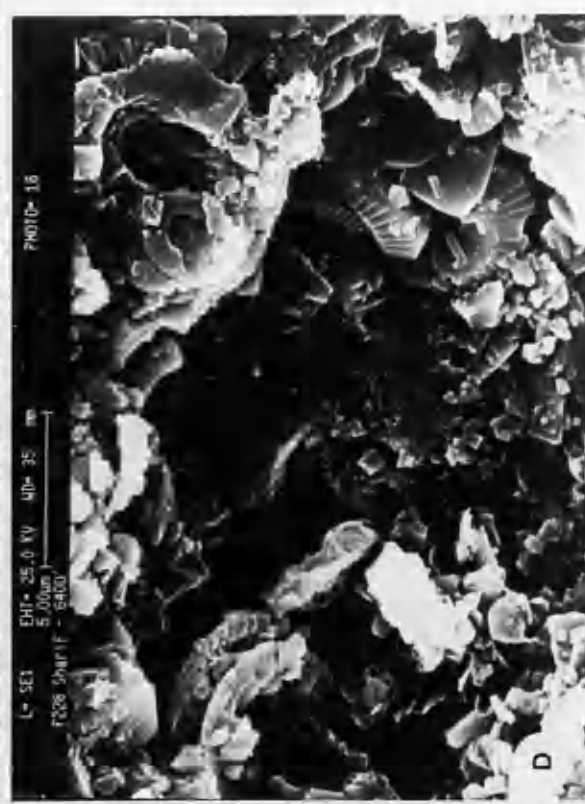
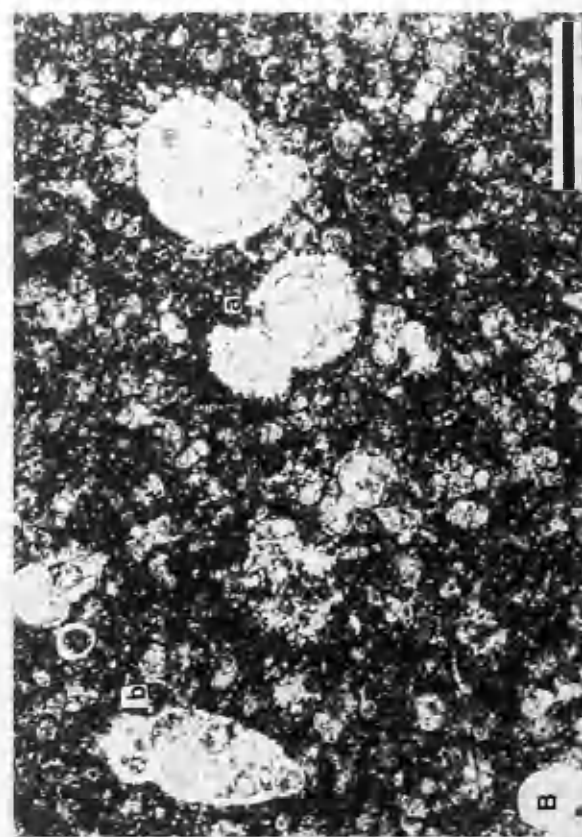
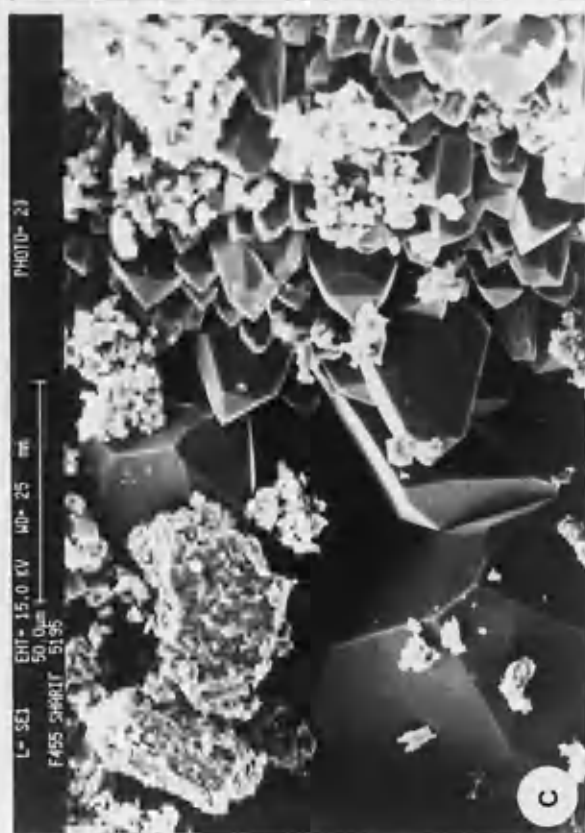
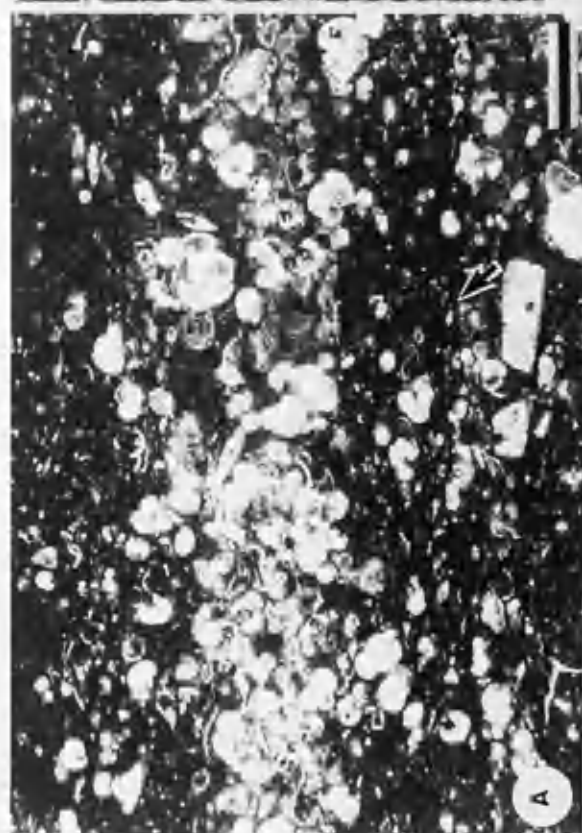


Plate 2.4

A,B) Photomicrograph under SEM of thoracosphaerids which form one of the essential component of the studied chalks. A) Three thoracosphaerids with large porespace. Bar scale=10 μ m. B) Internal view of thoracosphaerid test showing the rhombic form of the individual elements and later calcite cement. Bar scale=5 μ m

C,D) Photomicrographs illustrating dolomite in the chalk. C) Isolated dolomite crystal "floating" in the chalk matrix. Bar scale=5 μ m. D) Dolomite present as clusters (arrow) but this is rare. Bar scale=20 μ m.

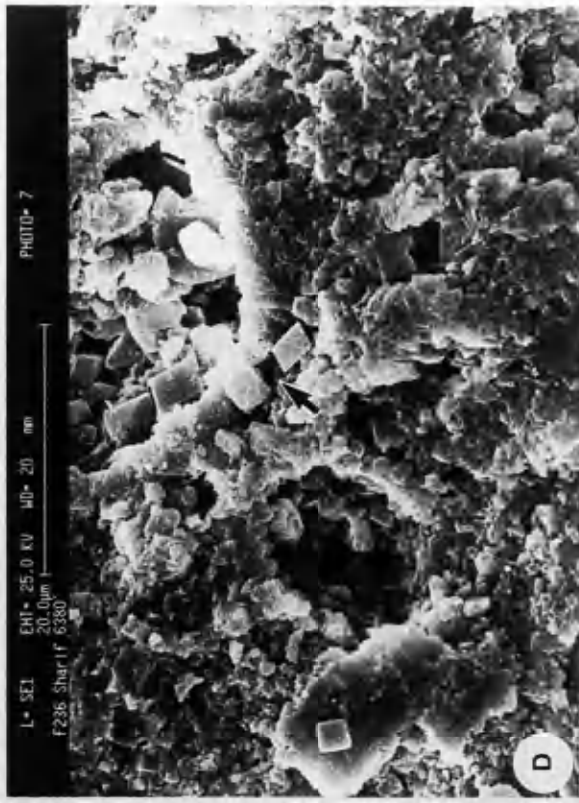
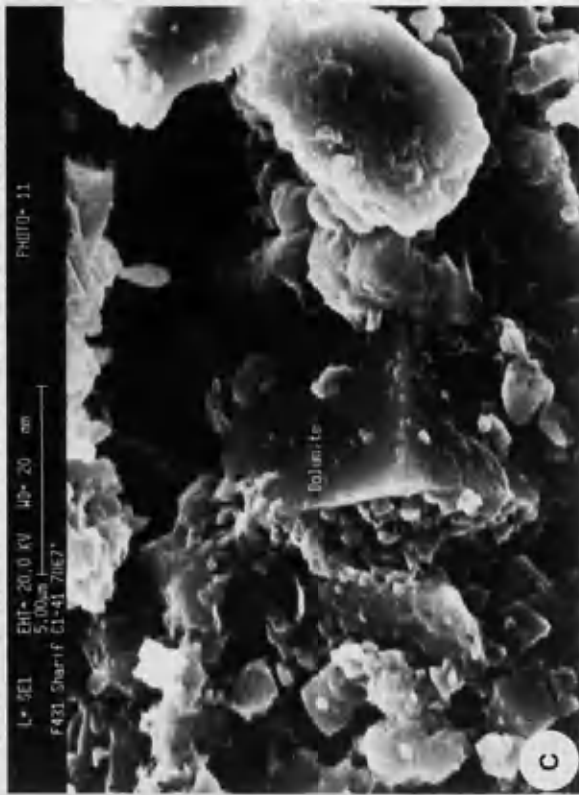
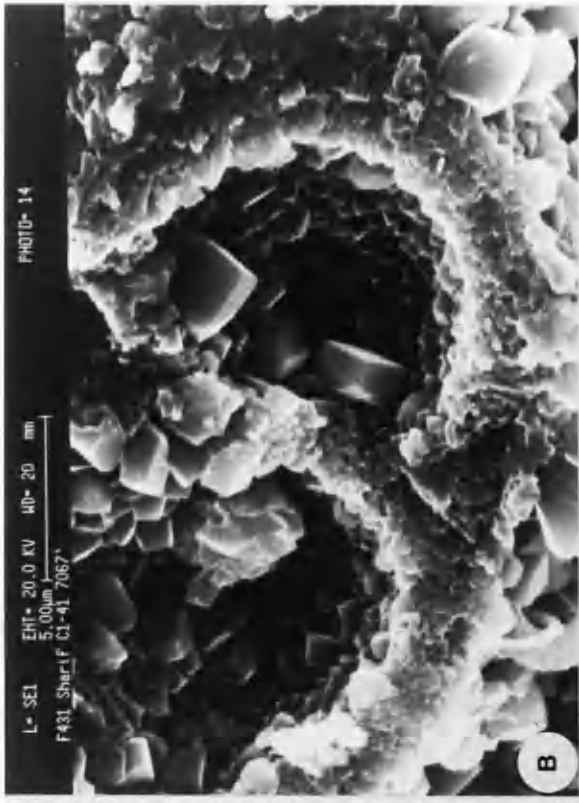
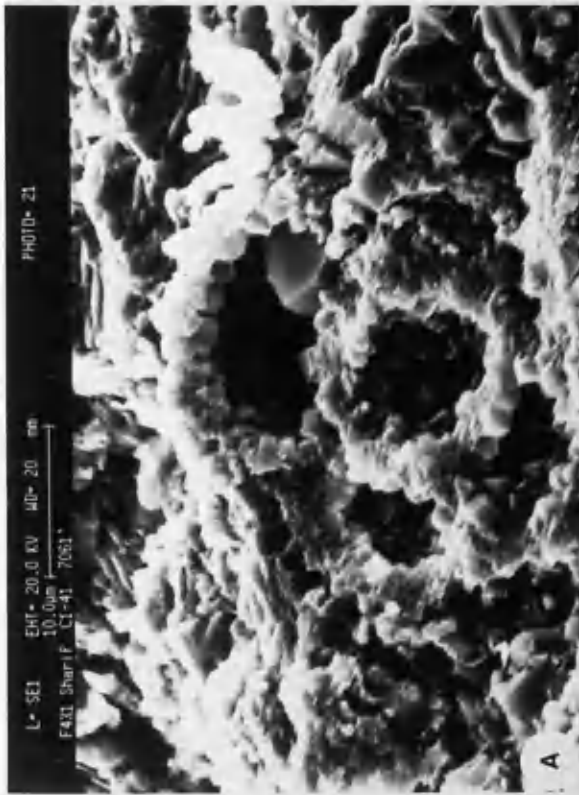


Plate 2.5

A-D) Photomicrographs showing characteristics of the pelletal packstone lithofacies. A) Small pellets interlock, possibly indicating little cement was present before compaction. Bar scale= 0.5mm. Well B2-41, depth 6550ft. B) With mollusc fragment (arrow). Well B2-41, depth 6510ft. C) Different sizes of pellets and *Alveolina* (arrow). Well B2-41, depth 6510ft. D) With Nummulite (arrow). Bar Scale in B and C=1mm. Well B2-41, depth 6510ft.

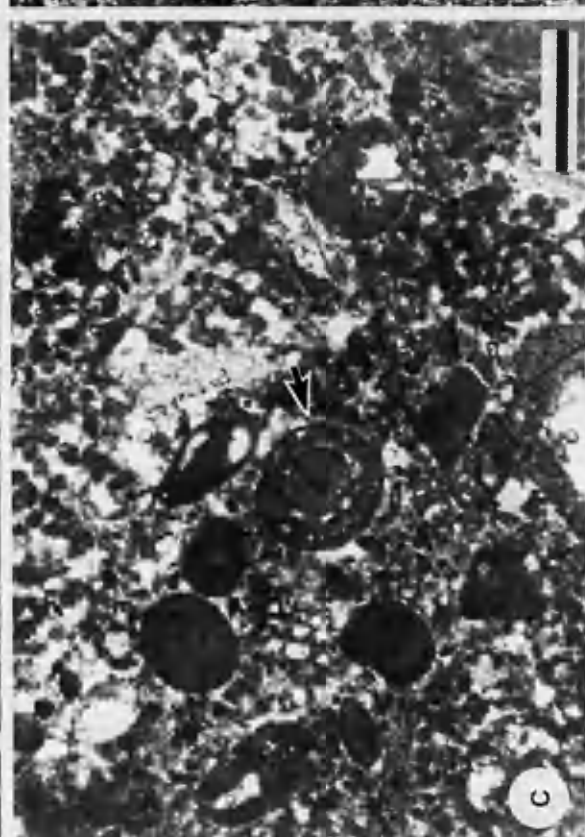
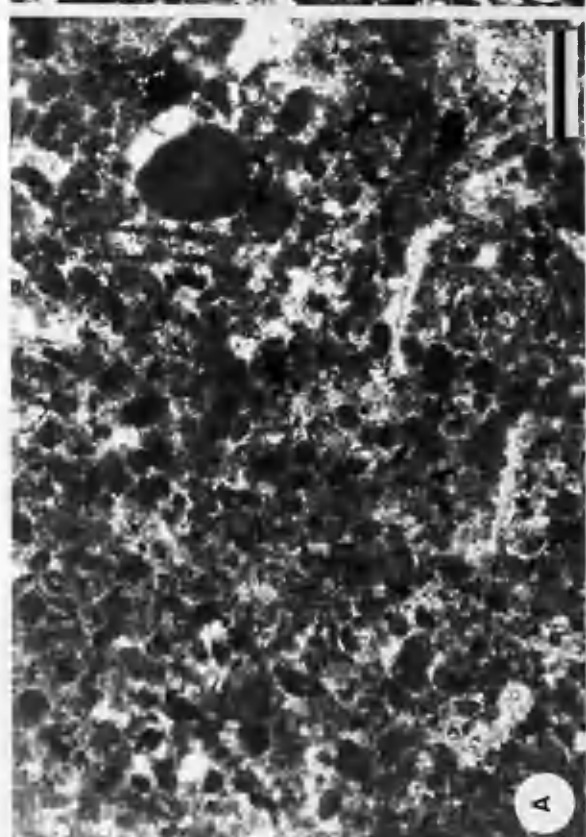
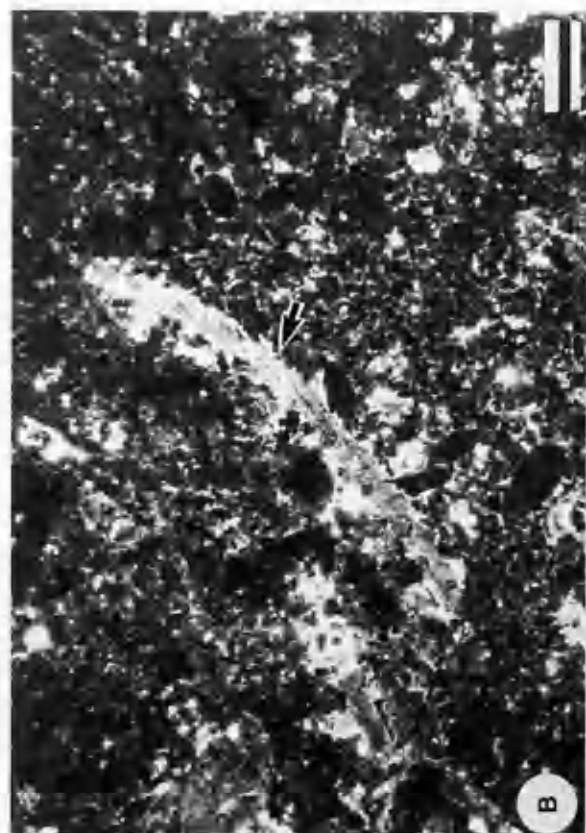


Plate 2.6

A) Photomicrograph of large nummulite packstone. Composed largely of *Nummulites gizensis* in which many chambers contain coarse blocky calcite cement (a). Note *Fusulina* in the top left. Bar scale=0.5mm. Well C1-41, depth 5199ft.

B,C) Photomicrograph of the small nummulites lithofacies. B) Consists almost entirely of small size nummulites. In (C) The chambers of the fossils are occasionally filled by calcite cement. Bar scale= 0.5mm. Well C1-41, depth 5188ft.

D) Photomicrograph of limestone showing mixed small and large size nummulites and considered as transitional between the two major lithofacies. Note the large nummulite with some pores filled by calcite cement while others remain empty (a). Bar scale=0.5mm. Well C1-41, depth 5199ft.



Plate 2.7

A) Photomicrograph showing packed nummulites with good intraparticle porosity (a), brachiopod fragment (b), echinoid fragment(c) and anhydrite cement(d). Bar scale=0.5mm. Well J1-41, depth 6123ft.

B) Photomicrograph of replacement of bioclast by spherulitic silica chalcedony in lithofacies F4. Bar scale=0.2mm. Well C1-41, depth 5192ft.

C) Photomicrograph of stylolite (arrow), most common in the large nummulite packstone. Bar scale=0.5mm. Well J1-41, depth 6123ft.



Plate 2.8

A,B) Photomicrographs of coarsely crystalline dolomite. A) Unimodal, planar-s, crystals with cloudy centres and clear rims. Well D1-41, depth 7688ft. B) Hypidiotopic dolomite crystals with few inclusions filling porespace. Bar scale=0.2mm. Well C1-41, depth 8968ft.

C,D) Photomicrographs of dolomite under SEM. C) Backscatter image showing the presence of pyrite in the dolomite. D) Interlocking crystals of fine crystalline dolomite. Note very low porosity. Bar scale=100 μ m

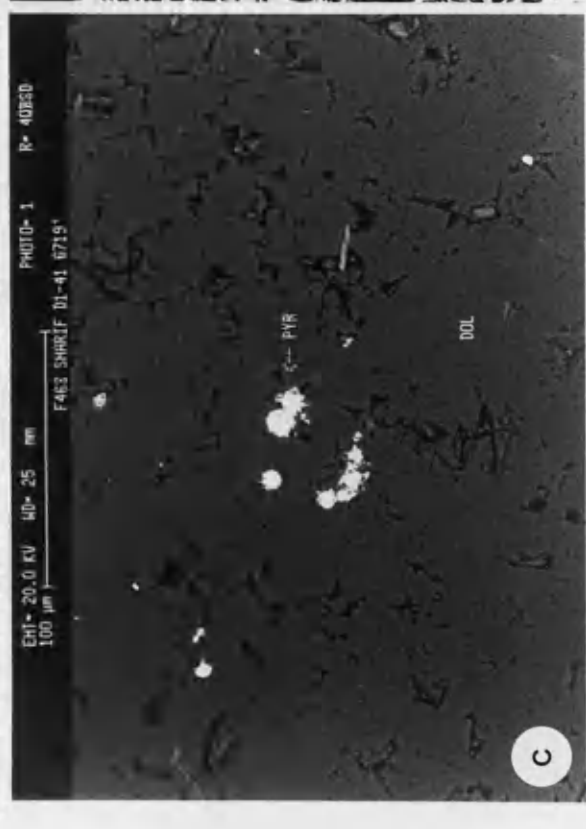
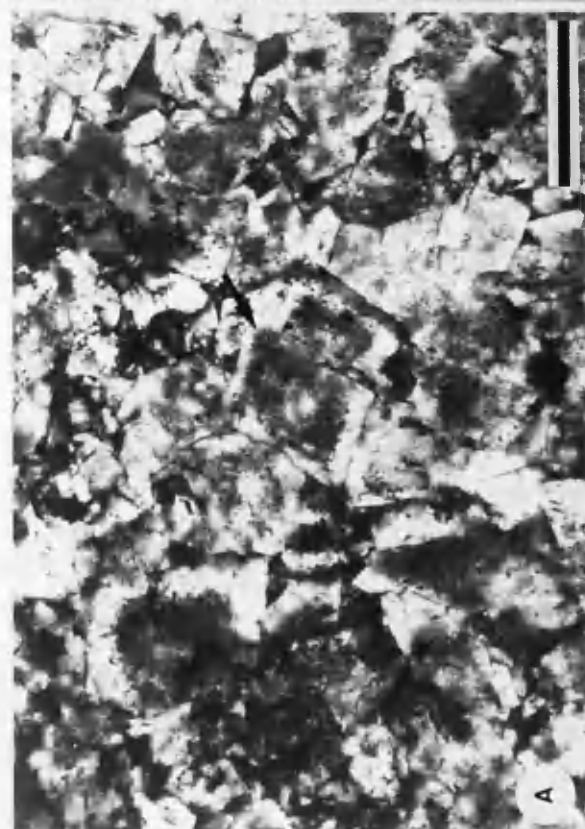
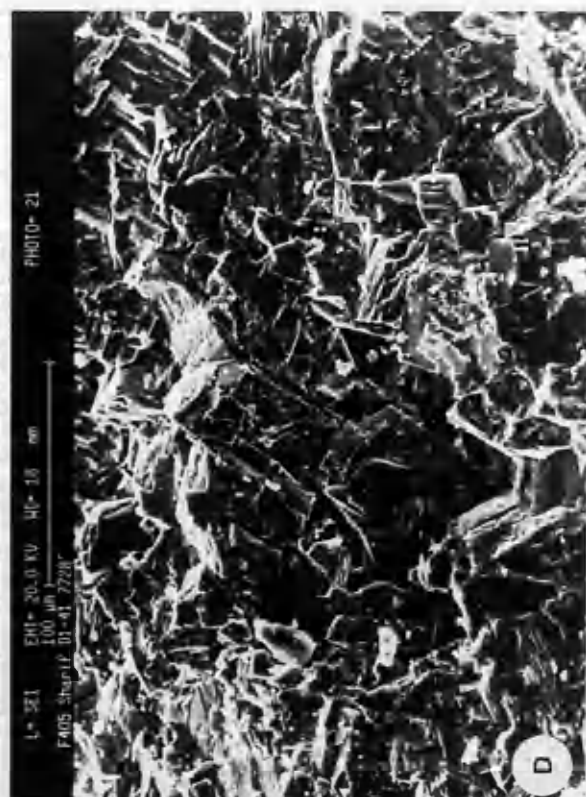
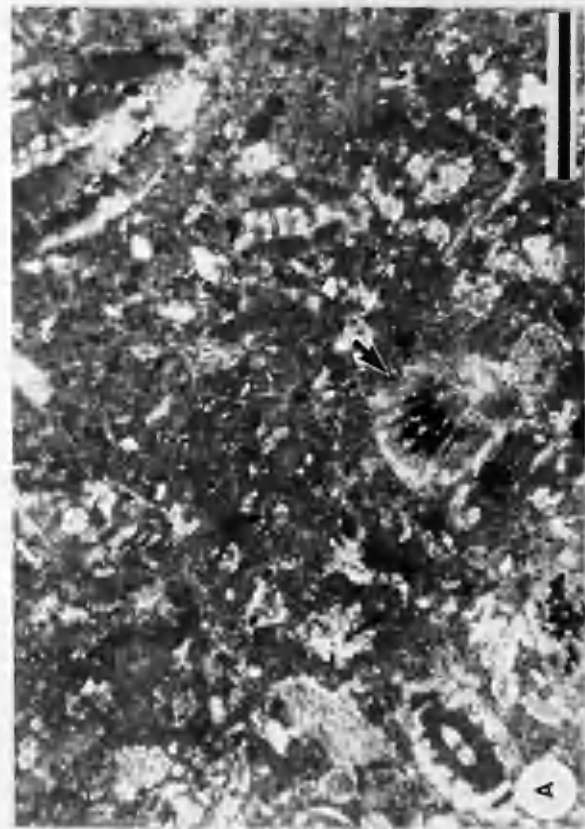
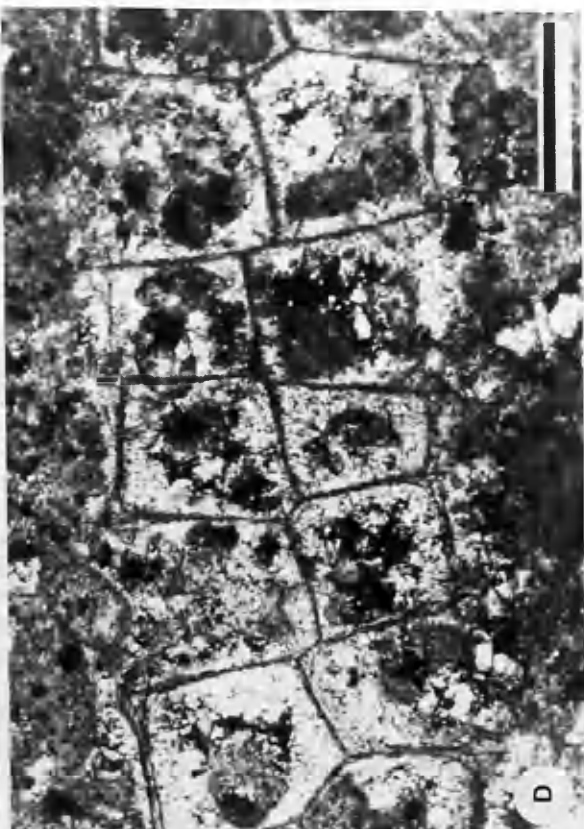
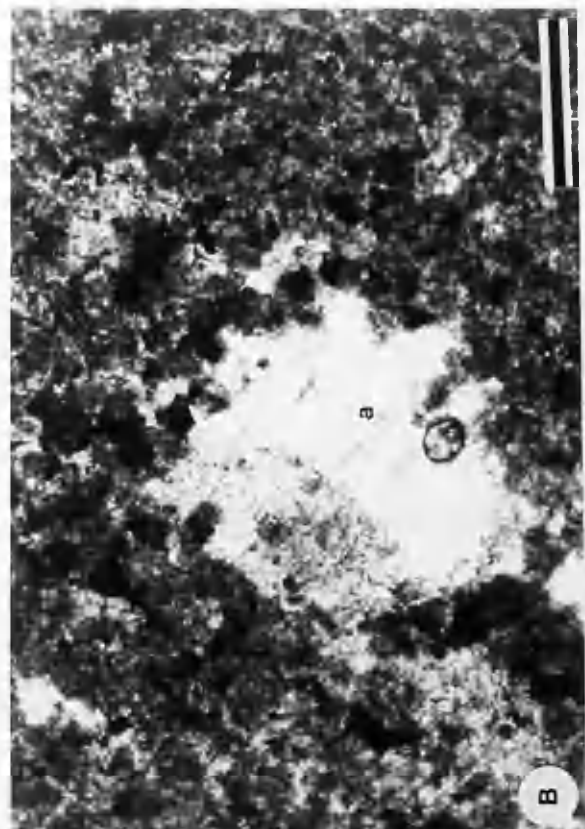


Plate 2.9

A) Photomicrograph of limestone replaced by dolomite in lithofacies F6 . Note partly mimetic replacement of bioclast (arrow) . Bar scale=0.2mm. Well D1-41, depth 5731ft.

B) Photomicrograph of replacive anhydrite (a) in lithofacies F6. The black spots are pyrite. Bar scale=0.2mm. Well C1-41, depth 7515ft.

C,D) Photomicrographs of replacement of bioclasts. C) Finely crystalline dolomite mimetically replaced fusulinid. Well D1-41, depth 5731ft. D) Partly mimetic replacement of bryozoan by finely crystalline dolomite. Bar scale=0.2mm. Well D1-41, depth 5735ft.



CHAPTER THREE

DIAGENESIS

Diagenesis is a continuous, composite course of post depositional processes which alter sediments. Some diagenetic events may so totally alter the original depositional texture of a sediment that it becomes difficult even to speculate about its origin. The rocks in the studied area generally vary from mudstones to packstones with rare grainstones. Most of the section was deposited in a slope environment, that is, chiefly in deep water. Usually the diagenetic history of pelagic sediments is strikingly less complex than that of shallow water deposits because the latter are composed of grains of different sizes, of variable unstable mineralogy, and are subjected to a variety of diagenetic environments and pore fluid chemistries during burial history.

Conventional petrography, cathodoluminescence (CL), and Scanning Electron Microscopy (SEM) for fine grained sediments and some dolomites, were utilized to reveal the diagenetic history of the studied core samples. The diagenetic changes were dominated by compaction, cementation, dolomitization and dissolution. The paragenetic sequence determined is given in Fig3.1. As mentioned earlier in chapter two, the rocks of the area are divided into seven separate lithofacies. Since chalk represents the predominant lithology and the volumetrically most

important, it is treated separately, whereas other lithofacies, which are diagenetically similar to each other, are discussed as one unit.

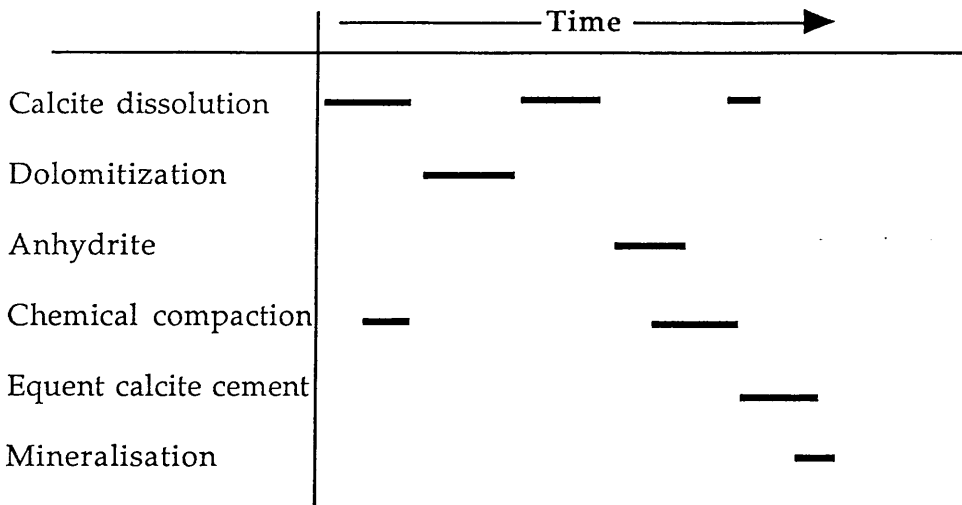


Fig. 3.1, Summary of the observed diagenetic events.

3.1 Chalk diagenesis

The chalk in the investigated area consists predominantly of coccoliths and other nannofossils (e.g thoracosphaerids) together with a small but significant quantity of pelagic Foraminifera such as Globigerinids. All of these composed during their life times of stable low Mg calcite. Chalk is a mineralogically stable sediment, deposited in relatively deep water environments. In the samples studied skeletal elements appear fresh with no evidence of either corrosion or of any overgrowth on the coccoliths. However, elsewhere there may be extensive overgrowth and coalescence of grains (Plate 3.1, C). No systematic variation in the distribution has been recognized. No examples of

hardgrounds have been recognized in the studied core samples. Stylolites and dissolution seams are common (Plate 3.2, A, B).

The initial stages of chalk alteration start immediately after deposition. As long as sedimentation continues the overburden will increase and most chalks undergo compactional dewatering. Biogenic activity, especially by burrowing organisms may enhance the expulsion of water so that the chalk becomes a grain supported framework. However, some early diagenesis of chalk involves more complex processes such as significant dissolution, cementation and replacement (Scholle, 1977). Synsedimentary sea floor cementation commonly known as hardground formation, has been observed in many areas, for example, by Bromley (1968), and Bathurst (1971). However, Scholle (1977), suggested that most chalks are little affected by sea floor cementation and that most changes are related to burial or post burial alteration. Davis (1986) related the inhibition of early diagenesis in chalks to low permeability which obstructs the movements of water through the matrix.

During burial, two main mechanisms appear to operate, mechanical compaction and chemical compaction. Another minor process is the imported of cement from external sources, but this is insignificant in low permeability sediments such as chalk because it demands the movement of large volumes of porefluid. Work by Bathurst (1971) found that chemical compaction, represented by pressure dissolution, plays an important part in subsurface cementation. This is defined as the process of

dissolution of minerals under non hydrostatic pressure (Scholle, 1977). Dissolution usually occurs at grain grain contacts where the stress is at a maximum (Weyl, 1959). This produces dissolved calcium carbonate which migrates mainly by grain boundary diffusion (Durney, 1972). But diffusion of this kind is not likely in porous granular materials such as chalk. The samples do not show overgrowth, therefore the carbonate was not reprecipitated nearby. Dissolution transfer can be a response either to overburden or tectonic stress (Scholle, 1977).

The presence of stylolites and dissolution seams is an indication that chemical compaction has taken place. The abundance of these features in the studied core samples testifies that pressure dissolution has been influential and should be therefore considered as a possible source for the production of calcium carbonate to form a cement. However, it is not easy to prove without any doubt that any cement is derived locally by dissolution transfer and not imported from external sources. No overgrowth has been observed on the coccoliths of the chalky lithofacies and this suggests that the calcium carbonate produced is going somewhere else. The burial depth at which solution transfer operates is not well known, although Dunnington (1967) suggested that 600 to 900m is the minimum for stylolite formation, while Neugebauer (1973, 1974) demonstrated that the production of cement by solution transfer is insignificant above 300m, but results in virtually complete lithification in chalks by 2000 to 4000m of burial. Once chalks have lithified through cementation dissolution becomes the dominant process and this is concentrated along discrete surfaces. Once porosity falls below 25% there is

transition from dissolution seams to stylolites (Scholle, 1977). Irrespective of whether cements in the chalk are derived internally by selective dissolution or from external source, it is likely that solution transfer rather than mechanical compaction is responsible for most porosity loss after the initial dewatering.

3.2 Other lithofacies

The remaining lithofacies share general characteristics. They are all wackstones, although the matrix is in varying proportions, and all have the same coarse grained cements in intragranular pores.

3.2. 1 *Cementation*

Cements of various sorts are considered to be one of major causes of porosity reduction, consequently reducing the potential of reservoir quality. The studied core samples reveal two kinds of cements, (a) Blocky calcite cement and (b) Calcium sulphate.

a) *Blocky calcite cement* : Equant blocky calcite is the dominant cement in the studied samples and is most evident in the large nummulitic packstones lithofacies (Plate 2.6, A) where it is predominantly present filling the intraskeletal chambers of foraminifera. A coarse mosaic of sparry calcite also occurs within fossil molds, and in interparticle pores and

cavities. The blocky cements in the studied samples have quite different CL signature from either the bioclasts or the matrix. They are typically dark and nonluminescent while the cement usually has dull red glow. Occasionally the cement crystals have darker centres and brighter edges. This is interpreted as a burial cement and the circumstances which lead to its formation are discussed below.

Large volumes of cements may be precipitated in porespace prior to significant burial (James and Choquette, 1984). Usually the source of the calcium carbonate for this cementation is provided by sources such as supersaturated marine water, evaporated marine water, or from dissolution of meta-stable carbonates. The volume of the cements is controlled by the rate of fluid flux in the porespace. In contrast, following burial, the volume of cement precipitated may be small and most of the fluids are in equilibrium with CaCO_3 . Subsurface cements are precipitated from fluids that evolve only slowly chemically, as a result of rock/water interaction over extremely long period of time (Moore, 1989). Under such conditions dissolution and precipitation work, if at all, in a closed system. Where this reaches equilibrium only pressure dissolution can provide the carbonate for further cement growth. The increase in temperature with burial favours cementation (Bathurst, 1986). The obvious problem remaining is to find an adequate source of CaCO_3 to form cement. Pressure dissolution, active during chemical compaction, is favoured as the CaCO_3 source for the bulk of the burial cements encountered in the rock record (Meyers, 1974; Scholle & Hally, 1985). In the study area these cements are not ubiquitous. This might be due to unsaturated flow or to a

flow rate too slow to support the growth of a number of nuclei.

b) *calcium sulphate cements*: In certain intervals in the investigated sections calcium sulphate, predominantly anhydrite, co-exists with dolomite (Plate 3.1, D). It is most common in wells C1-41 and D1-41 and occurs in both finely crystalline and coarsely crystalline dolomites with a xenotopic fabric. The anhydrite is present both as a replacement of dolomite and as a coarse cement filling porespace which include vugs and molds of fossils. Anhydrite is also occasionally present as a fracture filling. Some anhydrite can be shown to have grown before minor compaction but elsewhere anhydrite follows compaction and postdates dolomitization.

Other cements are either very rare or present in amounts which make them volumetrically unimportant. They include dolomite, calcite (as a cavity or fracture filling), rhombohedral cement in some of the forams (Plate 3.1, B), and baroque dolomite.

3.2.2 *Dissolution*

More than one stage of dissolution has been distinguished. The first stage which is inferred preceded the principle dolomitization event. This is indicated by the presence of moulds of some bioclasts, especially *Globigerina*, in the lithoclast bearing mudstone and chalky mudstone

lithofacies indicating dissolution. This was followed by dissolution which appears to have been contemporaneous with or shortly after the dolomitization had taken place. This is suggested by the occurrence of moulds of bioclasts in a generally dolomitized matrix and results locally in a well developed moldic porosity. At some horizons these pores have been partially or completely occluded by the growth of calcium sulphate (anhydrite). This irregular distribution may indicate either a lack of sufficient CaSO_4 for crystal growth or the development of additional new porosity by dissolution which followed sulphate precipitation. Brecciation is also present in the dolomite and this is suggested as a very late effect of evaporite dissolution by meteoric water. Thus, the irregular distribution of the CaSO_4 can be interpreted as due to the late development of porosity.

3.2.3 *Compaction*

Compaction is a well known and important process in the diagenesis of carbonate rocks. It commences soon after the initial deposition of the sediment. In the studied area many features have been recognized which might indicate that the area was subjected to compaction. Stylolites are present in most of the lithofacies studied but are more pronounced in the dolomites (Plate 3.2) and the nummulitic facies (Plates 2.7, C and 3.1, A). Stylolites are usually irregular and are commonly of low amplitude although high amplitude forms are also present. They are characterized by the dissolution of soluble phases, and the concentration of relatively insoluble or less soluble phases along the surface. The chalky

mudstone lithofacies is characterized by the occurrence of dissolution seams rather than stylolites (Plate 3.2, A, B). These are irregular, and unserrated with a brown insoluble residue. Wispy anastomosing seams of organic residues or other insolubles form what are usually called horsetail structures.

Compaction in general is divided into two courses. 1) Mechanical compaction, which starts shortly after deposition and 2) Chemical compaction, which operates only after deposition of considerable overburden. In mechanical compaction the weight of the overburden reorders the grains forming the sediment so that they become more closely packed. This re-ordering certainly occurs in areas where there are no early marine cements. Sediments such as muds may also be subjected to significant compaction, but there is little evidence of this in the core studied, this may be because there was an early marine cement to prevent compaction but there is no trace of this remaining. Muddy sediments are usually deposited with a high porosity which may reach more than 60%. This high primary porosity may dramatically decrease by grain rearrangement and the assumption of tight packing from the influence of compactive stresses. As soon as the overburden increases substantially chemical compaction replaces mechanical compaction and further reduces porosity. Chemical compaction is evident in the core samples in the presence of pressure dissolution seams and stylolites.

Stylolites and microstylolites are most common in the matrix of muddy sediments which are more prone to this style of compaction. Thus, the facies present in the area deposited in a slope are considered an ideal place for such features. The waters in these deep marine sediments were not continuously exchanged because the sediments were fine grained and relatively impermeable, such properties may prevent early cementation. Thus, the deep marine deposits are more highly compacted and stylolitized than the shallower water sediments. Usually deep water sediments are known by their high porosity and very low permeability, but the development of such features may enhance the petrophysical characteristics (porosity and permeability) of these rocks.

3.2.4 Mineralisation

Mineralisation is rare in the area studied. Late stage PbS mineralisation has been revealed by the use of the SEM Backscattering technique which shows lead sulphide to be present as small granules replacing quartz grains (Plate 3.3, A) and calcite in the debris flow within lithofacies F4. The source of Pb remains a puzzle. As a speculation in the absence of any other source such as a hydrothermal centre, the lead might have been introduced to the system from concentrated brines. The reaction between S and Pb usually occurs under reducing conditions.

Pyrite occurs in most wells and in many intervals, but it is more prominent in the deeper parts of the sequence. The pyrite occurs as

irregular granules in the micrite matrix or within chambers of the foraminifera in the nummulitic facies where significantly, it has usually been introduced after cementation. It is also common in the dolomite (Plate 2.8, C). Pyrite is known as an authigenic iron sulphide precipitating in reducing environment with sluggish circulation of porefluids. It commonly forms during or soon after deposition, but obviously generated after burial cement.

3.2.5 *Dolomitization*

Dolomite is abundant in the studied samples and is considered to be the most influential process affecting the studied area. Dolomitized fabrics are dominant especially in the Paleocene section in wells C1-41 and D1-41. Dolomitization usually obscures the primary depositional texture of the precursor, although some features remain and others may be inferred. A detailed study of the dolomitization and the suggested model for emplacement will be discussed in chapter five.

3.3 Cathodoluminescence (CL)

In recent years cathodoluminescence (CL) microscopy has become an essential tool in the study of carbonate rocks. It often reveals fabrics that are invisible in normal transmitted light. It has been widely used in the study of cement stratigraphy which is defined as the correlation of cements in carbonate rocks by interpreting equally luminescing zones within crystals as diagenetically coeval. Cement sequences (e.g Meyers, 1974) can be used to establish local and regional mapping of distribution which can be related to regional patterns of variation in the chemistry of pore waters (e.g Grover and Read, 1983), and the time sequence of diagenetic changes (e.g Machel, 1985).

The cathodoluminescence of calcite and dolomite is thought to be due to the presence of a number of trace elements of which Mn^{2+} is the most important activator and Fe^{2+} the most important quencher. The exact concentrations of these two elements needed to activate or quench CL, are poorly constrained. The relative proportions of Mn^{2+} and Fe^{2+} also affect the intensity and colour of luminescence, and reflect pore-fluid chemistry prevailing during precipitation. The chemical environment of crystal growth can be revealed by means of CL, but interpretation should only be undertaken with extreme caution. Crystals such as calcite and dolomite tend to grow layer by layer into voids. During their growth they incorporate different amounts of activators and quenchers which are proportional to the composition, to temperature, pH, Eh and other

properties of the depositing fluid. Variations in these parameters result in crystal banding or zonation which can sometimes be traced over tens, even hundreds of square kilometres (Meyers, 1974). Non luminescent calcite is normally always a result of Mn^{2+} concentration. A decrease in Eh would yield first an increase in Mn followed by a simultaneous increase in both Mn^{2+} and Fe^{2+} (Meyers, 1989). Non luminescent cement suggest is probably formed from waters that had high redox potential and that were oxidizing (Garrels and Christ, 1965; Ogelsby, 1976), while precipitation of bright and dull cements indicates a change from oxidizing to more reducing porefluids (Ogelsby, 1976; Meyers, 1978).

In the studied area no well defined CL zones have been recognized within individual crystals. This might be related to the general deficiency of Mn^{2+} in the studied samples (see chapter four). However, an attempt has been made to correlate similar CL signatures of sediments in order to construct regional geochemical variation over the stratigraphic interval and between the four wells studied (C1-41, B2-41, D1-41 and J1-41), although two wells J1-41 and C1-41 have poor core coverage. The distribution of these luminescence types is shown in Fig 3.2. The response of the Early Eocene sediments in the studied area to CL is varied. It includes four types of luminescence, type I, is present in the chalky mudstone lithofacies in well C1-41, the most westerly well studied and also the most distant from the platform. The matrix and the granular cement filling *Globigrina* tests are relatively bright. In well B2-41 to the east, and upslope, the matrix becomes brighter and there is also a bright cement (Plate 3.5, A). Type II, occurs in the chalky and nummulitic lithofacies in

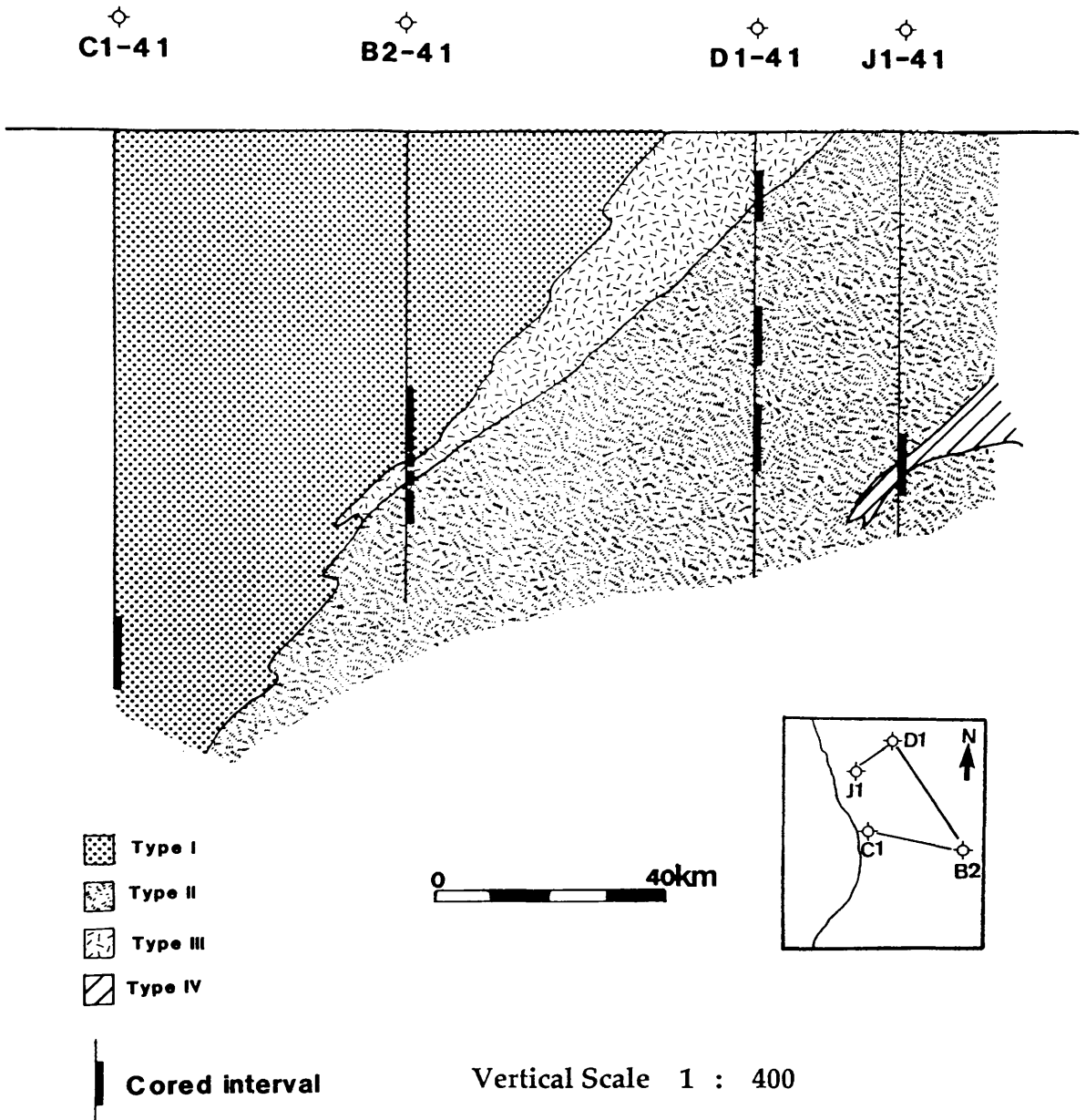


Fig. 3.2, X-section illustrate the correlation of similar CL signature in the Early Eocene sediments. Datum is the top of L. Eocene.

well D1-41 the most northerly area, and also low in the sequence in well B2-41. Bioclasts and matrix both show a general dull luminescence but this becomes relatively bright upward in the succession. Type III, is present in the upper part of the studied interval in the north, in both chalky and nummulitic lithofacies. In this the matrix is dull but the cement within the forams shows an early dull zone and a later bright zone (Plate 3.5, B-D). Finally, type IV, occurs only at the base of the interval studied in wells J-41 in the nummulitic lithofacies where both the matrix and the bioclasts are non-luminescent.

The distribution of non-luminescent cements has been used to interpret sources and flow directions of paleometeoric ground waters (Meyers, 1991). In Fig 3.2 the small patch of non-luminescent calcite which is confined exclusively to the lower part of the stratigraphic sequence in the northern part of the area may be interpreted as reflecting a position near the recharge area. This was apparently the Cyrenaica Platform which during the Tertiary was subjected to emergence most of the time. The dull-bright luminescence dies-out down section leaving only bright calcite in the lower part of the section. The slope provided the necessary elevation head to drive oxic water from the recharge area but this gradually changed to a reduced state down slope.

This lateral change is apparently paralleled by a similar change up section and it is thought that this implies progressive subsidence or burial and the expansion of the area reduction with time.

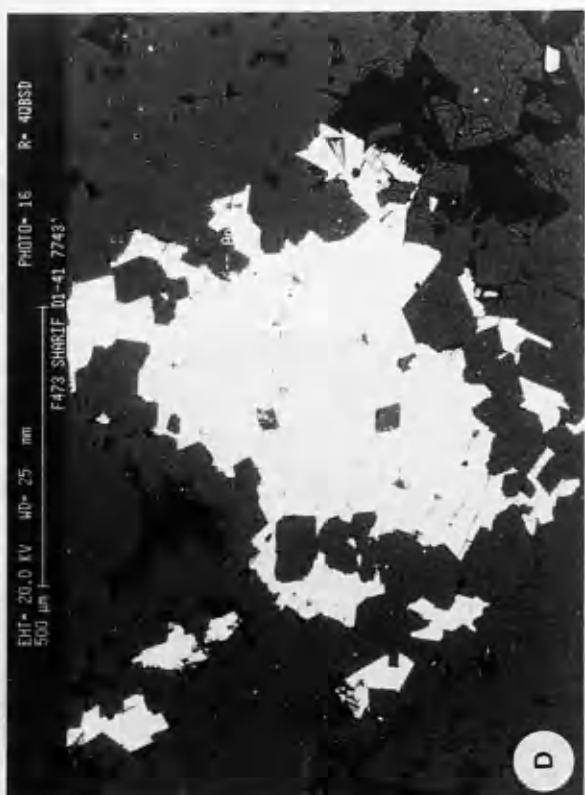
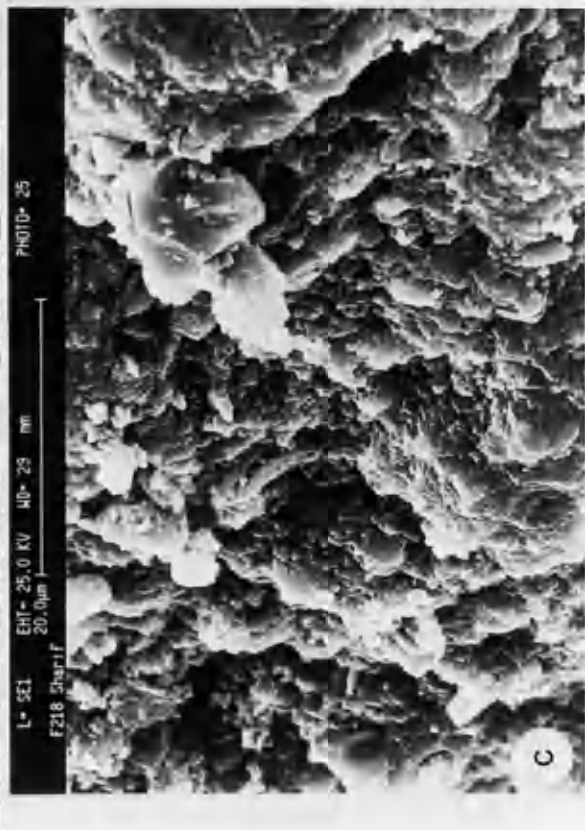
Plate 3.1

A) Photomicrograph of lithofacies F4 showing compaction. Mechanical and chemical compaction (arrow) affecting the nummulitic lithofacies. Bar scale=0.5mm. Well D1-41, depth 5199ft.

B) Photomicrograph of intragranular pores of foram showing rhombohedral calcite cement cement. Bar scale= 0.5mm. Well C1-41,depth D1-41, depth 5185ft.

C) Photomicrograph of cementation in chalk, most original biogenic grains have been obscured by overgrowthcementation. Bar scale=20 μ m. Well B2-41, depth 6430ft.

D) Photomicrograph of lithofacies F7 showing cementation by anhydrite. Backscattered image of dolomite in which anhydrite is present as a replacement and as a cement as well. Bar scale=500 μ m.



L-SEI EHT-25.0KV WD-23mm
F218 Sharif PHOTO-25

EHT-20.0KV WD-25mm
500µm F473 Sharif PHOTO-16
R-408SD

Plate 3.2

A,B) Photomicrographs of chemical compaction in chalk. A) Dissolution seams are frequently present in lithofacies F2. Bar scale=0.5mm. Well C1-41, depth 6730ft. B) Stylolites (arrow) which are less common than dissolution seams in the studied chalk. Bar scale=0.3mm. Well C1-41, depth 6415ft.

C,D) Photomicrographs of chemical compaction in dolomites of lithofacies F6. C) Dissolution seam in lithofacies F6 truncated by fracture filled with calcite (arrow). Bar scale=0.5mm. Well D1-41, depth 6719ft. D) Stylolites are also common in the dolomite (arrow), low amplitude stylolite characterized by dissolution of soluble , and concentration of less soluble phases along surface. Bar scale=1mm. Well C1-41, depth 8970ft.

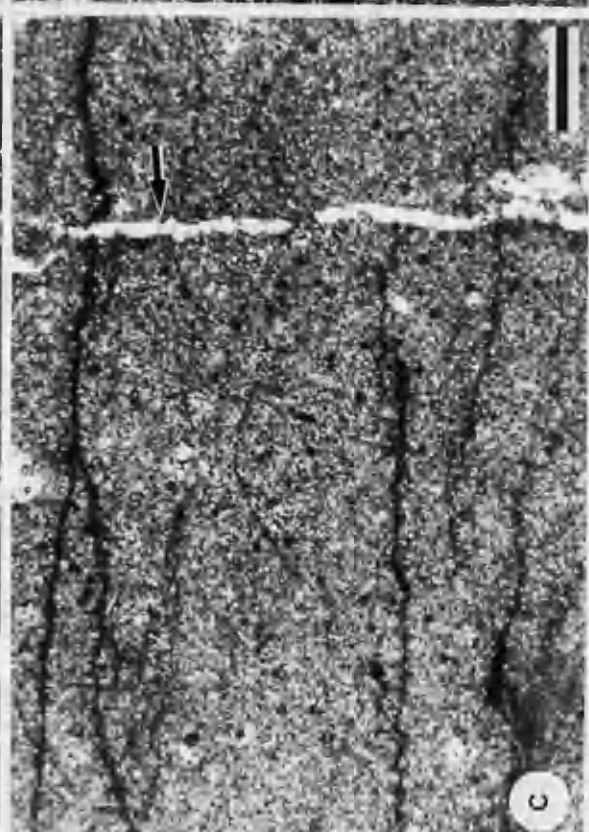
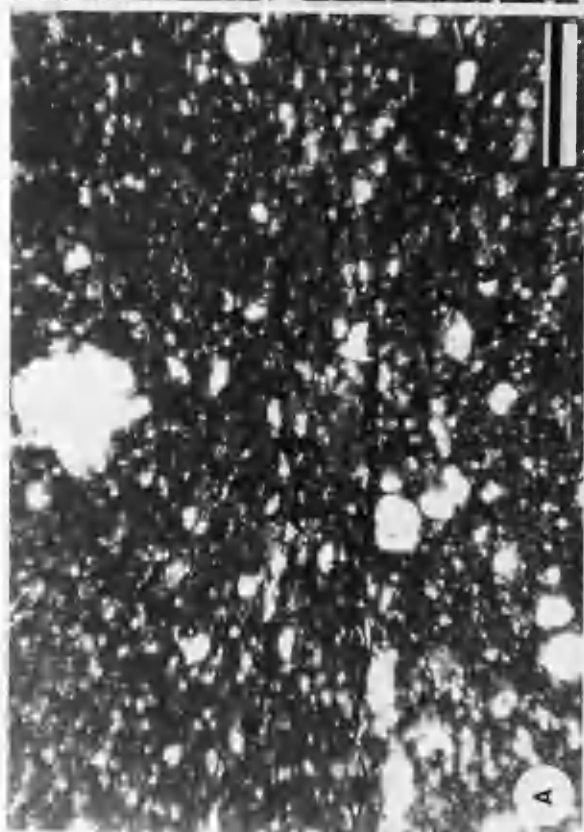
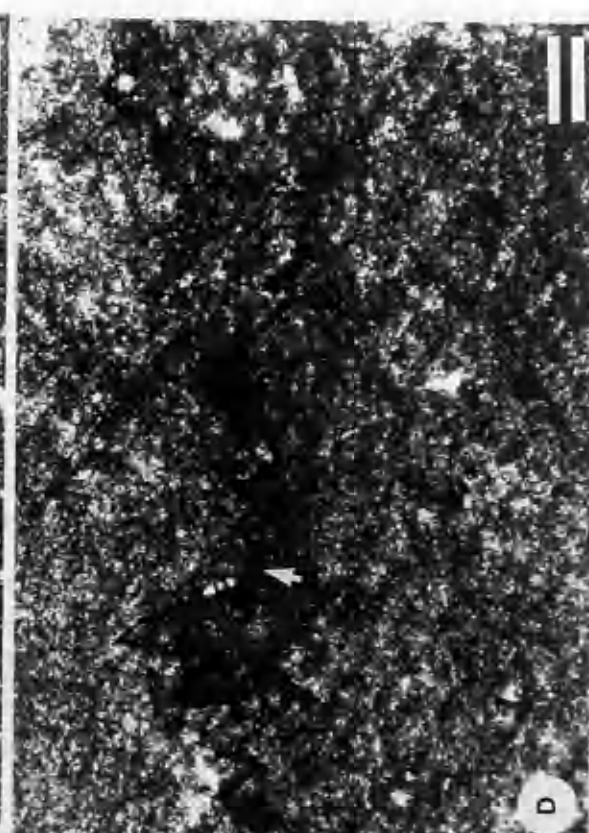
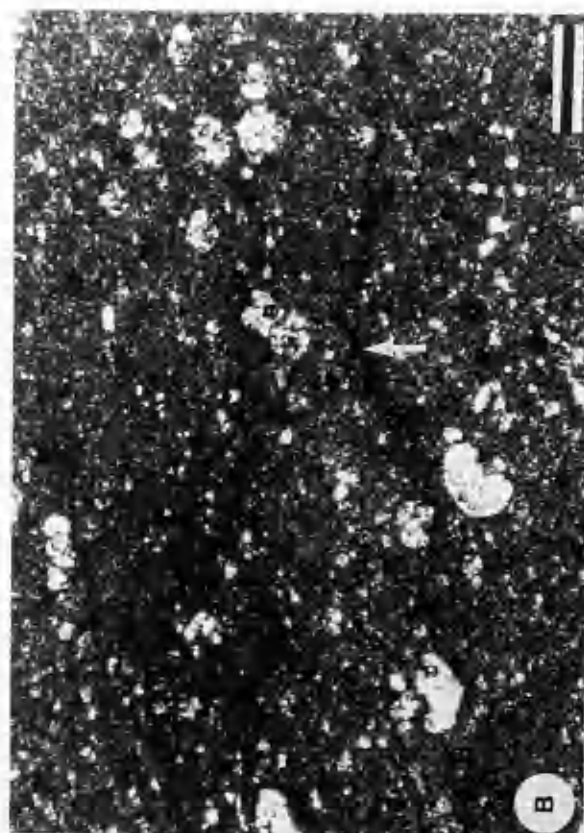


Plate 3.3

A) Photomicrograph of back scattered image of sandstone pocket in lithofacies F4. Note Pbs mineralisation. This looks like a replacement because it cuts the edges of quartz grains. Bar scale=200 μ m.

B) Photomicrograph of bladed anhydrite growing in porespace in the studied chalk. It is suggested that the anhydrite is responsible for porosity destruction. Bar scale=10 μ m.

C,D) Photomicrographs document the presence of NaCl. C) Sodium chloride crystals are present in trace amounts in the studied section. Bar scale=20 μ m. EDX spectrum illustrating analysis of the NaCl crystals in (C).

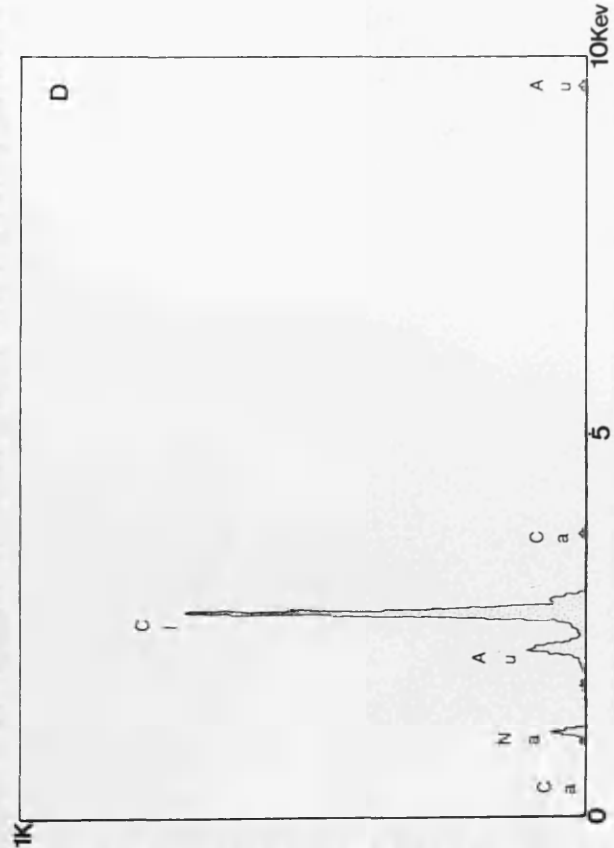
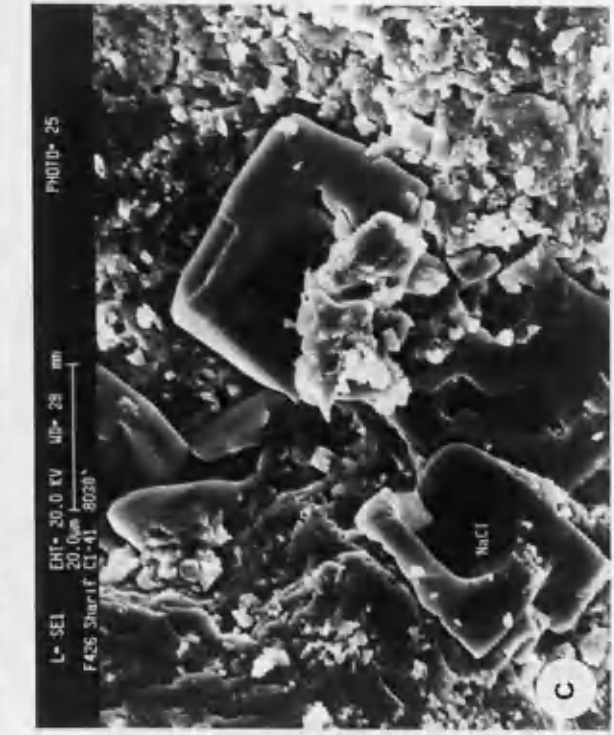
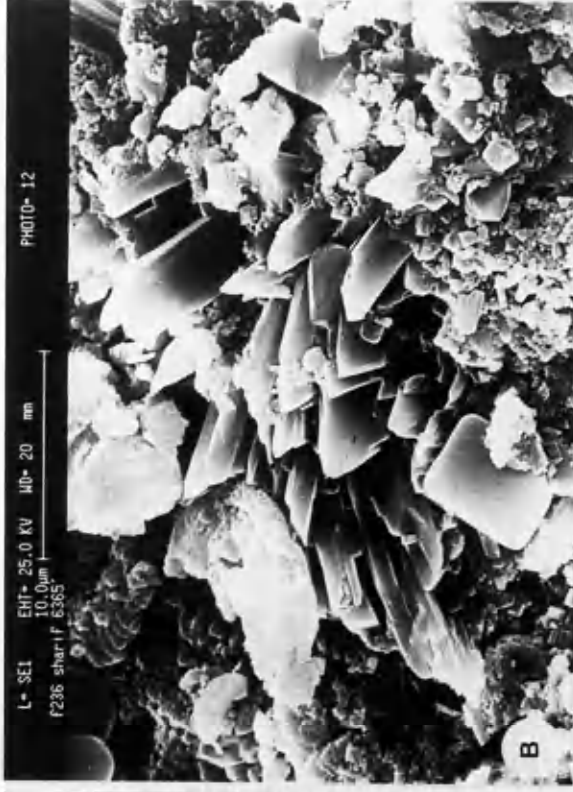
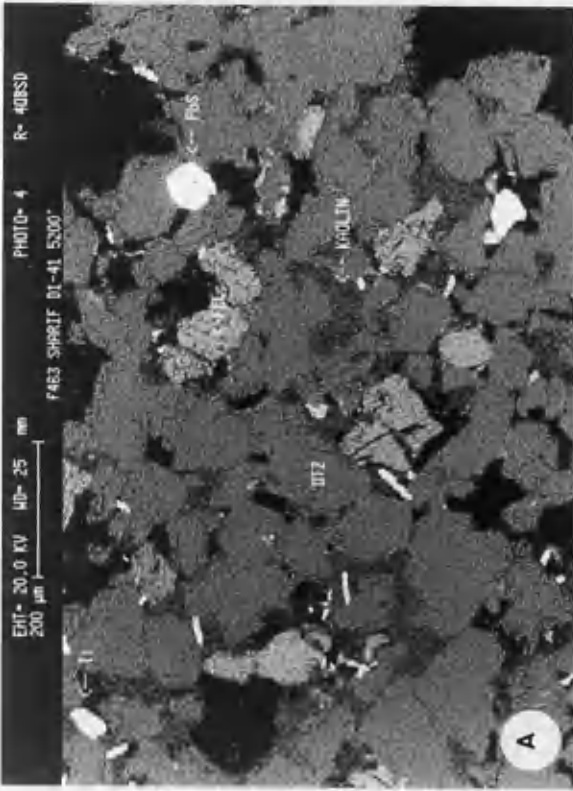


Plate 3.4

A,B) Photomicrographs showing porosity in the chalks. A) Globigerinid lime mudstone in which the bioclast tests are preserved and partially filled by sparry calcite, while void remain open (arrow). Bar scale=0.3mm. Well B2-41, depth 6380ft. B) High porosity in the chalk which might be attributed to the dissolution of bioclasts. Bar scale=0.2mm. Well B2-41, depth 6350ft.

C) Photomicrograph exhibiting the high intraparticle porosity (a) in the large nummulite packstone lithofacies. Bar scale=0.2mm. Well J1-41, depth 6136ft.

D) Photomicrograph (SEM) of porespace in coarse crystalline dolomite lithofacies. Bar scale=50 μ m.

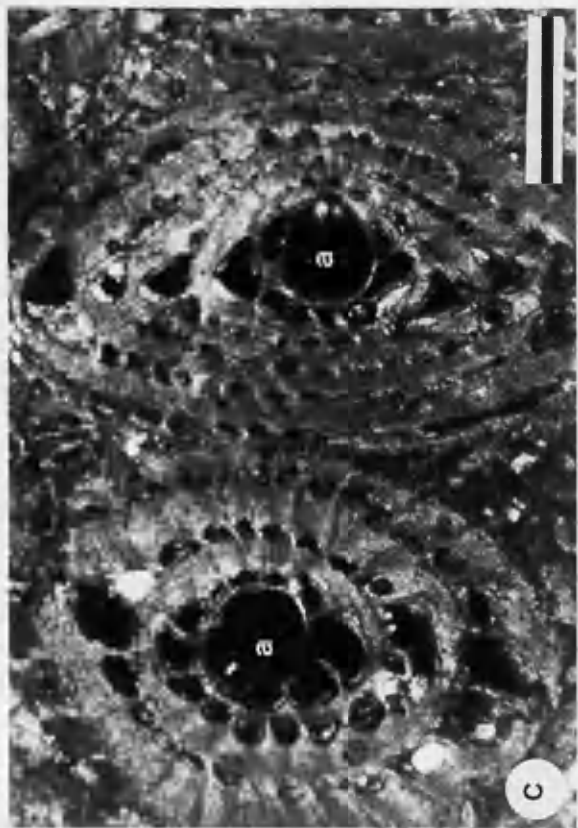
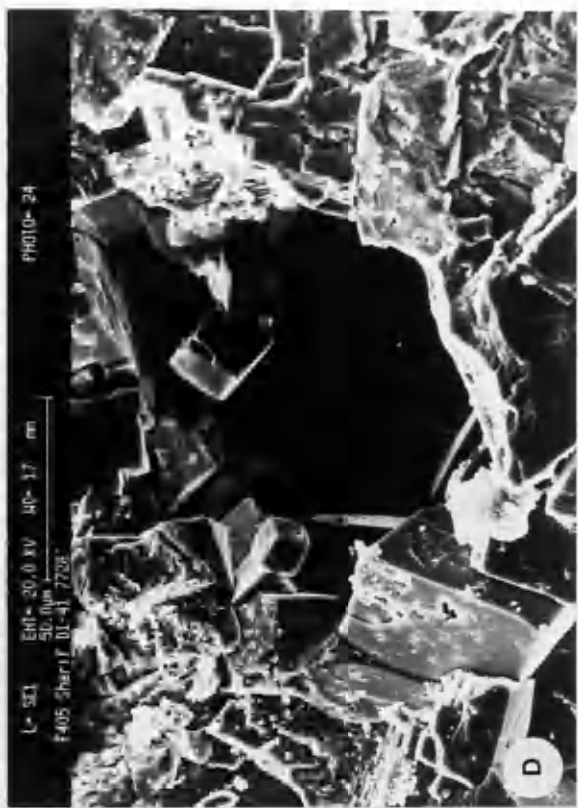
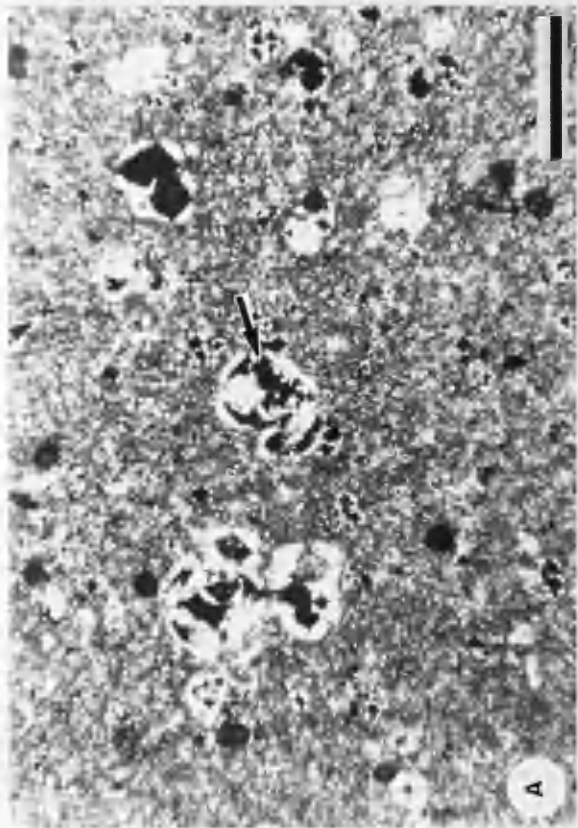
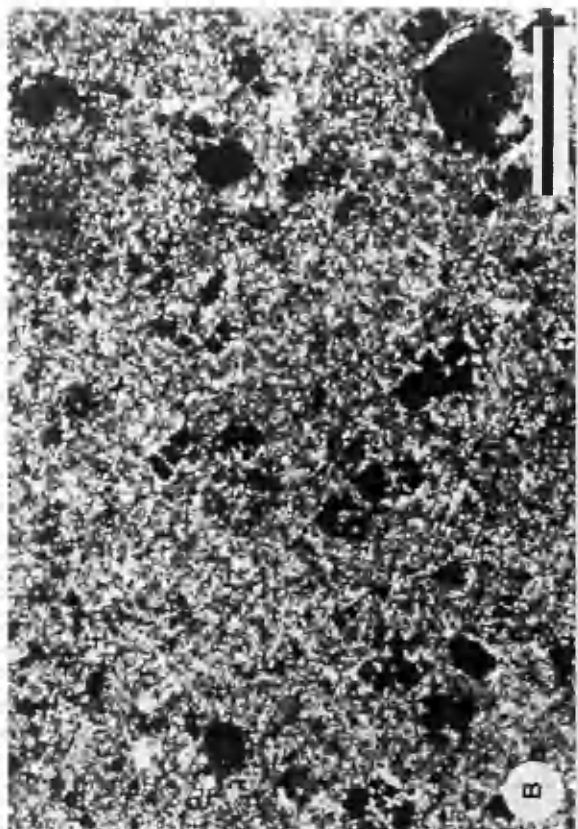
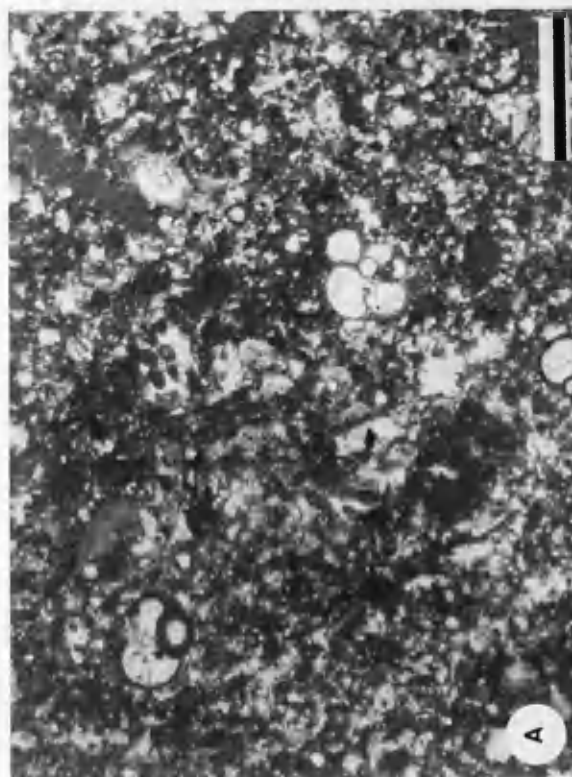
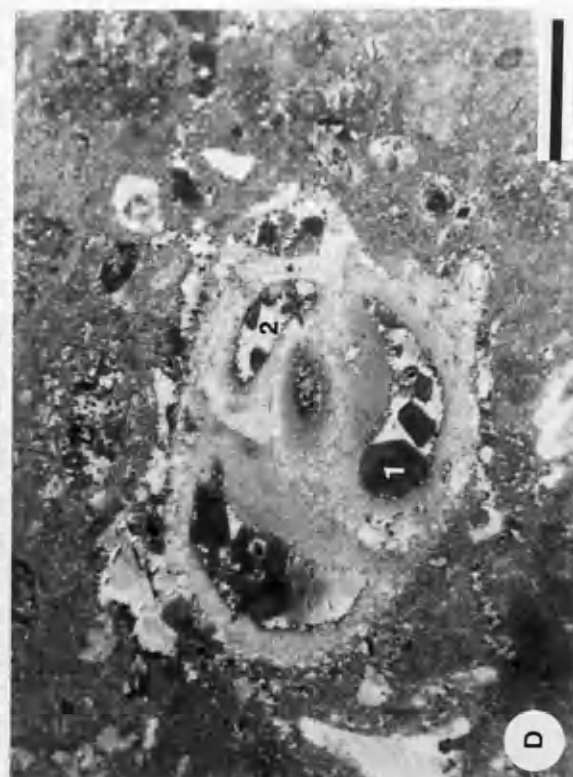


Plate 3.5

A) Photomicrograph with cathodoluminescent light of lithofacies F2 showing type I luminescence. The matrix and the cement in the chalky mudstone lithofacies are relatively bright. Bar scale= 0.3mm. Well B2-41, depth 6275ft.

B-D) Photomicrographs with cathodoluminescent light illustrate type III luminescence. B) Globigerinid in lithofacies F2 showing two cement stages the earlier (1) and the later (2). Bar scale=0.3mm. Well B2-41, depth 6430ft. C) Dull matrix and two cement stages in lithofacies F4. Bar scale=0.2mm. Well D1-41, depth 5185ft. D) Relatively dull matrix and two cement stages inside foraminiferan in lithofacies F4. Bar scale=0.3mm. Well J1-41, depth 6129ft.



CHAPTER FOUR

GEOCHEMISTRY

The geochemical analyses carried out during the course of study of the investigated core samples from the Paleocene and Early Eocene sedimentary rocks are discussed in this chapter. These analyses comprise the analysis of the elemental composition and concentration, and the isotopic signature of these sediments, specifically relating to oxygen, carbon and sulphur. Samples were first analysed by X-ray diffraction in order to ascertain dolomite and calcite contents and ratios. More than 50 samples, mostly dolomites, were prepared to establish the major and trace element contents by X-ray fluorescence. Carbon and oxygen stable isotope analyses were carried out on more than 20 samples, mostly from dolomites. Sulphur isotope analyses were performed on 5 calcium sulphate (anhydrite) samples.

The scope of this geochemical study was to identify the bulk composition of the studied sedimentary rocks and, by using the presence of trace elements such as iron, investigate the origin of the dolomitizing fluid. The analysis of stable isotopes, $\delta^{18}\text{O}$ and $\delta^{13}\text{C}$, has been used to reveal the circumstances under which dolomite formed and also the probable source for the dolomitizing fluid. The sulphur isotopic analysis $\delta^{34}\text{S}$ was carried out for the sake of gaining information about the

diagenetic calcium sulphate. In other words, the geochemical analyses were carried out in the hope of establishing a dolomitization model in the investigated area.

4.1 Methods and technique

4.1.1 X-ray Fluorescence analyses (XRFS)

Analyses were carried out using a Philips PW1450/20 automatic X-ray fluorescence spectrometer and on-line Superbrain microcomputer for data processing. The major elements were analysed from fused glass discs of 0.375g of 100 mesh powder and 2.09g of spectroflux (Lithium tetraborate). These were prepared according to the method of Harvey *et al.* (1973). For the trace elements, pressed powder pellets made of 0.375g of 100 mesh powder and 1.0g of thermal binder (phenolformaldehyde) were used (Leake *et al.* , 1969).

By using the above technique a total of 10 major oxides (e.g SiO₂, MnO, MgO, K₂O, etc.) and 16 trace elements (e.g Sr, Ba, Pb, etc.) have been analysed. The elemental and compound composition and concentrations obtained are given in Tables 4.1- 4.8. The equation for CO₂ calculation are given in the Appendix A. The detection limits are generally low, 0.165% for MgO, 0.006% CaO, 0.045% for Fe₂O₃, 0.012% for MnO and 1.5 ppm for Sr. The precision of the obtained results depends on the accuracy of calibration used and the effect of variation in mineralogy within the samples analysed

OXIDES in Wt%	D E P T H								
	12908	12829	12817	12808	12116	11602	11106	11100	11096
SiO ₂	9.86	4.07	9.59	26.86	42.17	3.71	40.8	40.4	40.3
TiO ₂	0.15	0.03	0.05	0.01	0.12	0.02	0.35	0.34	0.38
Al ₂ O ₃	3.74	0.85	1.48	0.63	3.24	0.49	6.70	6.53	6.84
Fetot	1.83	0.28	0.48	0.34	2.87	0.19	3.62	3.53	2.52
MnO	0.11	0.03	0.14	0.01	0.07	0.01	0.05	0.07	0.02
MgO	1.97	1.12	1.36	1.47	2.26	2.2	2.85	2.61	2.39
CaO	44.47	51.53	50.4	40.2	28.3	51.74	25.6	24.6	24.1
Na ₂ O	0.23	0.42	0.30	1.1	0.31	0.45	1.36	0.47	0.82
K ₂ O ₅	0.22	0.11	0.12	0.11	0.10	0.07	0.54	0.47	0.66
P ₂ O ₅	0.07	0.05	0.07	0.05	0.01	0.06	0.36	0.33	0.36
CO _{2cal}	37.0	41.6	41.0	33.1	24.6	40.6	23.2	22.14	
Total	99.7	100	102	103	104	99.5	105	101	99.9

Table 4.1, Chemical analyses for major elements from cored intervals in wellA1-41.

T-elmnt. in ppm	D E P T H								
	12908	12829	12817	12808	12116	11602	11106	11100	11106
Zr	28	5	4	b.d.l	37	b.d.l	52	81	67
Y	8	5	5	7	12	9	9	12	12
Sr	719	641	872	1096	977	1422	1672	1029	1012
U	5	b.d.l	3	5	b.d.l	0	4	4	1
Rb	11	2	5	7	6	3	21	28	22
Th	b.d.l	0	b.d.l	1	4	b.d.l	6	7	6
Pb	b.d.l	b.d.l	b.d.l	0	b.d.l	b.d.l	3	5	5
Ga	5	0	2	0	4	1	10	11	8
Zn	14	5	10	4	15	22	59	69	67
Cu	0	b.d.l	3	1	9	9	3	3	3
Ni	9	b.d.l	5	5	15	1	11	12	15
Co	2	194	b.d.l	b.d.l	4	b.d.l	5	194	191
Cr	41	178	18	21	71	8	76	278	265
Ce	18	534	13	8	16	4	44	534	546
Ba	68	481	47	44	786	1326	236	481	481
La	10	225	3	6	13	3	16	225	226

Table 4.2, Chemical analyses for trace elements from cored intervals in well A1-41

b.d.b=below detection limit.

OXIDES in Wt%	D E P T H								
	6550	6525	6430	6350	6305	6275	6185	6175	5185
SiO ₂	0.00	0.11	0.83	0.59	0.40	0.11	0.12	0.00	1.93
TiO ₂	0.01	0.03	0.03	0.04	0.04	0.11	0.02	0.01	0.03
Al ₂ O ₃	0.14	0.48	0.78	0.46	0.50	1.11	0.34	0.29	0.29
Fetot	0.06	0.18	0.31	0.17	0.20	0.53	0.16	0.10	0.14
MnO	0.05	0.01	0.87	0.04	0.04	0.00	0.1	0.04	0.01
MgO	1.07	1.05	50.6	1.87	0.97	4.24	1.9	1.09	1.98
CaO	55.8	52.88	0.37	51.29	54.19	49.3	52.9	55.1	52.09
Na ₂ O	0.36	0.61	0.37	0.28	0.73	0.53	0.63	0.77	0.47
K ₂ O ₅	0.05	0.21	0.28	0.21	0.21	0.19	0.14	0.12	0.14
P ₂ O ₅	0.01	0.35	0.29	0.14	0.18	0.08	0.06	0.08	0.15
CO _{2cal}	44.9	42.6	55.5	42.2	42.5	43.2	43.5	44.4	43.0
Total	102	98.5	110	97.3	99.6	99.5	99.9	101	100

Table 4.3, Chemical analyses for major elements from cored intervals in well B2-41.

T-elmt. in ppm	D E P T H								
	6550	6525	6430	6350	6305	6275	6185	6175	
Zr	8	b.d.l							
Y	6	19	16	13	11	9	9	6	
Sr	322	678	1161	1022	1207	1039	1212	1644	
U	1	4	3	0	3	b.d.l	b.d.l	2	
Rb	0	3	4	2	4	1	3	2	
Th	b.d.l	b.d.l	b.d.l	b.d.l	b.d.l	b.d.l	b.d.l	b.d.l	b.d.l
Pb	b.d.l	b.d.l	b.d.l	b.d.l	b.d.l	b.d.l	b.d.l	b.d.l	b.d.l
Ga	1	0	3	1	1	0	1	3	
Zn	b.d.l	76	90	77	146	38	19	49	
Cu	b.d.l	19	27	10	15	6	6	6	
Ni	1	38	37	25	35	17	6	7	
Co	b.d.l	b.d.l	1	b.d.l	0	b.d.l	1	b.d.l	
Cr	5	75	58	28	36	19	18	18	
Ce	4	7	0	7	3	11	10	0	
Ba	b.d.l	10	8752	39	17	15	25	179	
La	1	6	9	6	3	1	1	3	

Table 4.4, Chemical analyses for trace elements from cored intervals in well B2-41.

b.d.b=below detection limit.

OXIDES in Wt%	D E P T H								
	8984	8929	8961	8038	7905	7610	7514	7064	6730
SiO ₂	0.00	0.00	0.00	0.00	0.00	0.00	0.00	0.00	5.9
TiO ₂	0.01	0.01	0.01	0.03	0.02	0.01	0.01	0.01	0.14
Al ₂ O ₃	0.18	0.17	0.14	0.19	0.35	0.12	0.19	0.43	1.9
Fetot	0.06	0.08	0.03	0.00	0.09	0.02	0.06	0.17	0.76
MnO	0.00	0.02	0.03	0.10	0.05	0.02	0.05	0.00	0.02
MgO	20.2	17.8	19.15	21.7	17.4	18.6	18.1	3.28	1.28
CaO	31.2	29.9	30.5	31.8	32.82	31.5	29.2	35.5	50.9
Na ₂ O	0.97	0.19	0.17	0.23	0.97	0.16	0.07	0.06	0.81
K ₂ O ₅	0.7	0.05	0.7	0.08	0.11	0.04	0.11	0.10	0.22
P ₂ O ₅	0.7	0.05	0.2	0.01	0.02	0.01	0.01	0.20	0.12
CO _{2cal}	46.4	43.3	44.8	48.6	44.6	34.8	42.6	31.4	41.3
Total	100	91.6	95.7	102	96.4	85.4	90.5	71.2	103

Table 4.5, Chemical analyses of major elements in cored intervals in well C1-41.

T-elmt. in ppm	D E P T H									
	8984	8979	8961	8038	7905	7610	7514	7064	7054	6730
Zr	19	15	14	18	16	14	18	11	8	1
Y	4	6	5	4	4	4	5	8	8	11
Sr	98	231	248	60	82	45	77	804	883	1736
U	3	9	3	2	6	3	4	5	3	b.d.l
Rb	3	4	4	3	4	3	3	7	3	6
Th	b.d.l	1	0	b.d.l	b.d.l	b.d.l	0	0	b.d.l	b.d.l
Pb	b.d.l	b.d.l	b.d.l	b.d.l	b.d.l	b.d.l	b.d.l	b.d.l	b.d.l	b.d.l
Ga	b.d.l	b.d.l	0	0	0	0	b.d.l	0	0	3
Zn	16	6	9	19	3	14	2	104	68	36
Cu	b.d.l	b.d.l	b.d.l	b.d.l	b.d.l	b.d.l	b.d.l	10	5	10
Ni	b.d.l	b.d.l	b.d.l	b.d.l	b.d.l	b.d.l	b.d.l	35	16	15
Co	b.d.l	b.d.l	b.d.l	0	0	b.d.l	b.d.l	b.d.l	b.d.l	2
Cr	9	11	8	11	11	0	18	65	28	20
Ce	0	2	4	4	1	b.d.l	b.d.l	4	5	11
Ba	10	4	25	7	16	10	10	16	3	58
La	b.d.l	1	b.d.l	b.d.l	b.d.l	b.d.l	2	1	1	3

Table 4.6, Chemical analyses of trace elements in cored intervals in well C1-41.

b.d.b=below detection limit.

OXIDES in Wt%	D E P T H								
	7743	7708	7688	7516	6179	6106	5735	5723	5195
SiO ₂	0.00	0.00	0.00	0.00	0.46	0.00	0.00	0.00	0.43
TiO ₂	0.1	0.01	0.01	0.01	0.30	0.00	0.01	0.01	0.02
Al ₂ O ₃	0.19	0.20	0.17	0.22	0.56	0.17	0.21	0.19	0.25
Fetot	0.03	0.06	0.03	0.07	0.22	0.04	0.01	0.09	0.10
MnO	0.04	0.65	0.05	0.01	0.04	0.00	0.13	0.14	0.01
MgO	18.98	21.8	20.2	17.4	17.8	17.72	0.55	1.30	2.01
CaO	32.54	32.5	32.6	29.8	31.67	27.15	57.36	57.16	52.99
Na ₂ O	0.11	0.46	0.05	0.55	0.97	0.98	0.59	0.45	1.03
K ₂ O ₅	0.05	0.06	0.05	0.08	0.24	0.07	0.06	0.05	0.13
P ₂ O ₅	0.02	0.12	0.06	0.07	0.34	0.01	0.01	0.01	0.18
CO ₂ cal	46.2	49.2	47.5	42.2	44.2	40.6	45.6	46.2	43.7
Total	98.3	105	100	90.4	96.9	86.7	104	105	100

Table 4.7, Chemical analyses of major elements from cored intervals in wellD1-41.

T-elmt. in ppm	D E P T H										
	7743	7725	7708	7688	7516	6719	6179	6106	5735	5735	5195
Zr	11	10	13	18	16	17	17	14	14	12	10
Y	4	4	5	5	5	9	14	10	6	5	5
Sr	267	392	135	83	123	133	218	200	271	280	528
U	4	6	4	6	5	8	5	4	8	7	3
Rb	2	3	3	3	3	6	4	5	4	4	5
Th	3	4	3	1	4	3	1	2	3	3	3
Pb	1	0	b.d.l	0	b.d.l						
Ga	b.d.l	b.d.l	b.d.l	0	0	0	1	1	0	b.d.l	2
Zn	7	6	5	11	13	25	63	30	6	5	33
Cu	b.d.l	b.d.l	b.d.l	b.d.l	b.d.l	b.d.l	2	b.d.l	b.d.l	b.d.l	b.d.l
Ni	b.d.l	b.d.l	b.d.l	b.d.l	b.d.l	4	30	13	3	0	5
Co	b.d.l	b.d.l	b.d.l	b.d.l	0	b.d.l	b.d.l	b.d.l	b.d.l	b.d.l	b.d.l
Cr	11	8	7	12	13	46	80	46	17	14	23
Ce	5	5	2	b.d.l	1	11	7	4	8	1	1
Ba	12	13	10	10	7	10	17	7	b.d.l	8	0
La	b.d.l	b.d.l	2	1	b.d.l	4	8	4	b.d.l	6	b.d.l

Table 4.8, Chemical analyses of trace elements from cored intervals in well D1-41.

b.d.b=below detection limit.

All trace element results are given in parts per million (ppm), while the major oxides are in weight percent (wt%).

4.1.2 *Stable isotope analysis*

The dolomite and sulphate isotopic analyses were determined in the Isotopic Laboratory of the Isotope Unit at the Scottish Universities Research Reactor Centre. The Isotope analyses of $\delta^{18}\text{O}$ and $\delta^{13}\text{C}$ were carried out using a VG isotech Sira 10 mass-spectrometer. The preparation of the samples for CO_2 extraction was following the procedures described by McCrea (1950). The isotope analyses of $\delta^{34}\text{S}$, were carried out using a VG isotech Sira 2 mass-spectrometer. Gas extraction (SO_2) was done using the technique described by Coleman and Moore (1978).

After analysing the samples using X-ray diffraction, dolomite samples were chosen among them for carbon $\delta^{13}\text{C}$, oxygen $\delta^{18}\text{O}$ and sulphur isotopic analyses. Anhydrite was present in some of the dolomite samples, and chemical separation was applied due to the difficulty of physical separation. The separations were done seeking dolomite samples free of impurities in the interests of precision of the measurements. The preparation of the analysed samples was started with the reaction of 14.8-20g of rock powder with 5ml orthophosphoric acid. The reactions of these samples were run under two different temperatures. One set of samples was retained in a hot bath at 25°C for three days, another set was kept overnight at 100°C . For accuracy reasons analyses of most the samples

Well no	Depth (ft)	$\delta^{13}\text{C}$ (PDB)	$\delta^{18}\text{O}$ (PDB)	$\delta^{18}\text{O}$ (SMOW)
D1-41	8963	1.650	-3.985	26.802
	7743	2.324	-6.126	24.595
	7725	2.204	-4.030	26.750
	7688	3.606	-2.898	27.923
	7708	2.532	-2.885	27.936
	7516	2.476	-4.801	25.961
	6719	0.920	-2.461	28.373
	6108	0.747	-2.400	28.430
	6106	0.648	-0.440	30.349
	C1-41	8984	1.605	-2.024
8979		1.672	-4.648	26.118
8976		1.724	-6.690	24.013
8970		1.548	-5.353	25.392
8969		1.357	-3.892	26.898
8963		1.740	-3.506	27.296
8961		1.536	-5.411	25.331
7905		0.779	-5.756	24.886
7728		2.029	-4.030	26.756
7612		1.946	-8.275	22.380
7610		1.952	-5.824	24.906
7514		1.988	-8.346	22.306

Table 4.9, Results of carbon and oxygen isotope analyses of dolomite, results are in Parts per mil.

Well no	Depth(ft)	$\delta^{34}\text{S}$ (CDT)
C1-41	7612	+21.50
	7610	+21.11
D1-41	7743	+20.84
	7725	+22.12
	7729	+21.61

Table 4.10, Result of sulphur isotope analyses of calcium sulphate in part per mil

were repeated. The liberated CO₂ gas was collected and analysed using the mass-spectrometer. The carbon $\delta^{13}\text{C}$ and oxygen $\delta^{18}\text{O}$ isotope results are given as per mil deviation relative to the Chicago CO₂ standard PDB (Table, 4.9). Oxygen isotope results in carbonate are sometimes reported relative to SMOW, but the PDB standard is more widely used. The equation of conversion between the PDB and SMOW, defined by Coplen et al. (1983), is given in the Appendix A.

The sample preparation for sulphur isotope analyses, consisted first of chemical separation of anhydrite from dolomite. The dolomite was dissolved in HCL and 10ml of BaCl added to precipitate the sulphate. 15-20 mg of the powdered calcium sulphate, 600mg of fine silica, and 200mg fine copper (Cu₂O) were heated to 1120°C. SO₂ was extracted after releasing other gases by vacuuming out. The $\delta^{34}\text{S}$ is (Table 4.10) given as per mil relative to troilite of the Canon Diablo meteorite (CDT).

4.2. Results and discussion

4.2.1 Trace elements

The study of the trace elements in the investigated area reveals a general consistency throughout the Palaeocene and Early Eocene core samples. The Sr contents are slightly low in the dolomite compared with other lithofacies. The Fe, Mn, Si, and Al contents, given in oxides are generally low. These elements will be discussed in detail below and the geochemical characteristics inherent to each lithofacies are presented in

Fig. 4.1-4.5.

a- *Strontium* (Sr) Strontium is one of the most important minor elements in sedimentary carbonate rocks. The Sr distribution is normally a function of the facies type and is not random (Veizer and Demovic, 1974). The Sr contents of carbonate rocks tend to decrease with increasing alteration by water of meteoric origin.

The influence of the Sr contents of the replaced (precursor) mineral upon the Sr contents of dolomite, has been discussed by Veizer and others (1978) who regarded the precursor influence as significant. Early dolomite with high Sr was interpreted as replacing aragonite while, in contrast, diagenetic dolomite low in Sr was interpreted as replacing other carbonates that lacked Sr (Veizer *et al.*, 1978).

In the studied core samples the slightly high Sr in the chalky lithofacies, in contrast with the slightly low Sr in the other lithofacies, could be related to a higher proportion of stable low Mg calcite in the original sediments of the latter. It is noticeable that the dolomite facies in wells C1-41 and D1-41 has slightly lower Sr compared with the calcite dominated facies in the same wells. This may be interpreted by the assumption made by Veizer and Demovic (1974) in which the loss of Sr is connected with observed high dolomitization.

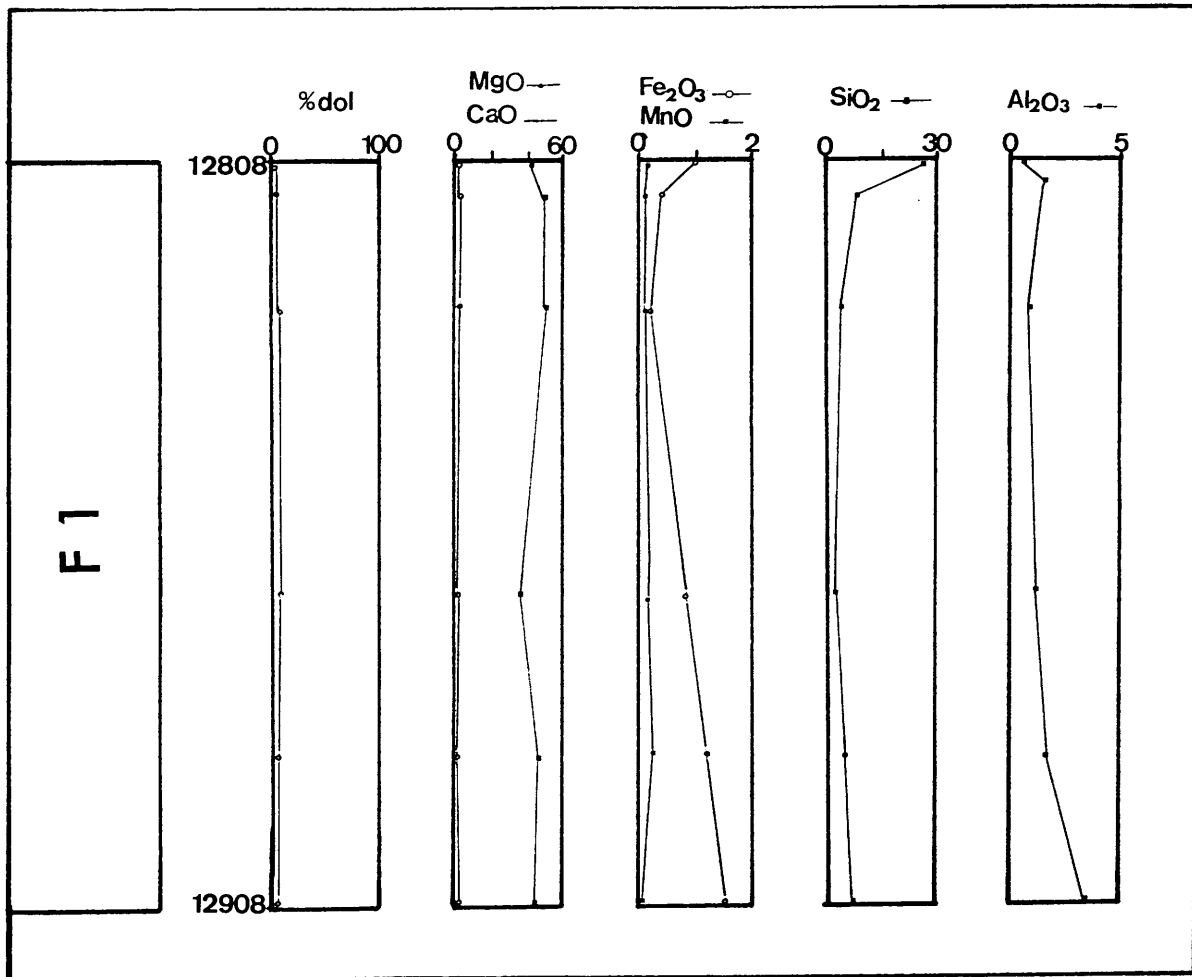


Fig. 4.1, Shows the vertical distribution of major and trace element concentration of the lithoclast bearing mudstone lithofacies in well A1-41.

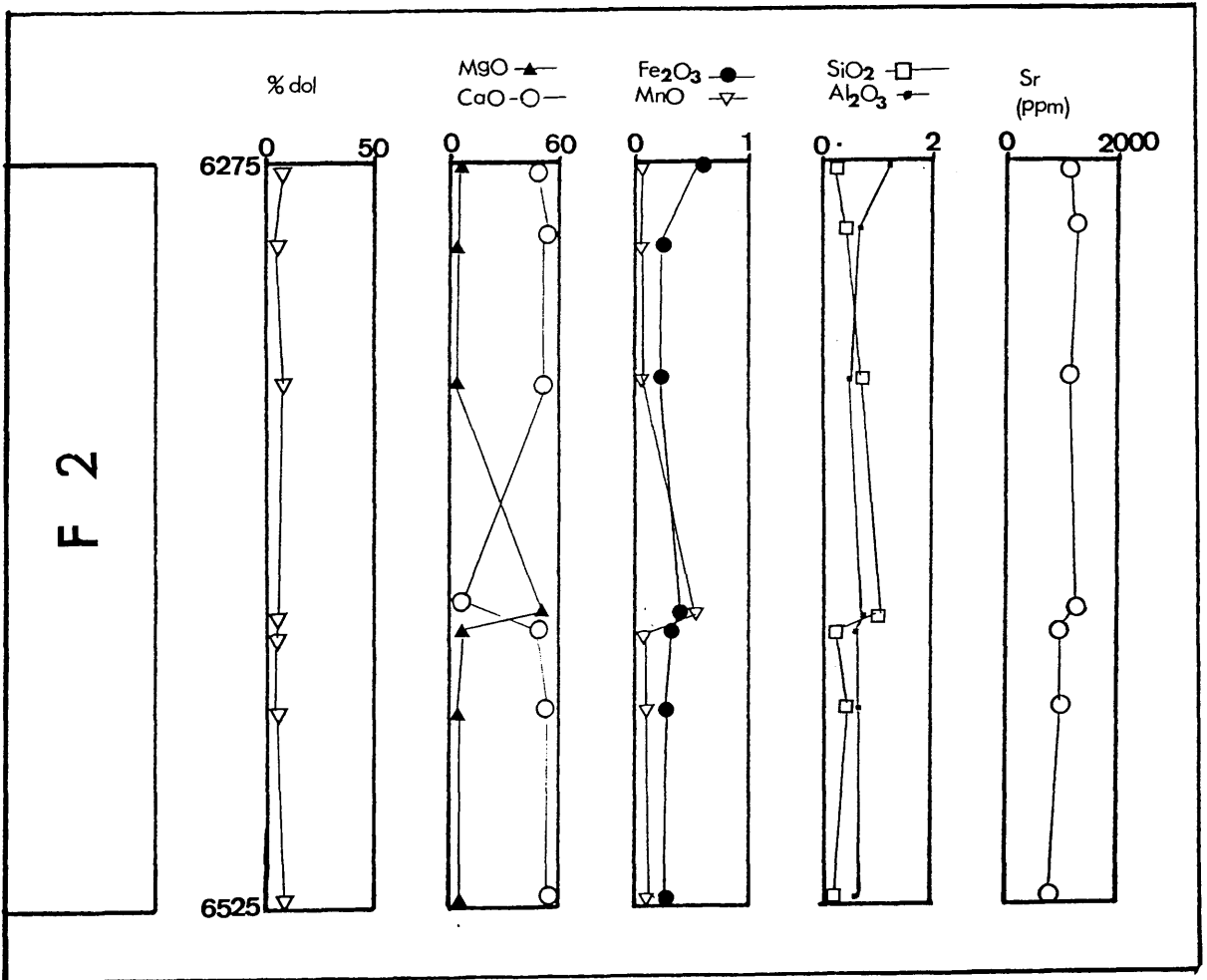


Fig. 4.2, Shows the vertical distribution of major and trace element concentration of the chalky mudstone lithofacies in well B2-41.

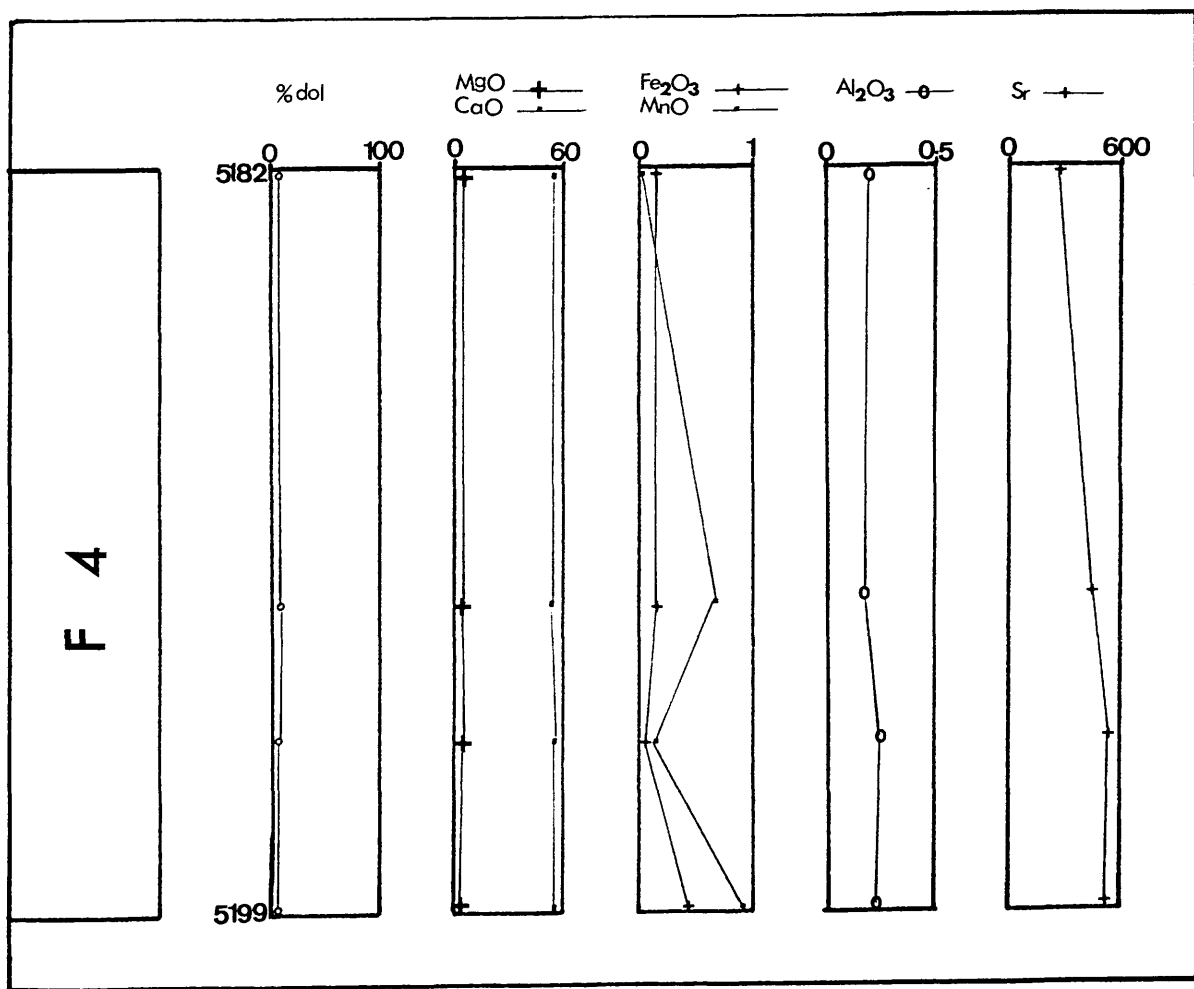


Fig. 4.3, Shows the vertical distribution of major and trace element concentration of the the large Nummulite packstone lithofacies in well D1-41.

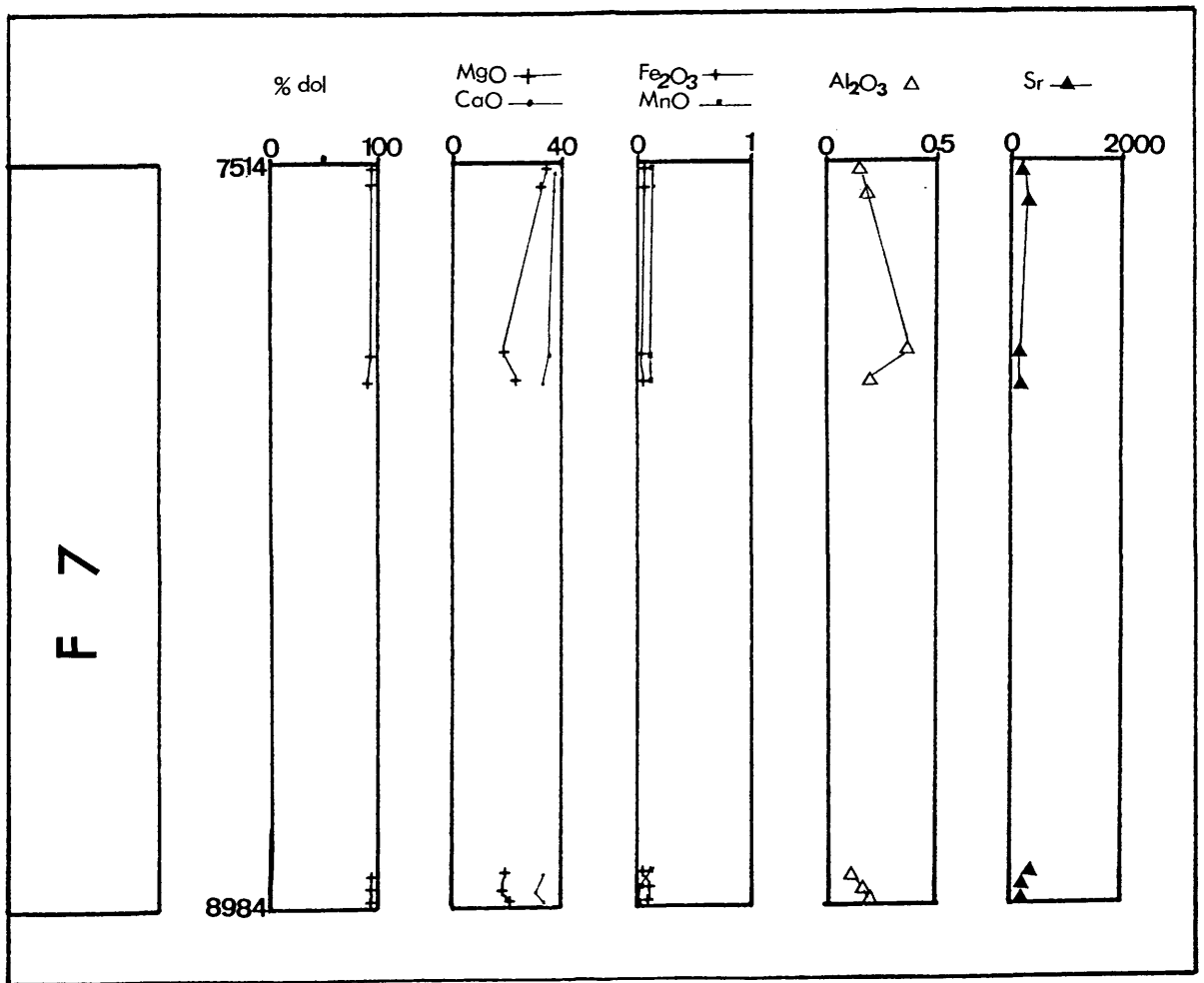


Fig. 4.5, Shows the vertical distribution of major and trace element concentration of the coarse crystalline lithofacies in well C1-41.

The Sr content has also been used to reveal the composition of the dolmitizing fluid and subsequently to assist in construction of a dolomitization model (Veizer, 1983). Usually a dolomitizing fluid which has more than 20% sea water would have an Sr figure close to the typical marine Sr content. When salinity increases the Sr content is also expected to increase, bearing in mind, however, that the most important factor which determines the amount of Sr in dolomite is the time of dolomitization. Early diagenetic finely crystalline dolomites have higher Sr contents than later diagenetic coarse dolomites. The range of Sr in late diagenetic dolomites is typically 90-300 ppm (Veizer and Demovic, 1974), and this figure fits very nicely with the range observed in the investigated dolomite section.

b- *Iron and Manganese* :Iron present in solution in sea water shows an approximate range of 0.002 to 0.020ppm (Sverdrup, Johnson and Fleming, 1942). In contrast, the Fe present in fresh water ranges from 0.031 to 1.67ppm with an average near 0.506ppm (Drum and Haffty, 1961). Manganese in solution in sea water ranges from 0.001 to 0.01ppm (Sverdrup, Johnson and Fleming, 1942), while Mn in fresh water has a value ranging from 0.002 to 0.185ppm with an average of 0.038ppm (Drum and Haffty, 1961). In general, fresh waters are weakly acidic and therefore, contain more soluble iron and manganese than do marine waters, which are generally alkaline. In general, therefore fresh waters contain higher levels of both Fe and Mn.

There are many views concerning the presence of iron in dolomite, but it appears to be enriched in dolomite formed under the anoxic conditions common after burial while there is little in dolomite formed under the oxidizing conditions characteristic of shallow water (Land, 1985). Mattes and Mountjoy (1980), pointed out in addition that early formed, pervasive burial dolomites are also iron poor. In general there is little difference in Mn content between primary and secondary dolomites, although usually secondary dolomites have slightly higher Mn, averaging 632ppm. The Mn distribution is believed to reflect the influence of precursor derived Mn.

The studied samples are generally poor in Fe and Mn. The iron content in the Tables is given in total Fe_2O_3 . This includes both ferrous (FeO) and ferric (Fe_2O_3) iron and reaches a maximum of 3.62 wt%. This low concentration does not allow discrimination between the two oxidation forms. The Mn oxides (MnO), reach a maximum 0.87 wt%. As the total iron concentration reflects the quantity of iron delivered to a site during deposition and diagenesis, the low iron content in the dolomite section may indicate a low terrigenous contribution to the precursor during its depositional history, and generally low iron contents of subsequent diagenetic fluids. Iron and manganese are both important elements to cathodoluminescence acting respectively as quenchers and activators. This will be discussed in section 3.2.6.

c- *Si, Al, and K* : These three elements, given in the form of oxides, show a variation in their distribution in the revealed lithofacies. The lithoclast bearing mudstone lithofacies contains the highest proportion of these elements, apparently due to the presence of hemipelagic siliciclastic muds and some platform derived quartz (Fig. 4.6). The chalky lithofacies contains less of these elements, but is generally still high and this may be interpreted as due to the presence of argillaceous chalk. The nummulitic facies also has high contents in some parts, especially in the form of SiO_2 . This may reflect the presence of small clastic pockets which are incorporated in the facies. In the dolomites Si, Al, and K are generally low which probably reflecting the lack of clay minerals in the precursor sediments. The derivation of these elements is usually due to the destruction of less resistant clay minerals and this source appears the most likely in the absence of any other apparent carrier of these elements. These clays are generally rich in the materials which comes from the platform.

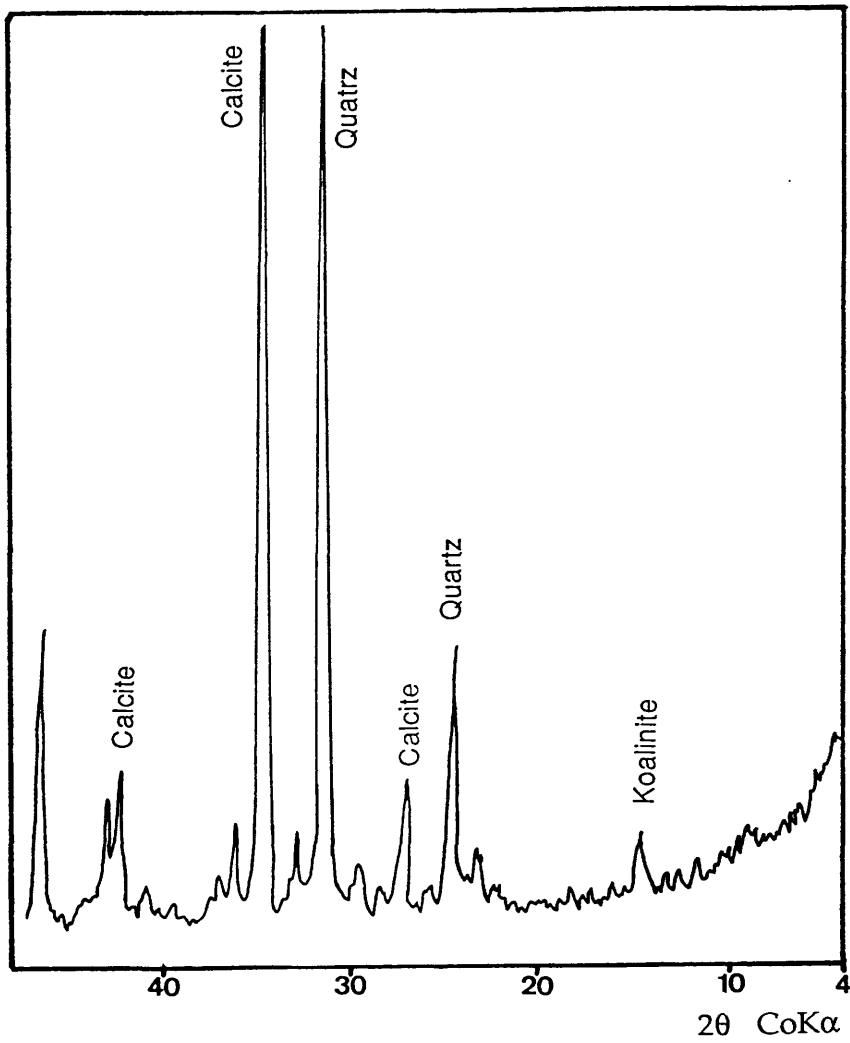


Fig. 4.6, X-ray diffraction pattern, showing the existence of quartz and trace of koalinite in the lithoclast bearing mudstone lithofacies. Depth 11106ft, well A1-41.

4.2.2 Stable isotopes

a- *Oxygen and Carbon* : The study of Stable isotopes has in recent years contributed significantly to the solution of many problems in earth science. Oxygen and carbon isotope analyses combined with chemical analyses and petrography have been used to infer a dolomitization model in the study area. Usually the $\delta^{18}\text{O}$ of diagenetically altered carbonate reflects the $\delta^{18}\text{O}$ of the reactive fluid, as well as the temperature of that fluid.. This includes the type of dolomitizing fluid and the circumstances which prevailed during the dolomitization process. This follows the work of Fritz (1971), Land (1980), Knauth and Beeunas (1986), Shukla (1988) and others who have used different isotopes to reveal solutions for the dolomitization dilemma.

The isotopic analyses of oxygen and carbon were carried out mostly on dolomite samples from two wells C1-41 and D1-41 in the northern part of the Agdabia trough. These show a general depletion in ^{18}O , that is, negative $\delta^{18}\text{O}$ values (relative to the PDB standard). The $\delta^{18}\text{O}$ values range between -2.4 to -8.3 per mil (PDB). In well D1-41 (Fig. 4.7), the relationships suggest lighter $\delta^{18}\text{O}$ with increasing in depth. The $\delta^{13}\text{C}$ values show homogeneity on a small scale but are more variable on a large scale and range between 0.6 to 2.5 per mil PDB, reflecting formation in water in equilibrium with marine sediments (Fig. 4.8). The narrow range in the $\delta^{13}\text{C}$ values probably reflects the resistance of carbonate to ^{13}C depletion during diagenesis, discussed by Land and others (1975). The $\delta^{18}\text{O}$ and $\delta^{13}\text{C}$ results do not allow any distinction to be made between the

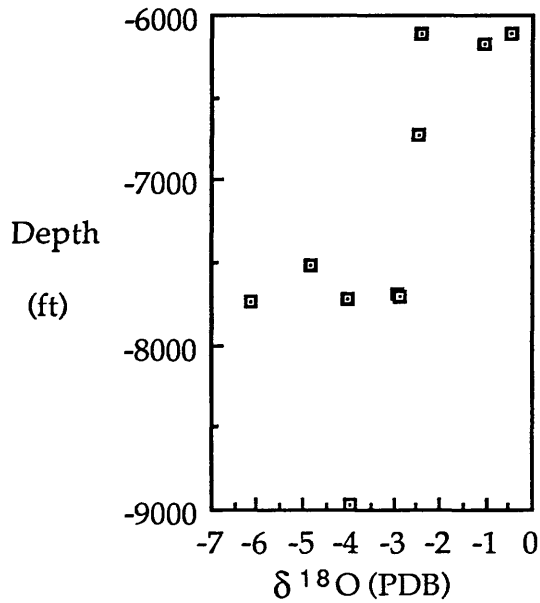


Fig. 4.7, Relationship between $\delta^{18}\text{O}$ and depth in the dolomite section (well D1-41). $\delta^{18}\text{O}$ suggest general depletion with depth.

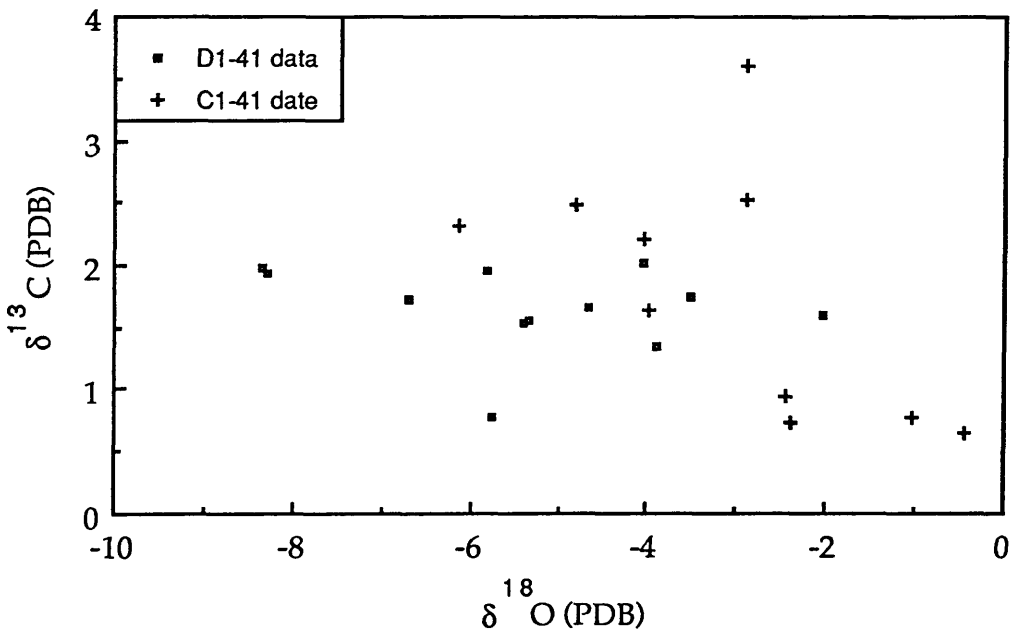


Fig. 4.8, Oxygen-carbon isotopic composition of dolomite. Note trend towards more depleted $\delta^{18}\text{O}$. $\delta^{13}\text{C}$ is homogenous on a small scale but variable on a large scale.

dolomites in the studied area.

The temperature of precipitation of dolomite can be determined from the equilibrium relationship between the $\delta^{18}\text{O}$ of dolomite, and the $\delta^{18}\text{O}$ of the precipitating water. Using the minimum, the average and the maximum values of $\delta^{18}\text{O}$ (22, 26 and 28 in SMOW) obtained from the analyses of the studied samples, the $\delta^{18}\text{O}$ of the water was calculated within a range of temperatures (25°C , 50°C , 75°C , and 105°C) where 105°C represents the average recorded temperature from the fluid inclusion petrography (Appendix B). The figures have been calculated using the dolomite - water fractionation equation given by Fritz and Smith (1970).

$$10^3 \ln \alpha \text{ dolomite - water} = 2.78 \times 10^6 T^2 + .11$$

Where

$$10^3 \ln \alpha \text{ dolomite - water} = \delta^{18}\text{O dol} + \delta^{18}\text{O water}$$

From the resulting Fig. 4.9, marine water has a $\delta^{18}\text{O} = 0$ per mil. Water able to precipitate dolomite has an isotopic range of ($\delta^{18}\text{O} = 22-28$ per mil), and therefore the inferred temperature of precipitation lay between $50-80^\circ\text{C}$.

The $\delta^{18}\text{O}$ of dolomite is dependant at least as much upon the $\delta^{18}\text{O}$ of the precipitating water (the dolomitizing fluid) and the temperature at which it formed, as upon the $\delta^{18}\text{O}$ of the carbonate

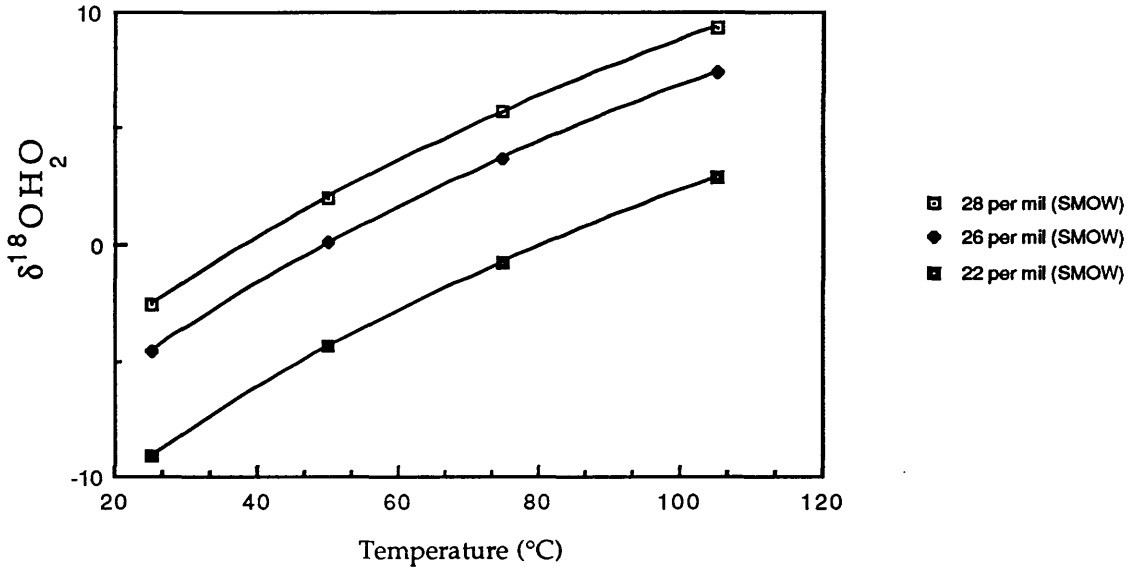


Fig. 4.9, Equilibrium relationship between $\delta^{18}\text{O}$ of dolomite (Curved lines), temperature, and the predicted $\delta^{18}\text{O}$ of water.

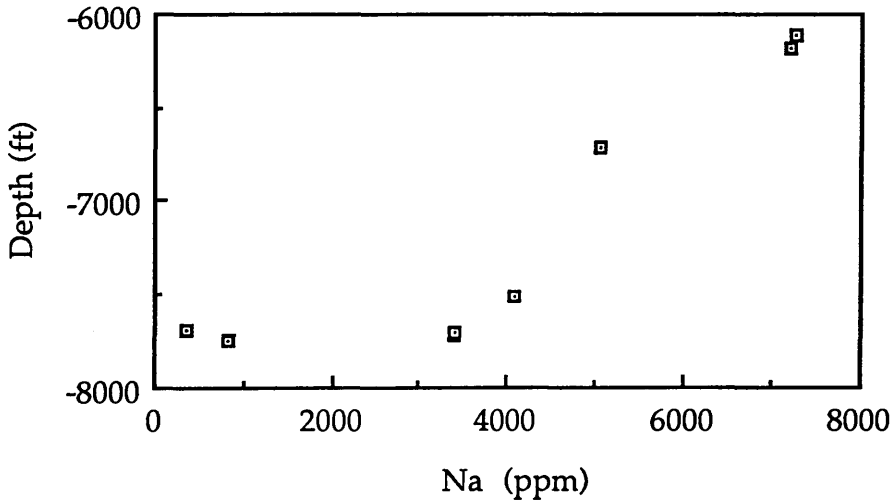


Fig.4.10, Relationship between depth and Na content in D1-41. There is a decrease in the Na content with depth.

precursor. Land (1985) pointed out that most dolomites which are depleted by more than -2 per mil must have been either formed from water depleted in ^{18}O with respect to sea water, or influenced by high temperature. Evaporite fluids can have low $\delta^{18}\text{O}$ values, because negative $\delta^{18}\text{O}$ values can occur if the brine consists of evaporated sea water mixed with early diagenetic meteoric water. This is due to the fact that meteoric water is usually depleted in oxygen while water which has been affected by evaporation becomes increasingly enriched in $\delta^{18}\text{O}$ with evaporation. For example, the natural brines from Bonaire and the Arabian Gulf, with salinities between 150-200ppt. are enriched in $\delta^{18}\text{O}$ by +1 to +5 per mil (Lloyd, 1966). During the early stages of the evaporation process the lighter oxygen isotopes are preferentially removed and the residual fluid becomes enriched. This would be different if the evaporation continued to the stage of halite formation where ^{18}O enrichment stops increasing and starts decreasing (Fallick, 1991; Hosler, 1979). Wu and others (1984) pointed out that there will be 19% depletion after the halite stage.

In the studied sections, dolomite co-exists with evaporites. This sheds some light on the type of fluids which dolomitized the rocks, because the deposition of such significant amounts of anhydrite and the presence of halite traces, indicates deposition from a highly saline fluid. This conclusion is also supported by the high Na content of the dolomites (Fig. 4.10). In addition, the revealed isotopic compositions of the water in the studied core samples average about +5 per mil (PDB).

Faure (1986) suggested that if dolomitization takes place soon after deposition, the enrichment in ^{18}O may be slight because the pore fluid is likely to be similar to sea water. On the other hand, if dolomitization occurs later by reaction with solutions having $\delta^{18}\text{O}$ contents different from those of sea water, the resulting $\delta^{18}\text{O}$ value of dolomite may be variable and unpredictable.

Many of the world major sedimentary basins contain significant accumulations of evaporites. During deposition there were millions of years when highly concentrated brines could have moved into underlying and surrounding sediments. The high densities of these brines allow them to sink into the lowest parts of the basins (Fritz and Frapre, 1982). Because of the strong density difference, meteoric water would be particularly ineffective at flushing out these dense brines (Demenico and Robins, 1985). In addition Knauth and Beeunas (1986) concluded that many formation waters with isotopic compositions supposedly indicative of meteoric origin are highly saline.

The interpretation of isotopic data for subsurface brines often depends critically upon assumptions regarding the isotopic composition of evaporated sea water. In the present samples there is an enrichment of $\delta^{18}\text{O}$ of water relative to SMOW. The influence of meteoric water can be ruled out since there is no any indication of any meteoric water in the section, at least before dolomitization, and usually meteoric waters are depleted in $\delta^{18}\text{O}$, which not the case here. Elevated temperatures are

suggested by both the isotope plot and fluid inclusion petrography but these usually give negative $\delta^{18}\text{O}$ values. The most probable explanation is that precipitation was from saline fluid formed from evaporated sea water. When salinity is high then the apparent temperature derived from $\delta^{18}\text{O}$ will also be high. This explanation is supported by the presence of anhydrite and halite in the section.

The $\delta^{13}\text{C}$ value of dolomites is in contrast with $\delta^{18}\text{O}$. The temperature and composition of pore fluids generally have little effect on it. It is mostly influenced by the isotopic composition of the precursor CaCO_3 . This is because the precursor minerals have more resident carbon than is present in the pore fluid. The most important factor in determining composition is the equilibrium fractionation of the carbon isotope which, in contrast with the oxygen isotope, is hardly affected by temperature. The carbon isotope values of minerals do not change when those minerals are subject to dolomitization. Although, the presence of oil and/or organic carbon can lighten the $\delta^{13}\text{C}$ values from the marine signature, this does not seem to have happened in the studied samples.

b- *Sulphur* : Faure (1986) assumed that the $\delta^{34}\text{S}$ values of marine sulphate minerals are representative of the isotopic compositions of S in the brines from which they were precipitated. The isotopic composition of sulphur varies widely . The reasons behind this variation lie mainly in sulphate reduction by anaerobic bacteria (Faure, 1986). It is known that the degree of isotope fractionation by bacteria is inversely proportional to the rate of

sulphate reduction, and consequently fractionation is regulated by either temperature or sulphate reduction or both.

Claypol and others (1980) studied in detail the sulphur and oxygen isotopes in marine sulphates and produced a plot illustrating $\delta^{34}\text{S}$ values through the Phanerozoic. From this plot $\delta^{34}\text{S}$ values during the Tertiary range between 19 to 22 per mil for marine evaporites. Thode and Monster (1965) point out that ancient evaporites usually carry almost the same isotopic composition as the parent water. This means that the $\delta^{34}\text{S}$ contents always reflect the sulphur isotopic composition of the water responsible for their crystallization. In the studied area the measured isotope values for the anhydrite present as a minor content within the dolomite vary between 20.8 to 21.50 per mil CDT with an average of 21.37 per mil. Generally these values fit the values suggested by Claypol *et al.* (1980) for Tertiary marine sulphates.

CHAPTER FIVE

DOLOMITE

Dolomite is a rhombohedral carbonate with an ideal formula $\text{CaMg}(\text{CO}_3)_2$. The intention of this study is first, to document the product and then to infer the formation processes. In other words, to study dolomite distribution and geochemistry in order to reach an adequate model to account for the presence of dolomite in the area investigated.

5.1 Distribution and description

Dolomite forms the predominant lithology in the Paleocene section of the wells studied, although it is only present as a minor component in the early Eocene samples. Dolomite abundance varies from 0 to 100 percent in the studied cores. Dolomitization is rare in A1-41 and common in J1-41 becoming more significant and pervasive in C1-41 and D1-41. The dolomite distribution patterns in the area show that the dolomitization gradient increased upwards towards the Cyrenaica platform. Rocks in C1-41 and D1-41 are preferentially and thoroughly dolomitized relative to the adjacent basinal facies (A1-41), and therefore, intervals containing more proximal lithologies are more extensively dolomitized than those containing more basinal lithologies. Murray and Luccia (1967) concluded that variation in the distribution of dolomite must

be controlled either by the distribution of the dolomitizing fluids or by the physical-chemical characteristics of the rocks themselves, including diagenetic modification of permeability pathways, increased reactivity of fine grained sediment, and mineralogic control on the sediment reactivity. These observations can be understood through the diagenetic potential of the original sediments (Schlanger and Douglas, 1974). The dolomitized sediments in the studied area were probably bioclast wackestones and bioclast packstones which were relatively coarser than basin sediments and thus more permeable, making them more susceptible to dolomitization. In addition, the most extensively dolomitized sediments in the area are those closest to the platform from which the dolomitizing fluid was derived.

Dolomite co-exists with evaporites in the core samples examined. The evaporites, which consist predominantly of anhydrite (Plate 3.1, D), range from trace amounts to approximately 10% in certain intervals. Anhydrite occurs mostly as a filling to vugs and some fossil casts, although it is also rarely present as a replacement. The anhydrite has most probably deposited first as gypsum, then dehydrated during was burial to form anhydrite. At temperatures below 50°C gypsum is the thermodynamically stable phase and should be precipitated instead of anhydrite (Hardie, 1967). Halite is present as a negligible amount only detected by SEM (Plate 3.3, C,D). Petrographic evidence suggests that the precipitation of the evaporites postdated dolomitization.

In the samples examined dolomitization was highly fabric selective, and was characterized by the obliteration of organic textures. The original fabric is only sparsely preserved, although it can be inferred in some places. The petrographic characteristics of the dolomite have been discussed in chapter two. Skeletal fragments in the dolomitized lithologies exhibit both mimetic and non mimetic replacement, as described by Sibley and Gregg (1987) these authors suggested that the mimetic replacement to the dolomite results from nucleation in optical continuity with the host, preserving its original microstructure and macroform. Non mimetic replacement results from destruction of the original microstructure during dolomitization. The degree of dolomitization of skeletal fragments in the samples varies greatly. Moldic porosity commonly developed in association with both mimetic and non mimetic replacements where molds and vugs in extensively dolomitized intervals are sometimes filled by geopetal dolomite sediments consisting of anhedral to subhedral crystals.

Abundant nucleation sites will lead to the formation of many small crystals. As the availability of nucleation sites decreases, fewer crystals form, but these may grow to a larger size (Sibly and Gregg, 1987). Thus differences in nucleation might be the reason for the presence of crystals of different sizes in the studied samples. Mimetic replacement of bioclasts is also controlled by the original crystal sizes. Fine grained microstructures provide abundant nucleation sites, resulting in their detailed preservation (Bullen and Sibley, 1984).

5.2 Geology of the area during the Tertiary

The Cyrenaica platform is located to the east and northeast of the studied wells and has had a significant influence on the depositional style in the Agdabia trough, beginning with the formation of the trough in the Upper Cretaceous. During the Paleocene the majority of Cyrenaica was dominated by Carbonate and evaporite deposits. The basin was characterised by deep water to the north and west where thick shales and carbonates were deposited, while on the Cyrenaica platform thin evaporites formed. Dolomite formation took place around the margins of the evaporitic platform with dolomites passing laterally into limestones and then limestones interbedded with shales in the deeper parts of the trough.

During the Eocene, the situation remained similar, evaporites were still confined to the middle of the platform which was surrounded by dolomite formation. This took place around the basin margins and dolomite again changes laterally towards the Agdabia trough, first to limestones, then to shales and limestones. Generally the depositional patterns in the Late Eocene were more or less the same as that in the Paleocene.

Usually in periods of lowstand of relative sea level, platform interiors should be more restricted, if not exposed and therefore more prone to the formation of evaporites. Thus, sea level changes may lead to

intervals of platform emergence and submergence, and are the kind of phenomena which might be responsible for the depositional pattern on the Cyrenaica platform where extensive evaporites have been deposited.

5.3 Geochemistry

In the studied area dolomite is relatively poor in iron. Land (1980) pointed out that there is commonly systematic variation in dolomite trace element content. The trace element content of crystals is proportional to the trace element composition of the solution from which the crystals forms. Diagenetic modification is believed to have been responsible for resetting both major and trace elements in dolomites. The analyses of oxygen stable isotopes (chapter four) are consistent with derivation from evaporated sea water. Sea water becomes increasingly enriched in ^{18}O with evaporation. The natural brines from Bonaire and the Persian Gulf, with salinities between 150-200 ppt., are enriched in ^{18}O by +1 to +5 per mil (Lloyd, 1966). Thus, the +3 to +7 from the studied dolomite would be a reasonable range of $\delta^{18}\text{O}$ derived from brines, at temperatures between 50-80°C.

5.3.1 *Fluid inclusions*

Fluid inclusion microthermometry was performed on a Leitz Dialux 20 EB microscope and a LINKAM TH 600 heating and cooling stage. Doubly - polished thin sections were prepared using low speed saws and ultraviolet (low temperature) curing epoxy to avoid reequilibration during

sample preparation.

a- *Introduction* : Fluid inclusion microthermometry is a technique by which the composition, salinity and temperature of entrapment of fluid inclusions may be determined. The homogenization temperature (T_h), is the temperature at which two-phase, liquid-vapour inclusions homogenize to liquid and is an indication of the minimum temperature of entrapment, provided that the inclusion was trapped as a homogeneous phase, that the volume of the inclusion has remained constant since time of entrapment and that there has been no leakage of fluid from the inclusion (Roedder, 1984). The homogenization temperature of the two-phase fluid inclusions was measured before any freezing was attempted, because expansion of ice can stretch the inclusion, thus violating the assumption of constant volume. The inclusions were heated slowly (about 10 °C/min) until the bubble homogenized. The inclusion was then cooled and the reappearance of the bubble carefully observed. If the bubble gradually expanded it was probably not completely homogenized. If the bubble failed to renucleate after cooling to room temperature, then the inclusion has probably been homogenized.

The major ions in solution can be recognized by their characteristic eutectic melting temperature. Their concentration can be calculated from freezing point. The inclusions were first frozen by cooling to about -70 °C. As the inclusion is re-heated the eutectic (T_e), the temperature at which the inclusion first melts, is recorded. Detailed eutectic melting phenomena cannot be observed because of the small size of the inclusions. The initial melting point in the samples examined was

commonly observed in the vicinity of -20°C . The eutectic melting point for the $\text{NaCl-H}_2\text{O}$ system is -20.8 , suggesting NaCl brines. The inclusions were warmed past the eutectic melting temperature at which the last ice melted and the temperature (T_m) recorded. Care was taken to make sure that the bubble was present during the final melting of ice or a metastable melting phenomenon result (Roedder, 1984). Salinity was calculated using the equation of Crawford (1981).

b- Discussion : Examination of the dolomite samples revealed two-phase fluid inclusions with an average homogenization temperature of 105°C and a freezing point depression (Appendix B) ranging between -12 and -18 . These translate to salinities of 162 and 210 ppt NaCl equivalent.

When interpreting fluid inclusion data in sedimentary rocks caution must be taken, because of the possibility of reequilibration, especially in carbonates which are more susceptible to reequilibration because of high solubility. Inclusions trapped at relatively low temperatures and later subject to higher temperature, perhaps through deeper burial or tectonism, would then record conditions of burial rather than precipitation (Goldstein, 1986). Fluid inclusions in carbonates may reequilibrate through wall stretching, without any change to the fluids. Inclusions which have stretched will yield anomalously high homogenization temperature values (Bodnar and Bethke, 1984). Since the revealed temperature from the isotopes is between $55-85^{\circ}\text{C}$, and the average recorded present bottom hole temperature is 85°C (from well logs).

The dolomite samples were carefully examined to check the anomalously high T_h , but no indications of reequilibration were found. This may not rule out the possibility that these fluid inclusions might have undergone reequilibration but the evidence is not clear. Since the sediments have experienced multiple stages of subsidence and burial. The temperature revealed by the isotope (55-85°C) will be adopted during the discussion of the mechanism of dolomitization.

5.4 Mechanism of dolomitization

The dolomites studied were precipitated from concentrated (162-210ppt NaCl equivalent) brines at quite high temperature. The presence of anhydrite in the samples, implies an association with evaporites or at least with CaSO_4 saturated fluid. The percentage of dolomite increases towards the platform, which was dominated by evaporites throughout the early Tertiary. Together these observation lead to the conclusion that the studied dolomites were dolomitized by fluid coming from the Cyrenaica platform.

It is suggested that platform brines were able to migrate down dip through rocks providing good permeability and promote dolomitization, there may also have been lateral migration into relatively permeable intervals. Fluid pumped from the platform had already been responsible for evaporite deposition and should have had a salinity within the field of gypsum precipitation (150-300ppt). The salinity determined from the fluid inclusions of the studied dolomites falls within this range

(162-210ppt). The stable isotope ratios obtained are also consistent with derivation from evaporated sea water which becomes increasingly enriched in ^{18}O with evaporation. The temperature under which the examined dolomites would have precipitated was between 50-80°C.

Three other dolomitization models have been considered. The mixing - zone, Dorag, dolomitization model (Badiozamani, 1973; Land, 1980) does not seem applicable to the studied samples, because the fluid inclusion study indicates that they were precipitated from brines which could not have originated from a mixing zone. Furthermore, stable isotope analyses also suggest that the dolomites precipitated from evaporated sea water.

Dolomitization by sea water is precluded by similar arguments. The $\delta^{18}\text{O}$ composition of the studied dolomites averages +5, thus they are heavier than normal marine water by +5 per mil. Furthermore fluid inclusions indicate that the dolomites were precipitated from highly saline fluids and thus could not have precipitated from normal sea water.

Dolomitization by seepage refluxion (Adams and Rhodes, 1960), offers an alternative explanation for the stratigraphic distribution of the dolomite observed in the area, where dolomitization increases progressively upward towards the platform. However, the most serious deficiency of this model is the lack of explanation for the high

temperatures revealed by both oxygen isotope and fluid inclusion studies.

In summary, the studied rock samples have been dolomitized by highly saline fluids derived from the Cyrenaica platform. The density of the brines and the difference in height between the platform and the basin provided the necessary gravity-driven hydraulic head for long-distance lateral flow of fluid (10-15km). Apparently dolomitization operated under considerable depth of burial. If the surface temperature is assumed to have been 25°C and the geothermal gradient in the area is 30°C/km then dolomitization occurred under more than 1km of burial.

CHAPTER SIX

POROSITY ANALYSIS

One of the essential aims of this study has been to evaluate the porosity distribution and development in the area, considering porosity as an important element in the determination of reservoir rock qualification. Many factors have hampered the study of porosity in the area and these include the domination of the studied samples by relatively poor porosity. This has been revealed by petrographic examination. Generally to date no commercial production has been obtained from the studied wells. Previous studies carried out by the National Oil Corporation attributed the lack of economic production of hydrocarbon to poor permeability.

Well logs have greatly enhanced our understanding of subsurface geology. They give access to lithological identification and consequently assist in prediction of the petrophysical characteristics of the sediment column through the measurement of physical properties. This is usually conducted through the drilled borehole. Wells have been drilled in the study area since the early 1960s, but the only log available at that time for measurement of porosity was the sonic log. Porosity and permeability can also be measured in the laboratory, but unfortunately such methods cannot be applied in the studied wells since the core samples are too small to make the plugs essential for such techniques.

6.1 Porosity determination

The available sonic logs are simply recordings versus depth of the time, t , required for a compressional sound wave to traverse 1ft of formation. Expressed as the interval transit time (Δt), this is dependent on the lithology type and porosity. This dependent upon porosity, when the lithology is known, makes the sonic log very efficient as a porosity log. The sonic log is also helpful in well to well correlation.

In order to calculate porosity from sonic logs the matrix interval time (Δt_{ma}) of a formation should be derived. In sedimentary formations the speed of sound depends on many parameters, basically, it depends on the rock matrix material (sandstone, limestone, etc.) and on the distributed porosity. Ranges of values of transit times for common rock matrices are

matrix	t_{ma} ($\mu s/ft$)
Sandstone	55.5
Limestone	47.5
Dolomite	43.5

Wyellie and others (1956), proposed, after numerous laboratory determinations, a relationship between porosity and transit time

$$\phi = (t_{log} - t_{ma}) / (t_f - t_{ma})$$

Where

t_{log} is the reading on the sonic log in $\mu s/ft$

t_f is the transit time of the saturating fluid (about 189 μ s/ft for a fresh water system).

Using this method a "quick look" interpretation of sonic well logs has been made for each of the seven lithofacies identified sedimentologically and petrographically in the studied wells. It is evident that only two lithofacies have good porosity and might be classified as potentially good reservoir rocks. These are, the chalky mudstone lithofacies and the nummulitic lithofacies. Other lithofacies have rather poor porosity. The factors which lead to poor porosity and permeability in the main lithofacies will be discussed below. The lithofacies will be discussed according to their age and stratigraphic position in the area.

6.2 Results and discussion

No signs of good porosity were found in the lithoclast bearing mudstone lithofacies during the petrographic study which might have been encouraging for later porosity calculation from well logs. The debris flow lithofacies is characterized by lithoclasts of different lithologies and sizes of shallow and deep water origin. The lithology apparently has poor porosity, attributed to the presence of mud between the lithoclasts. This implies poor reservoir characteristics. Although many other carbonate debris flows can be economically significant in petroleum exploration for example, in the Permian of west Texas several producing reservoirs appear to be allochthonous debris, transported basinward from the central

platform, basin facies are not usually considered to be good reservoirs. However, any possibility of the lithoclast bearing mudstone lithofacies in the Agdabia trough to be good reservoirs is precluded by poor porosity distribution. In addition, due to the lateral poor coverage of the cores it is possible that the debris flows are local and lack wide lateral extent.

The chalky mudstone lithofacies is widely distributed in the area especially in wells B2-41 and C1-41 (see chapter two). This has an average of 25% porosity (fig. 6.1, porosity calculated from sonic logs) which is reasonable for chalk buried by more than 2000m (see chapter four). One of the main targets for company exploration in the area was the chalk facies, but drilling and later studies have shown that permeability is the main element which might prevent hydrocarbon production from the chalk.

Fracturing is an important factor in the location of hydrocarbon reservoirs in chalk, because fractures most often improve permeability. Usually fractures enhance the effective permeability of the chalk and efficiently channel oil and gas from the matrix pores to the well bore. This is less obvious in the case of gas production because of the greater ease of getting gas to move through the extremely small pore throats and overall low permeability of deeply buried sediments. A fracture system can be enlarged through dissolution (Woods, 1963), so that in some areas, despite very low matrix permeability chalk is considered to provide a major zone for fluid movement. However, the fracture system may undergo

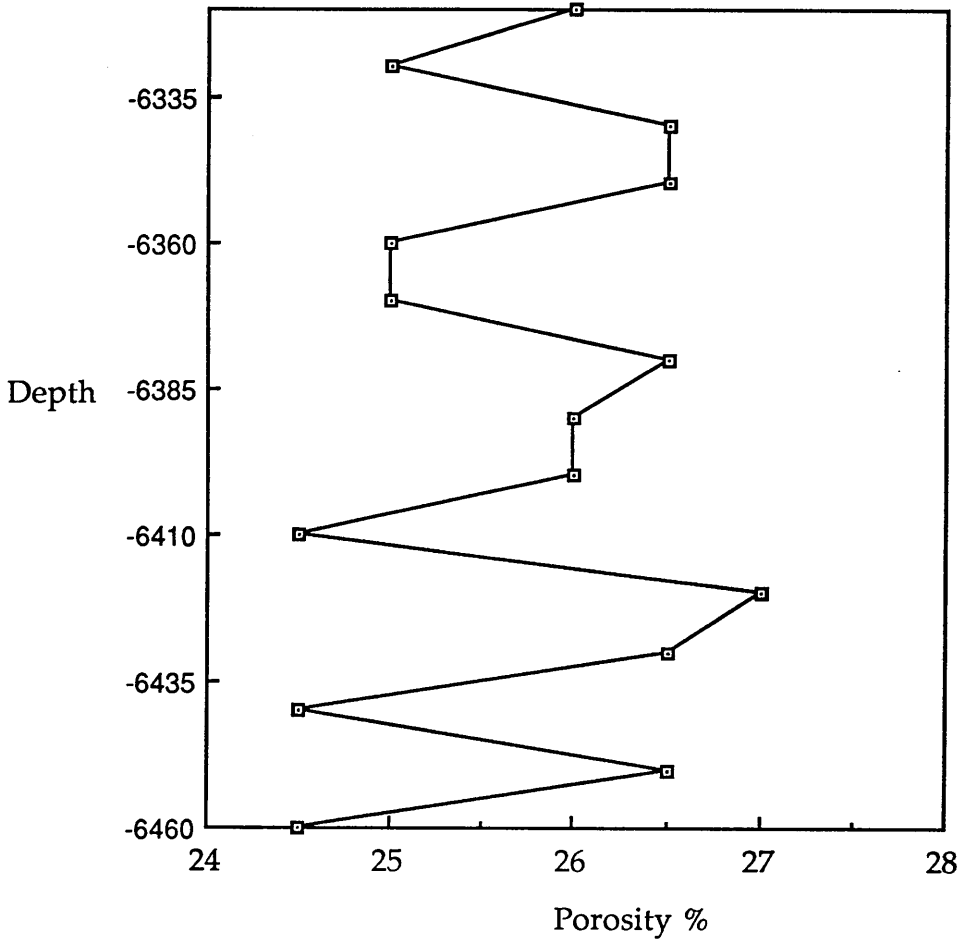


Fig. 6.1, Calculated sonic porosity in a cored interval in the chalky mudstone lithofacies (well B2-41).

cementation with calcite or other minerals and became ineffective as a fluid conduit. Thus some areas that might be expected to have good reservoir potential because of fracturing, may be virtually impermeable due later cementation of fractures. Unfortunately the prediction of these conditions prior to drilling is very difficult. The remarkably low permeability values (<1mil darcy) in the drilled wells, suggest that fractures, which might increase permeability, are poorly developed.

Some generalizations can be made. Production from chalk depends on the presence of a number of factors such as porosity and permeability. Shallow burial allows retention of porosity and hydrocarbon storage capacity of the formation. The chalk in the studied area has not been deeply buried and is characterized by reasonable intraparticle porosity (Plate 3.4, A, B), although under SEM some of the porosity is obstructed by growing anhydrite (Plate 3.3, B). The anhydrite, which is responsible for reducing the porespace may also drastically impede permeability by narrowing pore throats. In addition, the variation in the log response (Fig. 6.1) might be attributed to the presence of argillaceous materials, which would also .

The dolomites in the wells examined also have low porosity and are characterized by disseminated diagenetic anhydrite, occurring mostly as a cavity filling. Dolomitization often enhances porosity by later dissolving bioclasts or by a volume reduction which occurs during alteration. Murray (1960), explained the influence of dolomitization on

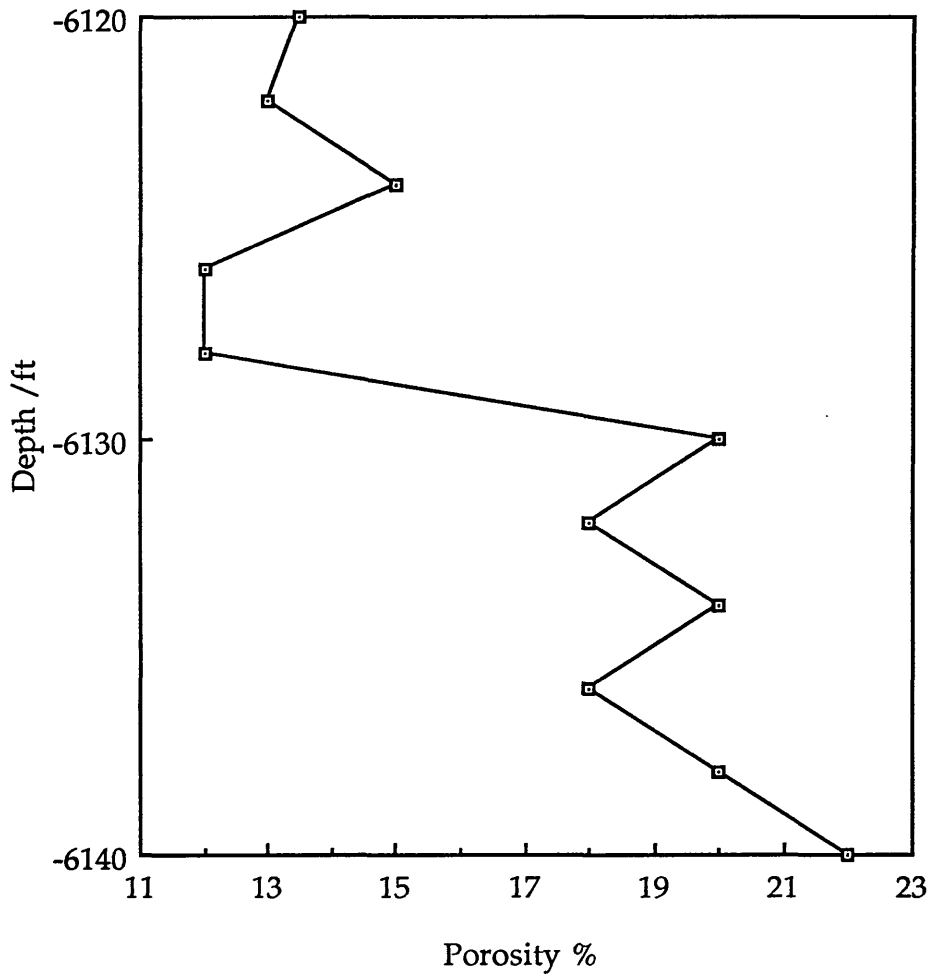


Fig. 6.2, Calculated sonic porosity in a cored interval in the large nummulite lithofacies (well J1-41).

porosity as reflecting the concurrent dissolution of calcite to provide the carbonate for dolomitization. If the dolomitization event only partially dolomitizes a sequence, and the remaining CaCO_3 is not removed by dissolution, the tendency is for enhancement of porosity (Anderson, 1985). Mattes and Mountjoy (1980) suggested that if a muddy sequence is laterally dolomitized, an interlocking dolomite mosaic may form, with actual porosity destruction. Lastly, dolomitization may occlude pre-existing porespace and yield a non porous rock. The porosity of the dolomite in the samples studied is relatively low (Plates 3.4, D) compared with other lithofacies and it is suggested that this lack of porosity might be due to the combined action of dolomitization and precipitation of anhydrite. The last would drastically decrease any porosity which might have resulted from dolomitization. (see Appendix C).

Finally, the nummulitic lithofacies which is wide spread in the Early Eocene rocks the area is characterized by two distinctive sizes of nummulites. The large nummulite lithofacies apparently contains excellent porosity, mostly as intraparticle porosity (Plate 3.4, C), although some of these porespace are occluded by blocky calcite. The porosity calculated for this lithofacies from well logs has an average of about 20% (fig. 6.2) and show a little increase down in the section. The low calculated porosity between 6120' and 6129' is due to the argillaceous materials.

The facies sequence represented by the nummulitic limestone may serve as a model hydrocarbon reservoir. Due to the bank with large

nummulities and high intraparticle porosity forms a potential reservoir while the adjacent lithofacies with small nummulites might serve as a potential source rock. Little is known about the permeability of this lithofacies, intraparticle pores are small and there is no obvious fracturing. More detailed petrophysical study is required to establish whether the variable porosity is sufficiently interconnected to transmit hydrocarbon.

CONCLUSIONS

Examination of Paleocene and Early Eocene rocks of the western margin of the Agdabia trough, has revealed details concerning their depositional environments and diagenetic history which have an important bearing on their potential as reservoir rocks.

1 - Seven lithofacies have been recognized. These are (1) lithoclast bearing mudstones, (2) chalky mudstones, (3) pelletal packstones, (4) large nummulite packstones, (5) small nummulite wackstones, (6) finely crystalline dolomites, and (7) coarsely crystalline dolomite. It is suggested that these lithofacies were deposited on a slope.

2 - The Slope sediments are normally located above the limit of the oxygenated water and extend from above to below wave base. The slope in the area studied extended from the edge of the Cyrenaica platform towards the basin centre for an estimated distance of more than 30Km. The domination of the slope environment produced relatively deep water sediments. These commenced at the base of the sequence with lithoclast bearing mudstones, interpreted as debris flow deposits, intercalated with hemipelagic muds and overlain locally by thin pelletal packstones. The later slope was covered by widespread chalk deposits which are in turn

capped by limestones dominated by nummulites. Dolomite is the predominant lithology of the Paleocene sediments in two wells C1-41 and D1-41, both located in the northern part of the area and the dolomite is often associated with calcium sulphate.

3 - Previous workers have noted that changes in the depositional pattern in the Eocene rocks of NW Libya produced a number of shallowing upward sedimentary cycles. One such cycle has been recognized in the area studied. This consist of packstones dominated by large nummulites which grade to a mixture of small and large nummulites then to wackstone with abundant small nummulites. Occasionally this cycle is interrupted by small scale debris flows. The cycle reflects the progradation of shallow water nummulitic banks over deeper water slope deposits as a result of sea level change.

4 - A series of diagenetic events have been deduced from petrographic examination. The diagenetic alteration is diverse, and commenced with dissolution and compaction followed by extensive dolomitization. This was itself followed by dissolution and by precipitation of anhydrite. The final stage was the precipitation of an equant calcite cement and Pb mineralization. Four types of luminescence has been recognized which correlate in the wells studied. Type I, is represented by bright matrix and cement. In type II, both bioclasts and matrix show a general dull luminescence. In type III the matrix is dull but the cement show two stages. Lastly, in type VI, both matrix and bioclasts are non luminescent.

The arrangement of the correlatable CL signature in the area, suggests an oxic water from Cyrenaica platform moves along the gradient accompanied by increasing in its reduced state. In addition, the lateral variation in the luminescence pattern postulated as been parallel by resembling change upward and explained by might be due to progressive subsidence or burial.

5- Geochemical investigations have revealed a number of remarkable points in the occurrence of trace and major elements and in isotopic analyses. Strontium is generally present within the range expected from carbonate rocks and has a ranges of 322 to 1600ppm and occasionally reach 1736ppm. The Sr content is slightly higher in the chalky mudstones. This might be attributed to the high proportion of stable low Mg calcite in the original sediments which retained its original Sr content. The dolomites have slightly lower strontium content (100-250ppm) compared with the calcite dominated facies, and the loss of Sr is interpreted as due to the dolomitization process. The dolomite section apparently also has low Fe and Mn contents. This might be related to the small amounts of these two elements which were incorporated into the system during deposition and the paucity of later cements which might have increased the amount of iron during diagenesis. Analyses of oxygen isotopes of the dolomites show depletion in ^{18}O ranging between -2.4 and -8.3‰, by using the fractionation factor, the $\delta^{18}\text{O}$ of water has an average of +5 relative to SMOW. This enrichment of $\delta^{18}\text{O}$ is compatible with precipitation from saline fluids formed from evaporated sea water. The temperature under which the dolomite formed, determined from the oxygen isotopes, ranged between 50-80°C. The $\delta^{13}\text{C}$ values are conformable with sediments formed

from marine water. The sulphur isotope values accord with the expected range of $\delta^{34}\text{S}$ for marine evaporites of Tertiary age. Fluid inclusion studies which were carried out exclusively on dolomites indicate quite high homogenization temperatures (105°C). These might be due to re-setting, but there is no any indication of this and such temperature is not so far from present bottom hole temperature (85°C). The measured freezing point depression of the fluid inclusions ranges between -12 and -18 values which correspond to 162-210ppt NaCl equivalent. Taken together these geochemical results suggest that Data from petrography, and geochemistry, the association of dolomite with evaporites, and the location of dolomite with respect to the Cyrenaica platform imply that hyper saline fluids from the Cyrenaica platform moved down slope and dolomitized existing limestones under more than 1Km of burial.

6 - Petrographic investigations and the interpretation of sonic well logs have been used to evaluate the porosity in the lithofacies studied. Generally most of the lithofacies are characterized by poor porosity, although the chalk and nummulitic lithofacies have reasonable porosity. The lithoclast bearing mudstones which are genetically interpreted as debris flows apparently have poor porosity due to the mud between the lithoclasts. The dolomites are also characterized by low porosity reduced further by the presence of disseminated anhydrite. The chalky lithofacies has been ruled out as a reservoir prospect due to low permeability attributed to a lack of fracturing, while the large nummulite lithofacies which is the most promising, shows porosity above average and might prove to be a good reservoir rock after detailed further study. Apparently

the porosity in the area in general was influenced by precipitation of calcium sulphate which has occluded available porespace with consequent deterioration of the effective permeability.

FUTURE WORK

Many questions have been raised during the course of this study, which have included the depositional environment, diagenesis and porosity analysis of Paleocene and Early Eocene sections.

1 - The Large Nummulites packstones are of particular interest. They show good porosity both in thin-sections and well logs and it has been suggested that they might potentially serve as a good reservoir. During the last stages of the study, two new wells have been drilled in the area. These may help in providing more information about the geology of the area in general and about the nummulitic lithofacies in particular. They will help to constrain ideas on the depositional environment, and may include data on the development of the nummulitic bank. They also offer the opportunity for further study of porosity and permeability using plugs from cores and for a more detailed correlation of porosity distribution in the area.

2 - The second question concerns the fluid responsible for the extensive dolomitization in the northern part of the area, to determine if there was any intervention of meteoric water during dolomitization. Analysis of formation waters for oxygen and hydrogen isotopes is in progress at the Scottish Universities Reactor Centre. The results of this will be used to test the dolomitization model proposed during the study.

3 - It is important to study the distribution and occurrence of anhydrite over a wider area. The introduction of the anhydrite was apparently responsible for the deterioration of the porosity and the destruction of

most of the permeability.

4 - Finally, the work completed suggests the study of facies distribution in areas towards the Cyrenaica platform where lithologies with greater hydrocarbon potential may be encountered.

REFERENCES

- Adams, J. E. and Rhodes, M. L.** (1960) Dolomitization by seepage reflux. *AAPG Bull.* **44**: 1912-1920.
- Adelseck, C. G., Geehan, G. W. and Roth, P. H.** (1973) Experimental evidence for selective dissolution and overgrowth of calcareous nannofossils during diagenesis. *Bull. Geol. Soc. Am.* **84**:2755-2762.
- Agoco Exploration Staff.** (1989). Geology of NE Libya. Unpublished report.
- Aigner, T.** (1982) Event-stratification in nummulite accumulation and in shell beds from the Eocene of Egypt. In *Cyclic and Events Stratification* Einsele, G. and Seilacher, A., (Eds.) p. 248-262; Springer-Verlag.
- Aigner, T.** (1983). Facies and origin of nummulitic buildups: an example from Giza pyramids plateau (Middle Eocene, Egypt). *Neues Jahrb.Geol. Palaent. Abh.* **166**: 347-368.
- Aigner, T. and Futterer, E.** (1978) Kolk-Topfe und- Rinnen (pot and gutter casts) im Muschelkalk- Anzeiger fur wattenmeer? *Neues Jahrb.Geol. Palaent. Abh.*, **156**: 285-304.
- Almond, D. C.** (1986) Geological evaluation of the Afro-Arabian Dome. *Tectonophysics*, **131**: 301-332.
- Anderson, J. H.** (1985). Depositional facies and carbonate diagenesis of the downslope reefs in the Nisku Formation (U. Devonian), central Alberta, Canada. *unpub. Ph.D. Dissertation.* the University of Texas/Austin, 393pp.

- Arni, P. and Lanterno, E.** (1972) Considerations paleoecologiques et interpretation des calcaires de l'Eocene du Veronais. *Arch. Sci. Geneve*, 25:251-283.
- Badiozamani, K.** (1973). The Dorag dolomitization model- application to Middle Ordovician of Wisconsin. *Jour. Sed. Pet.* 43: 965-984.
- Banerjee, S.** (1980) *Stratigraphic Lexicon of Libya*. Industrial Res. Cenere, Tripoli.
- Barr, F. T.** (1978) *Lower Tertiary Stratigraphy and Tectonics of northeast Libya*. 2nd symp. on the Geology of Libya, Al Fateh University, Tripoli, abst. P. 13-14.
- Barr, F. T. and Berggren, W. A.** (1980) Lower Tertiary biostratigraphy and tectonics of northeastern Libya. In: *The Geology of Libya* (M. J. Salem and M. T. Busrewil, eds) Academic Press. 1: 163-192.
- Barr, F. T. and Hammuda, O. S.** (1971) Biostratigraphy and Planktonic Zonation of upper Cretaceous Atrun Limestone and Hilul Shale, northeastern Libya. In: *Proc. 2nd Int. Conf. Plankt. Microfossils* (Rome, 1970) (A. Farinacci, ed.). 27-40.
- Barr, F. T. and Walker, B. R.** (1973) Late Tertiary Channel System in northern Libya and its implication on Mediterranean sea level changes. In: *Initial Rep. D.S.D.P.* (W. B. F Ryan, K. J. Hsu, eds) 13: 1244-1251.
- Bathurst, R. G. C.** (1971) *Carbonate sediments and their diagenesis*. New York, Elsevier, 620pp.

- Bathurst, R. G. C.** (1986) Carbonate diagenesis and reservoir development: conservation, destruction and creation of pores. In: J. E. Warme and W. Shanley (eds.) *Carbonate depositional Environments, Modern and Ancient*. part 5: Diagenesis I. Colorado School of Mines Quarterly, **81**: 1-25.
- Berggren, W. A.** (1969) Biostratigraphy and planktonic foraminifera zonation of the tertiary system of the Sirte basin of Libya. North Africa. In: *Proc. 1st. Int. conf. plank. Microfossils (P. Bornnemann and H. H. Renz) Leiden*. 104-120.
- Berggren, W. A.** (1974) Paleocene benthonic foraminiferal biostratigraphy, biogeography and paleoecology of Libya and Mali. *Micropaleontology*, **20**: 449-465.
- Berner, R. A.** (1965) Dolomitization of the mid-pacific Atolls. *Science*, **147**: 1297.
- Black, M.** (1953) The constitution of the chalk. *Proc. Geol. Soc. London*, **1499**: 81-86.
- Black, M.** (1965). Coccoliths. *Endeavour*. **24**: 131-7.
- Blondeau, A.** (1972). Les Nummulites. *Vuiberted*, Paris, 254pp.
- Bodnar, R. J. and Bethke, P. M.** (1984) Systematic of stretching of fluid inclusions I: Fluorite and sphalerite at 1 atmosphere confining pressure. *Economic Geology*. **79**: 141-161.
- Bramlette, M. N. and Martini, E.** (1964) The great change in calcareous nannoplankton fossils between the Maastrichtian and Danian. *Micropaleontology*, **10**: 291-322.

Bromley, R. G. (1968). Burrows and boring in hardgrounds. *Geol. Soc. Denmark Bull.* 18: 247-250.

Bromley, R. G. (1979) Field meeting in southern Scandinavia, 18-28 Sept. 1975: *Proc. Geologists Assoc.* 90, p. 181-191.

Brown, S. E. , Fairhead. J. D. and Mohamed. I. I. (1985). Gravity study of the White Nile Rift. Sudan. and its regional tectonic setting. *Tectonophysics*, 113, 123-127.

Bukry, D. (1974) Coccoliths as paleosalinity indicators- evidence from Black Sea, In: *The Black Sea - geology, chemistry, and biology.* AAPG Mem. 20:353-363.

Bullen, S. B. and Sibley, D. F. (1984) Dolomite selectivity and mimic replacement. *Geology.* 12: 655-658.

Claypool, G. E., Hosler, W., Kaplan,I., Sakai, H.and Israel, Z. (1980) The age Curves of Sulfur and oxygen isotopes in marine sulphate and their mutual interpretation. *Chemical Geol.*28: 199-260.

Colman, M. L. and Moore, M. P. (1978) Direct reduction of sulphate to sulfur dioxide for isotopic analysis. *Anal. Chem.*50:1594-1595.

Conant, L. C. and Goudarzi, G. H. (1967) Stratigraphic and tectonic framework of Libya. *AAPG Bull.* 51:719-730.

Conley, L. D. (1971) Stratigraphy and lithofacies of the Lower Paleocene rocks, Sirte basin. In: *The Geology of Libya* (M. J. Salem and M. T. Busrewil, eds) Academic Press. 1: 127-140.

- Cook, H. E. , Mc Daniel, P. N., Mountjoy, E. W., and Pray, L. C. (1972)** Allochthonous Carbonate debris flows at Devonian bank (reef) margins Alberta, Canada. *Bull. Can. Petrol. geol.* 20:439-497.
- Cook, H. E. and Egbert, R. M. (1981)** carbonate submarine fans along a Paleozoic, prograding, continental margin, Western United states. *AAPG Bull.* 65:913-914.
- Coplen, T. B., Kendall, C. and Hopple, J. (1983).** Comparison of stable isotope reference samples. *Nature*, 302:236-238.
- Crawford, M. L. (1981)** Phase equilibria in aqueous fluid inclusions In: Hollister, L. S. and Crawford, M. L. (eds.) *Fluid inclusions: Application to petrology.* Miner. Assoc. Canada Short Course Handbook. 6:75-100.
- Crevello, P. D. and Schlager, W. (1980)** Carbonate debris sheets and turbidites, Exuma Sound, Bahamas. *Jour. Sediment. Pet.* 50: 1121-1147.
- Davis, B. K. (1986)** Velocity changes and burial depth in Chalk of the southern North Sea basin In: *Petroleum Geology of North west Europe* . J. Brooks and K. W. Glennie(Eds). 1:307-313.
- Dickson, J. A. D. (1966)** Carbonate identification and genesis as revealed by staining. *Jour. Sed. Petr.* 36: 491-505.
- Domenico, P. A, and Robbins, G. A. (1985)** The displacement of connate water from aquifers. *Geol. Soc. Amer. Bull.* 96:328-335.
- Drum, W. H. and Haffty, J. (1961)** Occurrence of minor elements in water: *U.S. Geol. Survey, Circular 445*,11p.

Dunnington, H. V. (1967) Aspects of diagenesis and shape change in stylolitic limestone reservoir. 7th World Petroleum Cong. Mexico City, Proc. 2:339-352.

Durney, D. W. (1972) Solution transfer, an important geological deformation mechanism. *Nature*. 235: 315-317.

El- Hawat, A. S. (1985) Submarine slope carbonate mass- movements in response to global lowering of sea level: Apollonia Formation, Lower-Middle Eocene, N. E. Libya. *6th European Regional meeting of IAS*. Lilda.

El- Hawat, A. S., Sanussi, R., Shelwi, S., Figi, O. , Zayani, A., Megassabi, M., Bital-mal, Y., Ammar, A., Salem, F. and S. Barasi (1986) Stratigraphy and Sedimentation of Eocene Nummulitic Bank Complexes, Darnah Formation, Libya. *12th Inter. Sed. Congr.* Canberra.

El-Arnauti, A. and Shelmani, M. (1985) Stratigraphic and Structural setting. In: Palenostратigraphy of N.E. Libya. B. Thusu and B. Owens (Eds) *Jour. Micropalaeo.* 4: 1-10.

Enos, P. (1977) Flow regimes in debris flows: *Sedimentology*. 24: 133-142.

Fallick, A. E. (1991) Personal communication.

Faure, G. (1986). *Principles of isotope Geology*, 2nd edition. John Wiley and Sons.

Friedman, G. M. (1959) Identification of carbonate minerals by staining methods. *Jour. Sed. Pet.* 29: 87-97.

- Fritz, P.** (1971) Geochemical characteristics of dolomite and the ^{18}O contents of Middle Devonian oceans. *Earth and Planetary Science Letters*, **11**: 277-288.
- Fritz, P. and Frape, S. K.** (1982) Saline ground water in the Canadian shield-a first overview. *Chem. Geol.* **36**:179-190.
- Fritz, P. and Smith, D. G. W.** (1970) The isotopic composition of secondary dolomites. *Geochim. et Cosmochim. Acta.* **34**: 1161-1173.
- Futterer, E.** (1982) Experiments on the distinction of wave and current Influenced shell accumulations.- In: Einsele, G. and Seilacher, A., (eds) *Cyclic and event stratification*. Springer-Verlag.
- Garrels, R. M. and Christ, C. L.** (1965) *Solutions, minerals, and equilibria*: Harper and Row, New York, 450p.
- Goldstein, R. H.** (1986). Reequilibration of fluid inclusions in low-temperature calcium carbonate cement. *Geology*. **14**:792-795.
- Goudarzi, G. H.** (1980). Structure of Libya. In: *The Geology Of Libya*, M. J. Salem and M. T. Busrewil (eds). Academic press, Tripoli, **3**: 879.
- Gregory, J. W.** (1911). The fossil echinoidea of Cyrenaica. *Quart. Jour. Geol. Soc. London.* 672/615.
- Grover, G. R. Jr. and Read, J. F.** (1983) Paleoaquifer and deep burial related cements defined by regional cathodoluminescence patterns. Middle Ordovician carbonates, Virginia. *AAPG Bull.* **67**: 1275-1303.

- Gualtieri, J. L. (1962) *Exploration of the Jefren gypsum-anhydrite deposits, Libya*: U.S Geol. Survey Open File Report.65p+11pls.,3figs.
- Gumati, Y. D. (1984) Crustal Extension. subsidence. and thermal history of the Sirte basin. Libya. *Ph.D. thesis*. University of south Carolina, 207p.
- Gumati. Y. D. and Kanes, W. H. (1985) Early Tertiary subsidence and sedimentary Facies. Northern Sirte Basin, Libya. *AAPG Bull.*, 69:39-52.
- Hakansson, E. , R. , Bromley, R. G. and Perchnielsen, K. (1974) Maastrichtian chalk of north-west Europe- a pelagic shelf sediment. In: *Pelagic Sediments: on Land and under the Sea*. K. J. Hsu and H. C. Jenkyns (Eds). Int. Ass. Sediment. Spec. publ.1: 211-233.
- Hampton, M. A. (1972) The Role of subaqueous debris flow in generating turbidity currents. *Jou. Sed. Pet.* 42:775-793.
- Hancock, J. M and Scholle, P. A. (1975). Chalk of the North sea. In: A. Woodland (ed.), *Petroleum and the Continental Shelf of Northwest Europe: the geology and environment*. Applied Sciences Press, London, p.409-422.
- Hancock, J. M. (1975) The petrology of the Chalk. *Geologist Assn. Proc.* 86:499-535.
- Hancock, J. M. and Kennedy, W. J. (1967) Photographs of hard and soft chalks taken with the scanning electron microscope. *Proc. Geol. Soc. London*, 1643:249-252.
- Haq, B., Hardenbol, J. and Vail. P. (1987) Chronology of fluctuating sea levels since the Triassic. *Science*. 235:1156-1165.

Hardie, L. A. (1967) The gypsum-anhydrite equilibrium at one atmosphere pressure. *Amer. Mineral.* 52: 172-200.

Harvey, P. K., Taylor, D. M., Hendry, R. D. and Bancroft, F. (1973) An accurate fusion method for the analysis of rocks and chemically related materials by x-ray fluorescence spectrometry. *X-ray specrometry.* 2:33-44.

Hattin, D. E. and W. A. Cobban. (1965). Upper Cretaceous stratigraphy, paleontology, and paleoecology of western Kansas. *State Geological Survey of Kansas*, 69+iipp.

Hay, W. W. and Mohler, H. P. (1967) Calcareous nannoplankton from Early Tertiary rocks at port labau France, and paleocene-early Eocene correlation. *Jour. paleont.* 41:1505-1541.

Honjo, S. (1975) Dissolution of suspended coccoliths in deep sea water column and sedimentation of coccolith ooze. In: W. V. Sliter, A. W. H. Be and W. H. Berger (eds.) *Dissolution of deep sea carbonates.* Cushman Fdn. Spec. Pub. 13: 114-128.

Hosler, W. (1979) Trace elements and isotopes in evaporation In: *Marine Minerals.* R. G, Burns (eds.). *Reviews in Mineralogy, Miner. Soc. Am.*, 293-346.

James, N. P. and Choquette, P. W. (1984) Introduction In: *Paleokarst*, N.P James and P. W. Choquette (Eds), . Springer-Verlag New York, 1-21.

Jenkyns, H. C. and K. J. Hsu. (1974). *Pelagic Sediments: on land and under the sea.* Int. Ass. Sediment. Spec. publs. 1: 1-10.

Johnson, A. M. (1970) *Physical processes in geology*: Freeman Cooper and Co. San Francisco.

Kinsman, D. J. J. (1969) Interpretation of strontium concentration in carbonate minerals and rocks. *Jour. Sed. Pet.* **39**:486-509.

Klen, L. (1974) *Geological map of Libya*; 1:250,000 sheet: Benghazi, Explanatory booklet. Ind. Res. Cent. (Tripoli) 56p.

Klitzch, E. (1963) Geology of the north-east flank of the Murzuk basin (Djebel Ben ghnema-Dor el Gussa area): *Inst. Francais Petrole Rev.* **18**:1411-1427.

Knauth, L. P. and Beeunas, M. A. (1986) Isotope geochemistry of fluid inclusions in Permian halite with implication for the isotopic history of ocean water and origin of saline formation water. *Geochim. et Cosmochim. Acta.* **50**:419-433.

Land, A. W. and Mountjoy, E. W. (1980) Burial dolomitization of the Upper Devonian Miette buildup, Jasper National Park, Alberta In: *Concepts and Models of Dolomitization*. D. H. Zenger, J. B. Dunham and R. L. Ethington (Eds) SEPM Spec. Pub. **28**: 259-297.

Land, L. S. (1980) The isotopic and trace element geochemistry of dolomite: the state of art In: *Concepts and Models of Dolomitization*. D. H. Zenger, J. B. Dunham and R. L. Ethington (Eds) SEPM Spec. Pub. **28**: 87-110.

Land, L. S. (1985) The origin of massive dolomite. *Jour. Geol. Educ.* **33**:112-125.

Land, L. S., Salem, M. R. I. and Morrow, D. W. (1975) Paleohydrology of

- Land, L. S., Salem, M. R. I. and Morrow, D. W. (1975) Paleohydrology of ancient dolomites: geochemical evidence. *AAPG Bull.* 59:1602-1625.
- Leake, B. E., Hendry, G. L., Kemp, A., Plant, A. G., Harvey, P. K., Wilson, J. R., Coats, J. S., Aucott, J. W., Lunel, T. and Howarth, R. J. (1969) The chemical analysis of rock powders by automatic X-ray fluorescence. *Chemical Geology.* 5:7-86.
- Leeder, M. R. (1982). *Sedimentology, Processes and Products*. George Allen & Unwin. London: 2nd edn. 344pp.
- Lloyd, R. M. (1966) Oxygen isotope enrichment of sea water by evaporation. *Geochim. et Cosmochim. Acta*, 30:801-814.
- Machel, H. G. (1985) Cathodoluminescence in calcite and dolomite and its chemical interpretation. *Geoscience Canada*. V 12:139-147.
- Mapstone, N. B. (1975) Diagenetic history of a North Sea chalk, *Sedimentology*, 22:601-614.
- Matter, A. (1974) Burial diagenesis of pelitic and Carbonate deep sea sediment from the Arabian Sea. In: R.B. Whitmarsh, O.E. Weser, D.A. Ross et al. , *Initial reports of the DSDB*, US Government Printing Office, Washington, D. C. , 23:421-469.
- Mattes, B. W. and Mountjoy, E. W. (1980). Burial Dolomitization of the Upper Devonian Miette Buildup, Jasper National Park, Alberta. In: D. H. Zenger, J. B. Dunham and R. L. Ethington (eds.), *Concepts and Models of Dolomitization*. SEPM Spec. Pub. 28:259-297.

Mc Intyre, A., and A. W. H. Be. (1967) Modern coccolithophoridae of the Atlantic Ocean, 1, Placoliths and Cyrtoliths: *Deep Sea Res.* **14**:561-597.

McCrea, J. M. (1950) On the isotopic chemistry of carbonates and a paleotemperature scale. *Jour. Chem. Phys.*:**18**:849-857.

Megerisi, M. and Mamgain, V. D. (1980) The Upper Cretaceous Tertiary Formations of Northern Libya, *a synthesis ind. Res. Cont.* (Tripoli). **12**:1-85p.

Meyers, W. J. (1974) Carbonate cement stratigraphy of the Lake Valley Formation (Mississippian), Sacramento Mountains, New Mexico. *Jour. Sed. Pet.* **44**:837-861.

Meyers, W. J. (1978) Carbonate cements: their regional distribution and interpretation in Mississippian limestones of South western New Mexico. *Sedimentology.* **25**:371-400.

Meyers, W. J. (1989) Trace element and isotope geochemistry of zoned calcite cements, Lake Valley Formation (Mississippian), Sacramento Mountains, New Mexico.: insights from water-rock interaction modelling. *Jour. Sed. Pet.* **65**:355-370.

Meyers, W. J. (1991) Calcite cement stratigraphy: an overview, In: *Luminescence Microscopy and Spectroscopy Qualitative and Quantitative Applications.* C. Barker and O. Kopp (Eds.) SEPM short course **25**:133-148 Dallas, Texas.

Middelton, G. V. and Hampton, M. A. (1973) Sediment gravity flows: Mechanics of flow and deposition: In: G. V. Middelton and A. H. Bouma

(eds), *Turbidites and deep-water sedimentation*, SEPM. Pacific Sec. , Los Angeles, California.

Moore, C. H. (1989). Carbonate Diagenesis and Porosity. *Developments in Sedimentology* 46. Elsevier. 338pp.

Mountjoy, E., Cook, H. E., Pray, L. C. and Mc Daniel, P. N. (1972) Allochthonous carbonate debris flows- world-wide indicator of reef complexes, banks, or shelf margin. *24th Int. Geo. Congress, Montreal*. Sect.6:172-189.

Mullins, H. T. & Cook, H.E. (1986) Carbonate apron models; alternative to the submarine fan model for paleoenvironmental analysis and hydrocarbon exploration. *sediment. Geol.* 48:37-79.

Mullins, H. T. , Heath, K. , Van Buren, H. M. and Newton, C. R. (1984) Anatomy of a modern open-ocean carbonate slope: northern Little Bahamas Bank. *Sedimentology.* 31:141-168.

Murray, R. C. (1960) Origin of porosity in carbonate rocks. *Jour. Sed. Pet.* 30:59-84.

Murray, R. C. and Lucia, F. J. (1967) Cause and control of dolomite selectivity. *Geol. Soc. Am. Bull.* 78:21-36.

Mutti, E. , Ricci-Lucchi, F., Sequestret, M. and Zanzucchi, G. (1984) Seismoturbidites: A new group of resedimented deposits. *Mar. Geol.* 55:103-116.

Neugebauer, J. (1973) The diagenesis problem of chalk- the role of pressure solution and porefluid. *Neues Jahrb. Geologie u. Palaontology Abh.*143:223-

245.

Neugebauer, J. (1974). Some aspects of cementation in chalk. In: *Pelagic Sediment: on Land and under the Sea*. K. J. Hsu and H. C. Jenkyns (Eds) Int. Ass. Sediment. Spec. publ. **1**, 149-176.

Oglesby, T. W. (1976) *A model for the distribution of manganese, iron, and magnesium in authigenic calcite and dolomite cements in the Upper Smackover Formation in eastern Mississippi*. unpubl. M.S. Thesis, Univ. of Missouri, Columbia.

Provasoli, L. (1963) Organic regulation of phytoplankton fertility. In: *The sea*. M. N. Hill (ed.) **2**:165-219. Interscience, New York.

Reid, R. E. H. (1973) The Chalk Sea. *Irish. Nat. J.* **17**:357-375.

Roedder, E. (1984) *Fluid inclusions*, In: Ribbe, P. H. (ed.) *Miner. Soc. Am., Review in Mineralogy*. **12**:644pp.

Rohlich, P. (1974) Geological map of Libya; 1:250,000 sheet: Al Bayda. Explanatory booklet. Ind. Res. Cent., (Tripoli) 70pp.

Rohlich, P. (1978) Geological development of jabal Al Akhdar, Libya. *Geol. Rundsch.* **V67**, 401-412.

Rohlich, P. (1980) Tectonic development of Jabal al Akhdar. In: *The Geology Of Libya*. M. J. Salem and M. T. Busrewil (Eds.). Tripoli Academic Press. **3**:923-931.

Roth, P. H. and W. H. Berger. (1975) Distribution and dissolution of coccoliths in the south and central Pacific. In W. V. Sliter, A. W. H. Be and W. H. Berger (Eds.) *Dissolution of deep sea carbonate*. Cushman Fdn. Spec.

Publ. 13:87-113.

Schlanger, S.O. and Douglas, R. G. (1974) The pelagic ooze-Chalk-limestone transition and its implications for marine stratigraphy. In: *Pelagic Sediments: on Land and under the Sea*. K. J. Hsu and H. C. Jenkyns (Eds.). Int. Assn. Sediment. Spec. publ. 1:117-148.

Scholle, P. A. (1974) Diagenesis of Upper Cretaceous Chalks from England. Northern Ireland, and the North Sea. In: *Pelagic Sediments: on Land and under the Sea*. K. J. Hsu and H. C. Jenkyns (Eds.). Int. Assn. Sediment. Spec. publ. 1:177-210.

Scholle, P. A. (1977) Chalk diagenesis and its relation to petroleum exploration: oil from chalks, a Modern Miracle, *AAPGBull.* 61:982-1009.

Scholle, P. A. and Halley, R.B. (1985) Burial diagenesis: out of sight, out of mind. In: N. Schneiderman and P. M. Harris (Eds.). *Carbonate Cements*. SEPM Spec. Pub. 36:309-334.

Seilacher, A. (1973) Biostratigraphy: The sedimentology of biologically standardized particles. In: R. N. Ginsburg (Ed.) : *Evolving Concepts in Sedimentology*. John Hopkins Univ.Press.

Shukla, V. (1988). Sedimentology and geochemistry of a regional dolostone: correlation of trace elements with dolomite fabric. In: *Sedimentology and Geochemistry of dolostones*. SEPM Spec. Pub. 43:145-157.

Sibley, D. and Gregg, J. (1987) Classification of Dolomite Rock Textures. *Jou. Sed. Pet.* 57: 967-975.

Sola, M. and Ozcick, B. (1990) On the hydrocarbon prospectivity of the north Cyrenaica region, Libya. *PRJ.* 2:25-41.

Stefanini, G. (1923) Fossil terziari della Cirenaica. *Paleontogr. Ital.* 27:101-146. In: Banerjee, S. (1980). *Stratigraphic Lexicon of Libya*. Tripoli.

Supko, P. R. (1970) Depositional and diagenetic features in the subsurface Bahamian rocks, Technical report 70-1-10 The Office of Naval Research, Univ. Miami

Sverdrup, H. U., Johnson M. W. and Fleming, R. H. (1942) *The ocean- their physics, chemistry, and general biology*. Prentice-Hall, New York.

Thode, H. G. and Monster, J. (1965) Sulfur isotope geochemistry of petroleum, evaporites, and ancient seas In: *Fluid in the subsurface Environments*. A. Young and J. Galley (Eds.). AAPG Mem. 4:367-377.

Veizer, J. (1983) Chemical diagenesis of carbonates, theory and application of trace element technique. In: *Stable Isotopes in Sedimentary Geology*. M. A. Arthur and T. Anderson (Eds.) SEPM short Course 10:3.1-3.100.

Veizer, J. and Demovic, R. (1974) Strontium as a tool in facies analysis. *Jour. Sed. Pet.* 44:93-115.

Veizer, J., Lemieux, J. Jones, B., Gibling, M. R. and Savello, J. (1978) Paleosalinity and dolomitization of Lower Paleozoic carbonate sequence, Somerset and Prince of Wales Islands, Arctic Canada. *Can. Jour. Earth Science*, 15:1448-1461.

Weber, J. N. (1964) Trace element composition of dolostones and dolomites and its bearing on the dolomite problem. *Geochim. et Cosmochim. Acta*,

28:1817-1868.

Weyl, P. K. (1959) Pressure solution and the force of crystallization-a phenomenological theory. *Jour. Geophys. Res.* **64**: 2001-2025.

Wilson, J. L. (1975). *Carbonate Facies in the Geologic History*. Springer-Verlag Berlin-Heidelberg -New York. 471pp.

Woods, D. J. (1963) Fractured Chalk oil reservoirs, Sabine Parish, Louisiana, *Gulf Coast Assoc. Geol. Soc. Trans.* **13**:127-138.

Wu, B., Tang, J. and Duan, Z. (1984) The variation of ^{18}O content of water in the Qaidam Basin. *27th Int. Geol. Congress, Moscow, Abstracts*, V:440pp.

Wyellie, M. R. J., Georgy, A. R. and Gardner, G. H. F. (1956) Elastic wave velocities in hetrogenous and porous media. *Geophysics.* **21**.

Zert, B. (1974) Geological map of Libya; 1:250,000 sheet: Darnah. Explanatory booklet. Ind. Res. Cent., (Tripoli) 49p.

APPENDIX A

A-1- Calculation of total CO₂ :

$$X1 = \text{MgO}(\text{XRF}) \times Y$$

$$X2 = \text{CaO}(\text{XRF}) \times Z$$

$$\text{CO}_2 (\text{cal}) = X1+X2$$

Where

$$Y = \text{CO}_2 (\text{mol. wt.}) / \text{MgO}(\text{mol. wt.}) = 1.0915$$

$$Z = \text{CO}_2 (\text{mol. wt.}) / \text{CaO} (\text{mol. wt.}) = 0.7848$$

A-2- Abbreviations

PDB	Pee Dee Belemnite
SMOW	Standard mean ocean water
CDT	Troilite of the Canon Diablo meteorite
PPM	Parts per million
PPT	Parts per thousand

A-3- Conversion between PDB and SMOW standards

$$\delta^{18} \text{SMOW} = 1.03091 \times \delta^{18} \text{PDB} + 30.910$$

$$\delta^{18} \text{PDB} = 0.97002 \times \delta^{18} \text{SMOW} - 29.98$$

APPENDIX B

B-1- Fluid inclusion data:

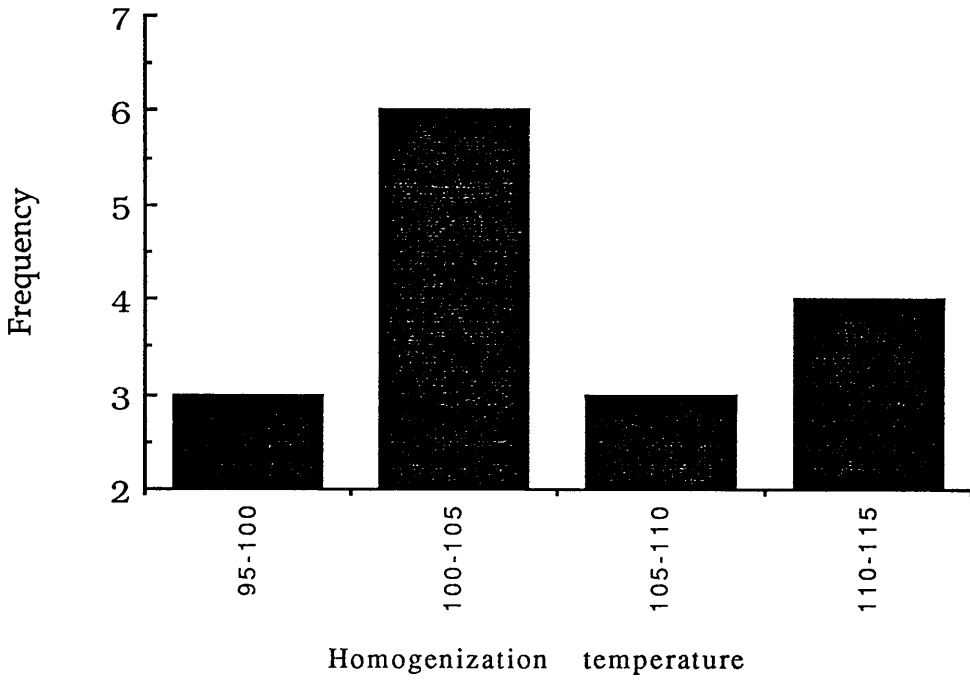
B-1-1- Homogenization temperature measurements (°C)

108	99
112	104
110	112
99	105
105	107
108	111
115	104
104	102
98	105
112	

B-1-2- Measurements of melting temperature (°C):

Initial melting	Final melting
-24	-15
-25	-14
-28	-17
-25	-10
-28	-19
-29	-12
-30	-13
-28	-15
-24	-17
-26	-14
-25	-16
-24	-15

B-1-3- Histogram illustrate the measured homogenization temperature in the dolomite:

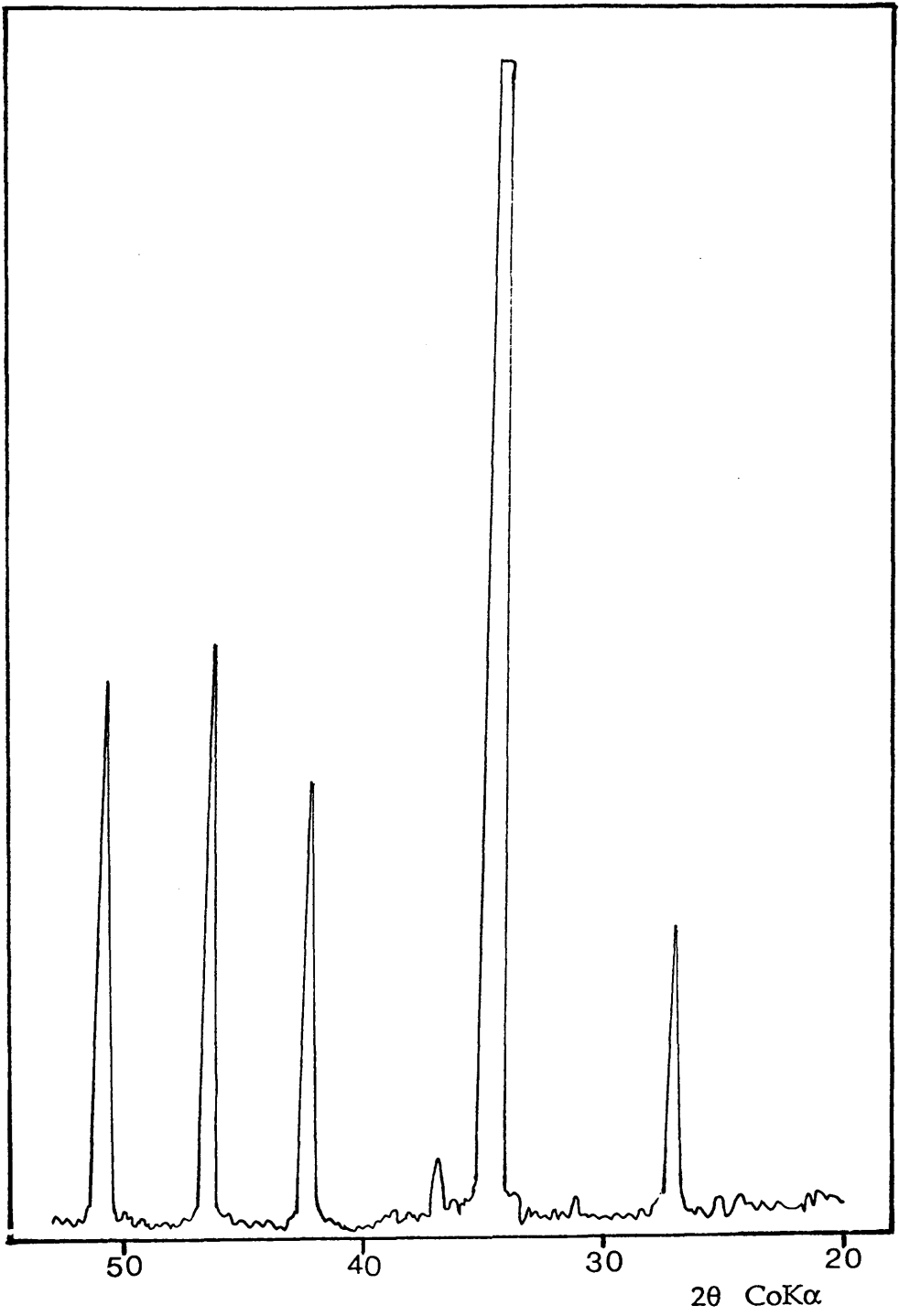


APPENDIX C

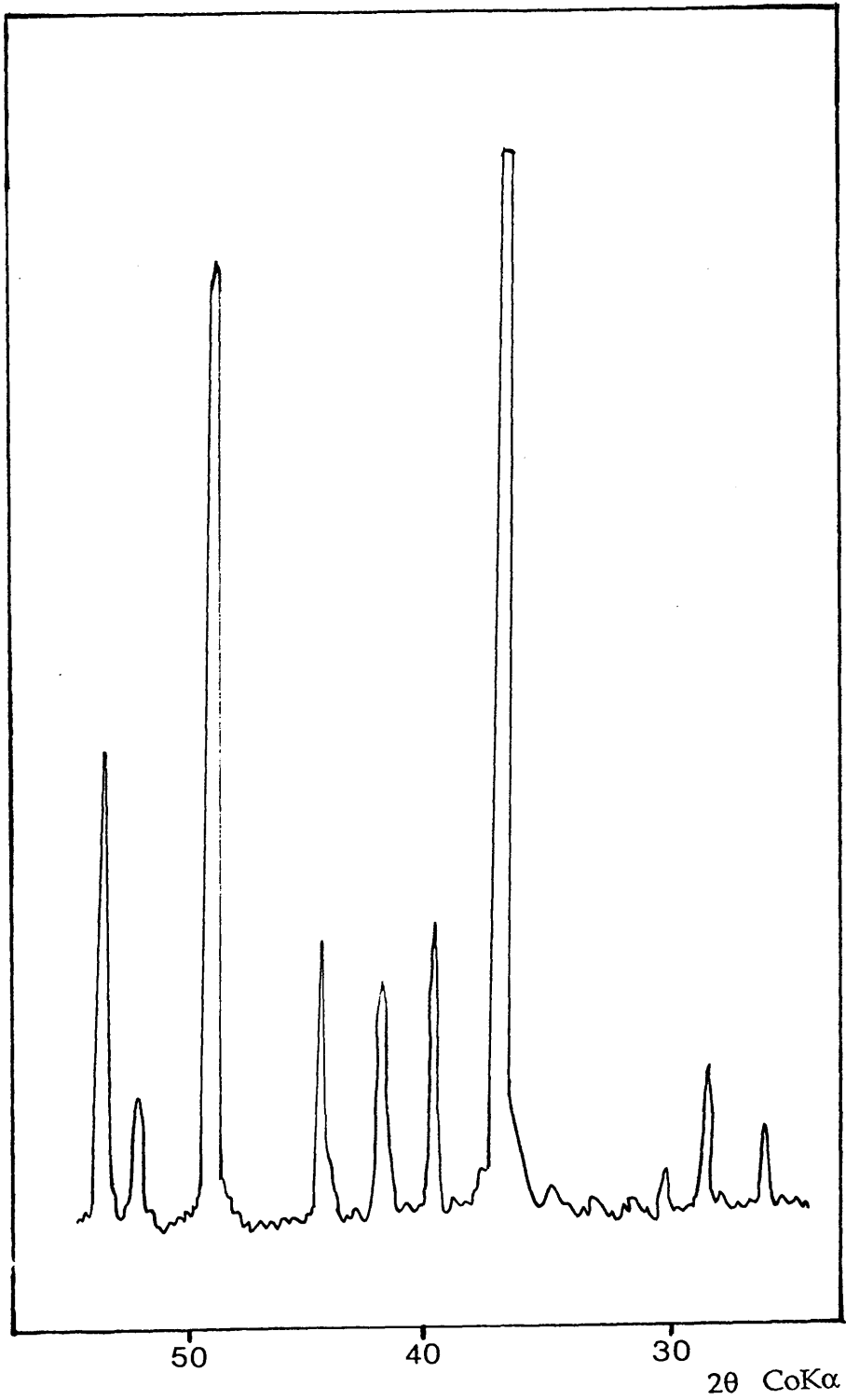
C-1- Observed porosity in the studied samples:

Well no	Depth (ft)	Porosity %	Well no	Depth (ft)	Porosity %
A1-41	12908	10	C1-41	8979	8
	12905	8		8970	10
	12829	7		8963	15
	12817	11		8038	13
	12814	9		7911	11
	12811	7		7905	9
	12807	8		7613	12
	11602	11		7610	16
	11106	6		7515	14
B2-41	6525	9		7067	18
	6510	12		7059	20
	6495	15		6730	22
	6480	18	D1-41		
	6460	22		7743	14
	6430	20		7728	18
	6350	25		7518	15
	6335	26		7516	14
	6320	23		6179	12
	6305	28		6109	9
	6290	22		5723	11
	6244	24			
	6230	20			
	6200	23			
	6185	18			
	6160	21			
	6130	25			
6115	22				
6080	18				

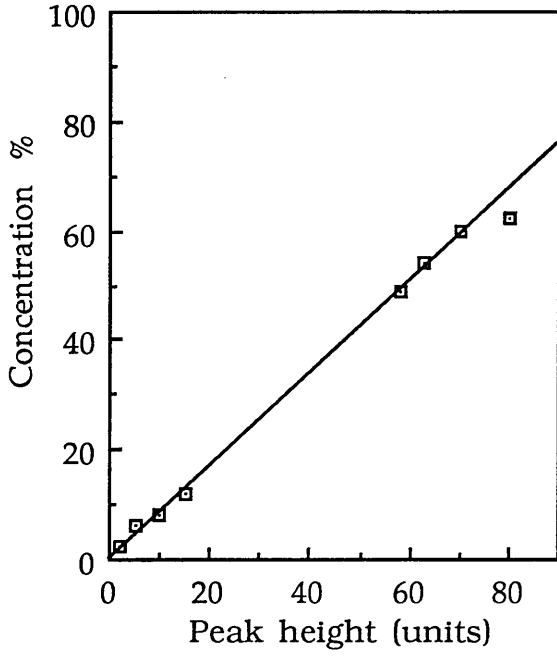
D-1-



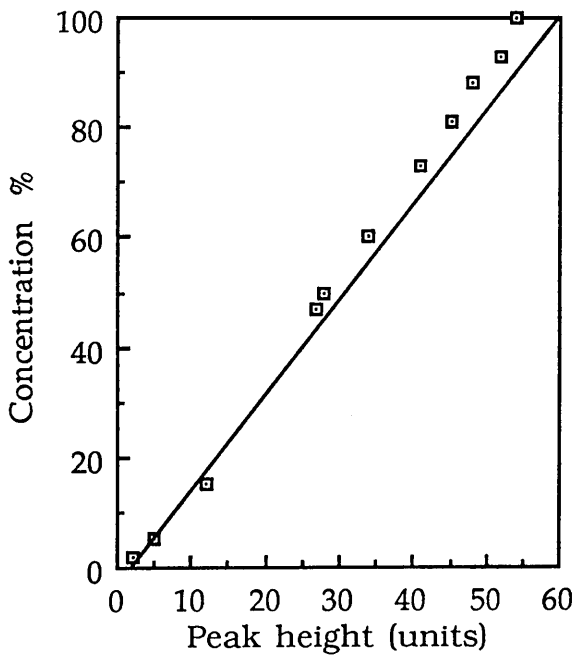
XRD trace of calcite standard



XRD trace of dolomite standard



D-2-Calibration graphs for dolomite (top) and calcite standard (bottom).



D-3- Results of semi- Quantitative analysis in the studied samples

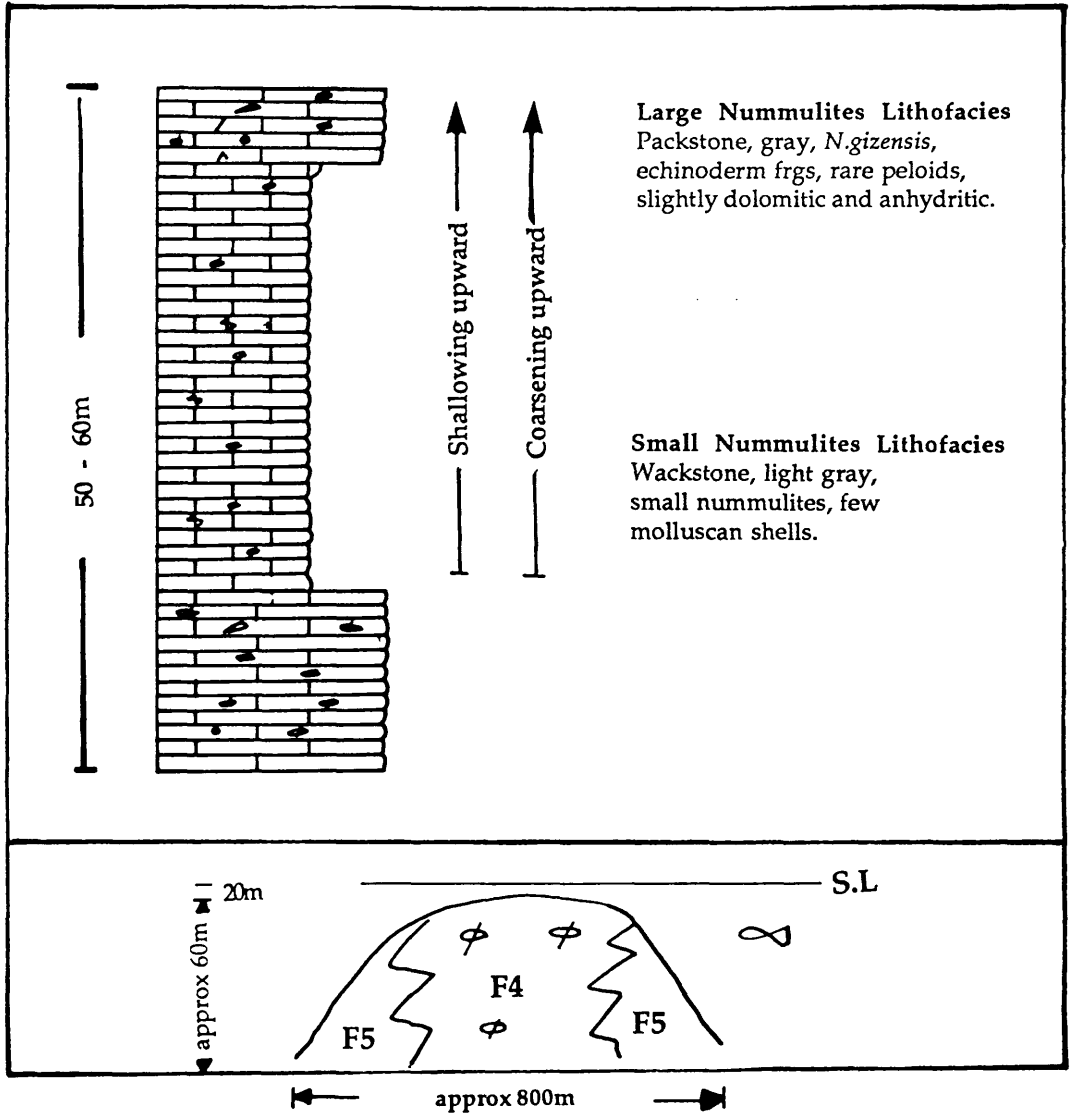
Well no	Depth (ft)	Calc. %	Dolom. %	Qtz %	Anh. %
A1-41	12908	81	3	6	
	12820	60		25	
	12817	92		4	
	12808	93		4	
	12116	50		20	
	11602	90	2	2	
	11106	55	2	21	
	11100	50	2	20	
	11096	48	4	19	
C1-41	8984		100		
	8979		98		1
	8961		96		2
	8038	5	94		
	7610	3	95		
	7514		98		1
	7054	88	10		
	6730	81	3		
B2-41					
	6550	93	1		
	6525	98	1		
	6430	97	1		
	6350	91			
	6305	96	2		
	6275	75	8	1	
	6185	90	3	1	
	6175	90	2	1	
D1-41	7743		88		9
	7725		84		14
	7708		92		4
	7688	1	87		
	6719		96		
	6275	75	8	1	
	6106		86	1	
	5735	99			
	5185	91	2	1	

APPENDIX E

E-1- Percentage of each constituent inherent to the studied lithofacies

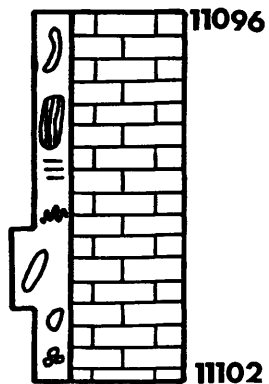
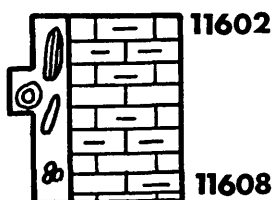
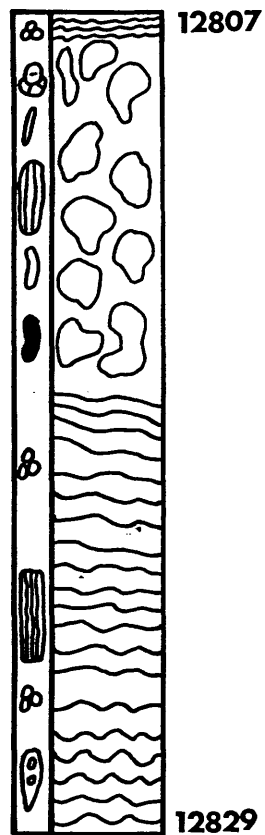
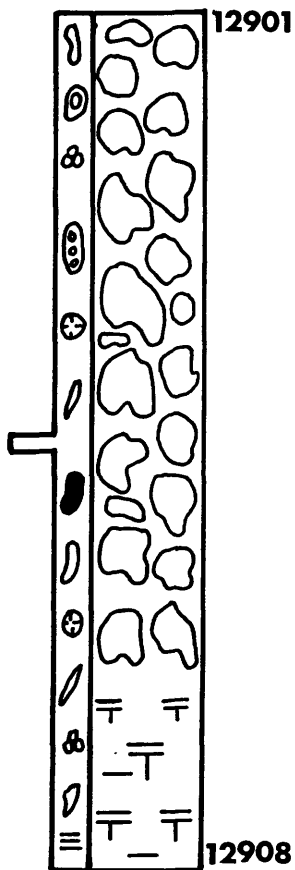
Numbers are in %		LITHOFACIES						
		F1	F2	F3	F4	F5	F6	F7
ALLOCHEMS	Lithoclasts	20	5	6				
	Globigerinids	10	18	7				
	Nummulites		1	2	60	45		
	Milioids		1	3	4	2		
	Fusulinids		2	1	2	3		
	Echinoid frag.	8	2	3	1	6	1	1
	Mollusca frag.	4	1	2	3	2	2	1
	Gastropoda	3	2	1	4	3		
	Peloids	8	3	26	1	1	1	
	Coccolith	9	27					
Dolomite		2	4	2	7	6	96	98
ORTHOCHEMS	Micrite	15	20	23	6	17		
	Sparite	6	4	17	5	7		
TERRIGEN. MAT.	Arg. material	4	9	6	2	8		
	Quartz silt	11			5			
	Colour	light brown	pale cream	brown	gray	light gray	tan gray	dark gray
	Other features	laminated hemipelagic	laminated bioturbated		stylolitic compacted	stylolitic pyritic	stylolitic	brecciated

E-2



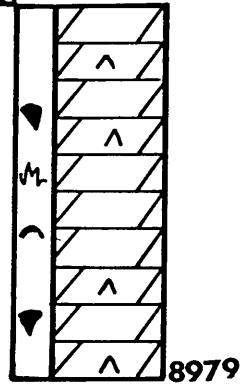
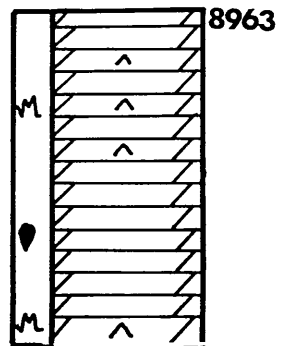
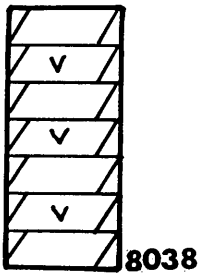
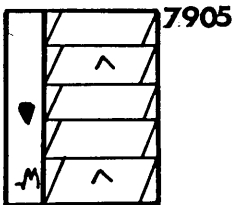
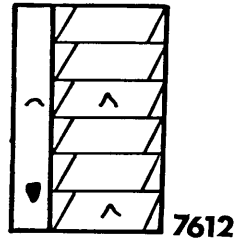
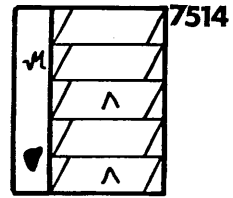
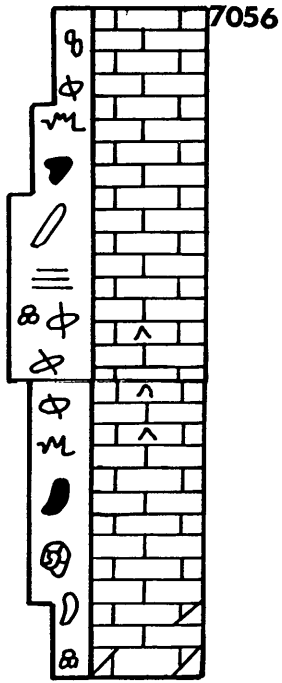
Depositional cycle in the nummulitic facies

E-3

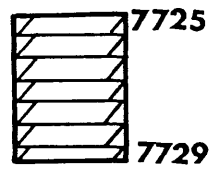
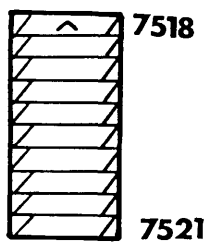
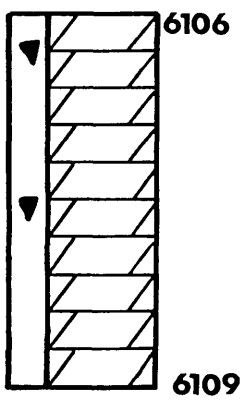
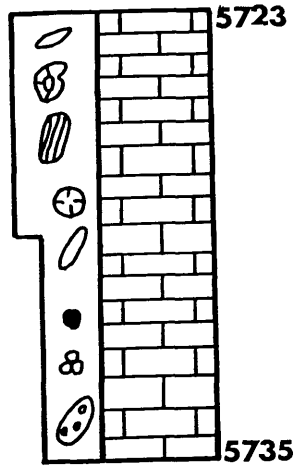
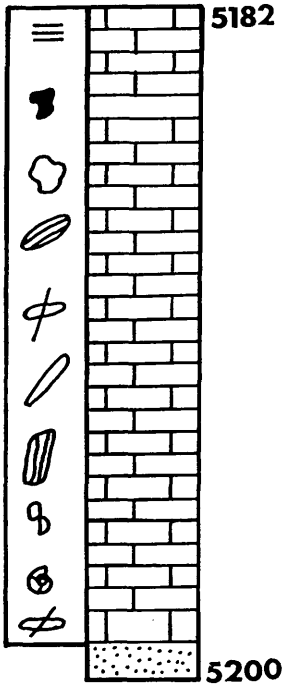


Lithological presentation of the cored interval in well A1-41

Note: key to symbols in P. 65.



Lithological presentation of the cored interval in well C1-41



Lithological presentation of the cored interval in well D1-41

